	GESTIÓN DE SERVICIOS ACADÉMICOS Y BIBLIOTECARIOS	**CÓDIGO**	FO-GS-15
UFPS Vigilada Mineducación		**VERSIÓN**	02
	ESQUEMA HOJA DE RESUMEN	**FECHA**	03/04/2017
		PÁGINA	1 de 1
ELABORÓ	**REVISÓ**	**APROBÓ**	
Jefe División de Biblioteca	Equipo Operativo de Calidad	Líder de Calidad	

RESUMEN TRABAJO DE GRADO

AUTOR(ES): NOMBRES Y APELLIDOS COMPLETOS

NOMBRE(S): LAURA TATIANA   APELLIDOS: MENESES BARRERA

FACULTAD: INGENIERÍA

PLAN DE ESTUDIOS: INGENIERÍA MECÁNICA

DIRECTOR:

NOMBRE(S): LEONEL   APELLIDOS: RINCON CANCINO

NOMBRE(S): MEIMER   APELLIDOS: PEÑARANDA CARRILLO

TÍTULO DEL TRABAJO (TESIS): "NUMERICAL ANALYSIS OF SPARK-IGNITED INTERNAL COMBUSTION ENGINES USING ETHANOL-GASOLINE BLENDS"

RESUMEN

In the present work, a spark ignition internal combustion engine is simulated using 0D and 1D models in AVL BOOST, using five ethanol-gasoline blends (E0, E20, E40, E60, E85) as fuels. The analysis includes varying the compression ratio of each blend (11, 12.5, 13, 14) by analysing engine performance and exhaust gas composition parameters, efficiencies, temperatures within the cylinder, and a brief economic feasibility analysis for blends that showed similar power data. The simulation was performed in AVL BOOST. The combustion model used was the Wibe model, taking its data from experimental studies from the literature. There was a 17% decrease in torque and power for the E84 blend compared to the gasoline RC 11. Blends such as E20 with a compression ratio of 13 and E40 with a compression ratio of 14 obtained torque and power values similar to gasoline. The lower calorific value of ethanol implies a higher specific consumption; there was a 9.7% decrease in consumption of E84 at RC 14 compared to E84 at RC 11.

PALABRAS CLAVES: Ethanol- gasoline blends, BOOST, Combustion, spark ignition, simulation

CARACTERISTICAS:

PÁGINAS: _179_ PLANOS: ___ ILUSTRACIONES: ____ CD ROOM: ___

NUMERICAL SIMULATION OF A SPARK IGNITION INTERNAL COMBUSTION

ENGINE USING ETHANOL-GASOLINE BLENDS

Laura Tatiana Meneses Barrera

UNIVERSITY FRANCISCO DE PAULA SANTANDER

FACULTY OF ENGINEERING

MECHANICAL ENGINEERING

SAN JOSÉ DE CÚCUTA

2020

NUMERICAL SIMULATION OF A SPARK IGNITION INTERNAL COMBUSTION

ENGINE USING ETHANOL-GASOLINE BLENDS

Submitted to the Faculty of Engineering in partial fulfillment of the requirements for the

degree of Mechanical Engineer

Advisor

PROF. LEONEL R. CANCINO, DR. ENG.

UFSC / BRAZIL

Co-Advisor

PROF. MEIMER PEÑARANDA, M.SC.

UFPS / COLOMBIA

UNIVERSITY FRANCISCO DE PAULA SANTANDER

FACULTY OF ENGINEERING

MECHANICAL ENGINEERING

SAN JOSÉ DE CÚCUTA

2020

ACTA DE SUSTENTACIÓN DE UN TRABAJO DE GRADO

FECHA: CÚCUTA, 29 ABRIL DE 2020   **HORA:** 04:30 PM

LUGAR: EXPOSICIÓN VIRTUAL

PLAN DE ESTUDIOS: INGENIERÍA MECÁNICA

Título de la Tesis: "NUMERICAL ANALYSIS OF SPARK-IGNITED INTERNAL COMBUSTION ENGINES USING ETHANOL-GASOLINE"

Jurados: ING. JOSÉ RAFAEL EUGENIO
                     ING. ORLANDO GUTIERREZ LOPEZ

Director: ING. LEONEL R CANCINO
Codirector: ING. MEIMER PEÑARANDA CARRILLO

Nombre de los estudiantes	Código	Calificación	
		Letra	Número
LAURA TATIANA MENESES BARRERA	1121290	CUATRO, OCHO	4,8

MERITORIA

FIRMA DE JURADO

Vo.Bo_____
GONZALO DE LA CRUZ ROMERO GARCIA
Coordinador Comité Curricular
Ingeniería Mecánica

CARTA DE AUTORIZACIÓN DE LOS AUTORES PARA LA CONSULTA, LA REPRODUCCIÓN PARCIAL O TOTAL Y LA PUBLICACIÓN ELECTRÓNICA DEL TEXTO COMPLETO

Cúcuta,

Señores
BIBLIOTECA EDUARDO COTE LAMUS
Ciudad

Cordial saludo:

Laura Tatiana Meneses Barrera, identificado(s) con la C.C. Nº 1090503467, autor de la tesis y/o trabajo de grado titulado NUMERICAL ANALYSIS OF SPARK-IGNITED INTERNAL COMBUSTION ENGINES USING ETHANOL-GASOLINE BLENDS presentado y aprobado en el año 2020 como requisito para optar al título de Ingeniero Mecánico; autorizo a la biblioteca de la Universidad Francisco de Paula Santander, Eduardo Cote Lamus, para que con fines académicos, muestre a la comunidad en general a la producción intelectual de esta institución educativa, a través de la visibilidad de su contenido de la siguiente manera:

• los usuarios pueden consultar el contenido de este trabajo de grado en la página web de la Biblioteca Eduardo Cote Lamus y en las redes de información del país y el exterior, con las cuales tenga convenio la Universidad Francisco de Paula Santander.

• Permita la consulta, la reproducción, a los usuarios interesados en el contenido de este trabajo, para todos los usos que tengan finalidad académica, ya sea en formato CD-ROM o digital desde Internet, Intranet etc.; y en general para cualquier formato conocido o por conocer.

Lo anterior, de conformidad con lo establecido en el artículo 30 de la ley 1982 y el artículo 11 de la decisión andina 351 de 1993, que establece que "**los derechos morales del trabajo son propiedad de los autores**", los cuales son irrenunciables, imprescriptibles, inembargables e inalienables.

FIRMA Y CEDULA

C.C. Nº 1090503467

Abstract

In the present work, a spark ignition internal combustion engine is simulated using 0D and 1D models in AVL BOOST, using five ethanol-gasoline blends (E0, E20, E40, E60, E85) as fuels. The analysis includes varying the compression ratio of each blend (11, 12.5, 13, 14) by analysing engine performance and exhaust gas composition parameters, efficiencies, temperatures within the cylinder, and a brief economic feasibility analysis for blends that showed similar power data. The simulation was performed in AVL BOOST. The combustion model used was the Wibe model, taking its data from experimental studies from the literature. There was a 17% decrease in torque and power for the E84 blend compared to the gasoline RC 11. Blends such as E20 with a compression ratio of 13 and E40 with a compression ratio of 14 obtained torque and power values similar to gasoline. The lower calorific value of ethanol implies a higher specific consumption; there was a 9.7% decrease in consumption of E84 at RC 14 compared to E84 at RC 11.

Resumen

En el presente trabajo se Simular un motor de combustión interna de encendido por chispa utilizando los modelos 0D y 1D en AVL BOOST, utilizando cinco mezclas de etanol-gasolina (E0, E20, E40, E60, E85) como combustibles. El análisis incluye la variación de la relación de compresión de cada mezcla (11, 12,5, 13, 14) analizando los parámetros de rendimiento del motor y composición de los gases de escape, eficiencias, temperaturas dentro del cilindro y un breve análisis de viabilidad económica para mezclas que mostraron datos de potencia similares. La simulación fue realizada en AVL BOOST. El modelo de combustión utilizado fue el modelo de Wibe, tomando sus datos de estudios experimentales from literatura. Hubo una disminución del 17% en el par y la potencia para la mezcla E84 en comparación con la gasolina a RC 11. mezclas como la E20 con una relación de compresión de 13 y la E40 con una relación de compresión de 14 obtuvieron valores de par y potencia similares a los de la gasolina. El menor poder calorífico del etanol implica un mayor consumo específico, se produjo una disminución de 9,7% en el consumo del E84 a RC 14 frente al E84 a RC11.

Keywords: Mezclas de etanol y gasolina, BOOST, Combustión, enc.endido por chispa, simulación

Table of Contents

List of tables

List of figures

List of Appendix

Introduction

The development of internal combustion engines has been going on since the early 1800s, advanced and improving significantly over the following decades. Among the most relevant events are the construction of the first engine based on the "four-stroke" operating system built by Nicolaus August Otto around 1832 and the development and construction of the compression ignition engine by Rudolf Diesel from 1892 onwards. (Pulkrabek, 1997).

Once the career of design started and looking for the improvement of internal combustion engines, multiple variations, methods and systems were introduced. (Heywood, 1988). One of the main classifications of internal combustion engines is by the method of ignition of the air-fuel mixture, among which are: ignition by spark and ignition by compression.

According to Merker (2012) in a spark ignition internal combustion engine, the mixture of air and fuel, introduced by the intake valve into the combustion chamber, is compressed and ignited by an electrical discharge produced by a spark plug. This electric discharge occurs between 10 and 40 degrees from the crank handle before the piston reaches the top dead center. (Heywood, 1988).

Research on engines, and specifically on the spark ignition internal combustion engine, has been constant and approached by both, experimentally and numerically methodologies. The latter was possible thanks to the advance of computers and the different simulation programs dedicated to the combustion area (CRFD- Computational Reactive Fluid Dynamics). These programs allow the researcher to represent in a simplified, economic and fast way (in comparison with experimental methods) the different processes that can occur inside an ICM during its operation, allowing to obtain relations and effects between the different inputs,

operation and output engine parameters. (Nigro, Storti, & Ambroggi, 1999). Note that these numerical simulation programs allow to perform optimization processes.

Currently, one of the most important simulation programs for internal combustion engines is the AVL AST, which, using different advanced models, provides a coherent prediction of engine operation and efficiency, as well as emissions and noise analysis. (AVL BOOST, 2019).

Despite the multiple benefits that the development of internal combustion engines has carried mainly in the transport area, they have also caused important problems for public health and the environment in terms of environmental pollution, more specifically due to the emission of greenhouse gases and other harmful gases. Due to the above, solutions have been continually sought to minimize emissions of pollutants into the atmosphere and one of the proposals of greatest acceptance and impact has been the use of biofuels, either as a main fuel or as an additive or mixed with fossil fuels. Biofuels are basically alcohols, ethers, esters and other chemical compounds produced from biomass. For example, herbaceous and woody plants, residues from agriculture and forestry; and a large amount of industrial waste, such as food industry waste (Stratta, 2000).

There are different types of biofuels, but for relevance ethanol will be treated. According to the National Petroleum Agency (ANP Brazil) ethanol is a biofuel of chemical formula C_2H_5OH (C_2H_6O) that can be obtained from sugar, corn, beet, potato, etc., and is used as a substitute for gasoline in spark ignition engines. Currently, different countries use ethanol as an additive to gasoline, among which they stand out: United States, Brazil, Canada and the European Union (National Petroleum Agency, 2019). Brazil is the first producer of ethanol based on sugar cane, but generally the second after the United States, which produces ethanol from

corn. Canada produces ethanol from corn and wheat, this country has the first and only plant provided to convert biomass fibers into ethanol through enzymatic technology and sells gasoline with up to 10% ethanol in some service stations (Government of Canada, 2018). For its part, the European Union (EU) aims to use 27% of energy in renewable energies by 2030, which is why biofuels are important (Suarez, Cairotte, Arlitt, Nakatani, Hill, Winkler,... & Astorga, 2017).

For its part, in Brazil the use of ethanol as a biofuel began with the PROÁLCOOL program in 1975, seeking to confront the oil crisis through the obligatory inclusion of ethanol in gasoline between 4% and 10%, and over the years the production of ethanol has fallen and increased according to the market and above all the price of oil, (Girardi, 2019). Ethanol is produced from sugar cane, both dehydrated ethanol (0.7% water) and hydrated ethanol (max. 7.4%) are produced and their ethanol consumption has intensified with the launch of Flex- Fuel vehicles which can work with hydrated ethanol, gasoline, or mixtures of any proportion (Nogueira, Dominutti, De Carvalho, Fornaro, & Andrade, 2014). Due to the above, about 50% of sugar cane crops are destined for ethanol production and since Brazil is also a world power in sugar production and export, sugar cane crops are of vital importance to the country's economy. By 2001 there were 320 plants in the sugar and alcohol sector and by 2007 a total of 360 and 120 more projects (De Cerqueira & Leal,). In addition, the gasoline market in Brazil today is regulated by the National Petroleum Agency (ANP) and in 2019 the ethanol content in gasoline is 27% (PETROBRAS, 2019).

As for Colombia, Law 693 of 2001 marked the country's entry into the era of biofuels, motivated by the Kyoto Protocol and the dynamics of oil prices (Amaris, Manrique, and Jaramillo, 2015) and based on environmental sustainability, improved fuel quality, agro-industrial development, employment generation, agricultural development and energy supply

(Serrato and Lesmes, 2016). This law promoted the use of fuel alcohol as an additive to gasoline (Congress of the Republic of Colombia, 2001) and introduced certain benefits such as: the exclusion of VAT on sugarcane, the exemption of oil palm income and the control of sales prices of bioethanol and biodiesel (Amaris, Manrique, and Jaramillo, 2015). In addition to Law 693/2001, Law 939 of 2004 was approved, which also encouraged the use of biodiesel (Congress of the Republic of Colombia, 2019).

Ethanol production in the country is possible because Colombia has available land, labor, geographic benefits, and aquifers that would give the country an important place in ethanol production, but different social, economic, and political problems may be delaying it. There are currently 7 ethanol production plants in Colombia, which are made from sugar cane (Mouthón, 2008).

In August 2018, Semana magazine presents a brief description of the use of ethanol in Colombia as a biofuel, which at the beginning was 8%, rising to 10% from 2018, being even lower compared to other countries such as Brazil and the United States. This low percentage is still due to the limitations of national agricultural and industrial production, despite having 7 bioethanol distilleries with 30.000 barrels produced daily. Additionally, in 2014 imports of ethanol were authorized when the national supply was not sufficient, but by 2017 free imports were authorized with the argument of not giving rise to shortage, bringing discontent of domestic producers, which claim to be at a disadvantage against such imports, generating a fall in domestic production (Semana, 2018).

In the present work, the aim is to simulate a spark ignition internal combustion engine using five blends as fuel: E0, E20, E40, E60, and E84. The mixtures named above are represented by the letter "E" which indicates that it is a mixture of gasoline with ethanol as

biofuel, followed by the volumetric percentage of ethanol in the mixture, therefore, E20 represents a mixture of ethanol and gasoline with 20% ethanol and 80% gasoline on a volumetric basis. And, using 0D and 1D models through the AVL-BOOST module of AVL-AST. Based on this simulation, the operating and output parameters of the engine, the emissions of CO, CO_2 and NOx, as well as other pollutant gases present in the combustion of ethanol will be analyzed, depending on the fuel mixtures used.

The research will be developed in the line of research in simulation of internal combustion engines, headed by Prof. Leonel R. Cancino, at the Federal University of Santa Catarina, Joinville Campus, this in addition to providing knowledge in the field of combustion and serve as a basis for possible future research, opens along with other research projects of UFPS students in the UFSC, the need to implement advanced studies in this area in the main campus of UFPS.

The document is developed by chapters, where the first one contains the problem studied, the objectives of the investigation and its scopes and limitations; the second chapter alludes to the referential framework, where the theoretical and legal bases used are presented, followed by chapter three where reference is made to the methodology used in carrying out the project, where each one of the steps and parameters used can be observed in detail. Chapter four shows the results obtained in the simulations; chapter five also shows the analysis of the results of chapter 4, followed in chapter six by the recommendations and difficulties presented and finally the bibliographical references used throughout the work and the corresponding appendix.

1. General presentation of the draft

1.1. Title

Numerical analysis of spark-ignited internal combustion engines using ethanol-gasoline blends.

1.2 Problem Approach

The internal combustion engines (ICM) were a great advance for humanity, since the arrival of these, there were significant changes in all areas, starting the industrial revolution and changing the manufacturing processes and the way to transport, mainly. But, they have also been participants and causes of the pollution of the planet and its consequent increase in temperature. For this reason, the production of energy by alternative means "within the primary consumption of global energy has significantly expanded the search for the reduction of air pollution and climate change generated by the consumption of fossil fuels in the last fifty years". (Mantilla, Aguirre, & Sarmiento, 2008).

This has focused interest on biofuels for automotive use, more specifically for ethanol spark ignition engines. On the other hand, ethanol and its gasoline blends have received great attention as an alternative fuel due to the reduction of greenhouse gas emissions and because it is produced from renewable sources. And although it is an attractive biofuel, as it contains the hydroxyl group OH its incomplete combustion causes high emissions of aldehydes. The aldehydes are highly reactive compounds involved in complex chemical reactions in the atmosphere. The aldehydes considered pollutants are those found in the gaseous state: acetaldehyde (C_2H_4O) and formaldehyde (CH_2O), which are toxic and have harmful effects on health, reaching highly toxic and potentially carcinogenic (Barros & Sodré, 2016).

In addition, another problem focuses on the low energy content of ethanol relative to gasoline and diesel. Therefore, having lower calorific value makes it necessary to burn more

ethanol compared to gasoline also producing more pollutants. In spite of this, ethanol relatively reduces the amount of CO_2 and CO due to its low carbon content, but as mentioned above its inefficient combustion produces other toxic emissions such as formaldehyde, acetaldehyde, ammonia, benzene, etc. (Biofuel, 2010).

Similarly, there have been studies with mixed results where an increase in the production of soot is observed with the increase of the ethanol mixture, attributing this behavior to the high value of ethanol vaporization enthalpy, which creates cooling load effects producing soot (Yang, Roth, Dubin, Shafer, Hemming, Antkiewicz,... & Karavalakis, 2019).

Brazil was the first country to implement the use of ethanol as an additive to gasoline and is currently one of its largest producers and consumers. A study carried out in this country showed that the highest values of formaldehyde have been recorded in the city of Rio de Janeiro, where they increased considerably between 1998 and 2004, while the levels of formaldehyde and acetaldehyde dropped sharply between 2004 and 2009. In the last period, values ranged from 1.52 to 54.31 ppbv for formaldehyde and from 2.36 to 45.60 ppbv for acetaldehyde. The authors attributed high concentrations of aldehyde to the increasing use of biofuels. Several authors have developed reaction pathways in the combustion of different biofuels and have concluded that, in general, such processes can be expected to produce carbonyl compounds, particularly formaldehyde (Noqueira, Dominutti, De Carvalho, Fornaro, & Andrade, 2014).

In 2001, Colombia began a path towards the use of ethanol as a fuel and more recently, in 2018, its mandatory use in blends with gasoline (E10) was ratified. It is therefore necessary to analyze the emissions produced by ethanol and blends of ethanol and gasoline, both regulated and unregulated emissions, including acetaldehyde and formaldehyde. For its part, the U.S. code

of regulations requires the analysis of non-methane gases (aldehydes) for mixtures above 25% oxygenated fuels (Girardi, 2019).

Therefore, in order to assess the causes of emissions from spark ignition internal combustion engines, as well as their efficiency and comparisons according to fuel type, it is necessary to know in advance the internal functioning and behavior of the operating parameters of an engine running on ethanol and ethanol/gasoline blends.

The simulation of the combustion of a spark ignition ICM can be performed in different models (0D, 1D, 2D, 3D) depending on the degree of accuracy and detail of the process. Since the project is a simplified simulation, the analysis will be carried out using 0D and 1D models, using the numerical simulation program AVL BOOST. This program also allows the variation of the composition of the fuel used, considering five fuels, including ethanol and four blends of ethanol and gasoline: E0, E20, E40, E60 and E84.

The numerical simulation will allow, via parameter variation, to know in detail the functioning of the engine from the numerical point of view, using the different models of heat transfer, fluid mechanics and combustion already available in the AVL-AST, in addition to calculating and knowing via chemical balance the concentrations of certain emissions at the end of the combustion process inside the cylinder. This generates the possibility to perform analysis for possible optimizations of the different subsystems of the engine to be simulated as for example: (a) spark release angle, (b) intake and exhaust pressure losses, (c) intake manifold geometry, (d) pollutant emission, (e) valve lift curve, among other possible focal points of analysis.

1.3 Justification

The system of transport and generation of energy is more and more demanding every day and as time goes by this demands improvements, seeking not only the energetic efficiency but also diminishing, in great percentage the footprint of pollution, it is for this reason, that it is necessary to know the operation of the internal combustion engines, both spark ignition and compression ignition engines. Since, starting from the knowledge of its behavior, the relation between the parameters of operation and exit, the form how the combustion is developed in the combustion chamber, the behavior of air in the collector of admission, among others, can have a base for its analysis, improvement and eventual modifications. As for the generation of emissions, both types of ECI generate CO, NO_X, HC, unburned HC, soot, among others, the amount of which depends on the characteristics and functioning of each one. It is recognized that most commercial vehicles are spark ignition vehicles and it is the gasoline to which ethanol is added, therefore, in this paper will focus on the spark ignition engine.

Global warming is a reality attributed primarily to the human extension of the "greenhouse effect" the warming that occurs when the atmosphere traps heat that radiates from the Earth into space. Over the last century, the burning of fossil fuels, such as coal and oil, has increased the concentration of carbon dioxide in the atmosphere. Some probable effects that this warming can bring are: increase in the temperature of the Earth, change in the humidity of certain regions and increase of precipitations, partial melting of glaciers, increase in the level of the sea, affectations to crops and general changes of the climate (NASA, 2019). On the other hand, much of the combustion of fossil fuels (oil) takes place in the transport sector, i.e., through the use of internal combustion engines.

This is why global warming and climate change have generated greater interest in the implementation of biofuels in internal combustion engines (Larsson, Stenlaas, Erlandsson, 2019). Now Garcia and Calderon (2012) say that the use of biofuels allows countries to diversify their energy basket and makes them less dependent on non-renewable fossil fuels, can have positive effects on the environment by reducing the level of greenhouse gas emissions, and, by relying on agricultural inputs, can have positive effects on countries' rural development (p. 1). Rogério & Manoel (quoted by De Cerqueira, Leal, 2007) also present three main reasons for the use of biofuels: the reduction in dependence on fossil fuels in terms of security of supply; the minimization of emissions; and the control of greenhouse gases.

The government of Canada affirms that ethanol is a cleaner fuel than gasoline in the sense of its net effects, because despite emitting emissions, although lower than those of gasoline, when analyzing that corn and wheat crops absorb carbon dioxide their net pollution is much lower. Low blended ethanol from corn produces 3 to 4 percent less greenhouse gas emissions than gasoline (Government of Canada, 2018).

The newspaper El Heraldo carried out a journalistic article titled "Imports displace 26% of ethanol production", in this one it is affirmed that "Only in February of this year 12 million liters were imported, which represented almost 30% of the national demand per month, which is of about 40 million liters", the previous shows that Colombia must promote the farming of sugar cane and the production of ethanol, contributing not only to the improvement of the environment but to the national economy (Mouthón, 2008).

Despite all the benefits of using ethanol as a fuel, studies have been conducted to confirm the risk of cancer from exposure to aldehyde emissions (Yüksel & Yüksel, 2004), (Ceviz & Yüksel, 2005), (Leong, Muttamara, Laortanakul, 2002).

The above demonstrates the importance of the use of biofuels in internal combustion engines, but also of their study and research in order to determine and implement the correct way in which they should be burned, in order to minimize emissions of greenhouse gases and also emissions of other gases highly toxic to health such as aldehydes. The comparison of the parameters and performance of an engine with respect to the content of ethanol in the fuel, allows to have an overview of this biofuel, as well as to continue with more in-depth research in each specific area.

In Colombia, the importance of the study of ethanol as a biofuel has been increasing since the creation of Law 693 of 2001, being this the first law that dictated norms on the use of fuel alcohols and created incentives for their production, commercialization and consumption in the country (Congress of the Republic of Colombia, 2001). Currently, through Resolution 40185, the government established a percentage of 10% ethanol in gasoline, increasing the need to know the advantages and disadvantages of the use of this biofuel, and therefore, the importance of an adequate combustion of the fuel to avoid emissions of toxic gases and obtain the maximum possible yield.

At the institutional level, the Francisco de Paula Santander University has as its mission the continuous improvement of research and extension processes, seeking the integral training of professionals committed to solving environmental problems in favor of sustainable development in the region. (UFPS, Francisco de Paula Santander University, 2016) This is why the development of research in conjunction with universities such as the Federal University of Santa Catarina in Brazil (UFSC), is an important contribution to institutional research and the strengthening of relations between universities, increasing the field of knowledge that can be acquired by the student.

On the other hand, the Mechanical Engineering program of the UFPS seeks to train ethical, moral and intellectual professionals capable of meeting the needs of society, through the use of technologies and applying creativity, in addition to promoting research and service to the community. In addition, as part of their occupational profile, mechanical engineers can formulate and promote policies to optimize the use of energy resources, promoting the development of machines, equipment and mechanical systems that transform and use them efficiently. According to the above, the agreements with Universities encourage joint research expanding the horizons of the same, in addition, the integration of theoretical concepts of combustion and computer-assisted simulations of this process increases the capabilities of solving engineering problems, allowing simple and effective representations of engines and their operation in search of the resolution of the different technical and environmental problems that these machines may present. (UFPS, Mechanical Engineering, 2018).

At the level of the student, to make a research in direction of a university of great academic transcendence as the Federal University of Santa Catarina, increases its knowledge on the area to investigate, allowing to assimilate new methods and systems of learning, in specific, acquiring knowledge in the handling and application of programs of Engineering and Numerical Simulation. Likewise, during the time of development of the research the student knows and learns about another culture and customs, and since Brazil is a country with a language different from the student's own, learning Portuguese is taken as an extra benefit of great importance. On the other hand, the student is favored by having the opportunity to participate in graduate scholarships offered by the Brazilian Government, in order to continue with the formative and research process.

1.4 Problem formulation

How do the parameters of a spark ignition internal combustion engine vary with the ethanol content in ethanol-gasoline blends?

1.5 Objectives.

1.5.1 Overall Objective.

Simulation of a spark-ignition internal combustion engine using 0D and 1D models in AVL BOOST by using five ethanol-gasoline blends (E0, E20, E40, E60, E85) as fuels. The analysis includes the compression ratio variation for each mixture (11, 12.5, 13, 14) analyzing the engine performance parameters.

1.5.2 Specific Objectives

- To develop a numerical simulation methodology for internal combustion engines using 0-D and 1-D models previously implemented in the AVL-BOOST software.

- To analyze engine performance parameters: torque, power and specific fuel consumption using five different fuels blends (E0, E20, E40, E60 and E84) and different compression ratio (11, 12.5, 13 and 14).

- To evidence of the behavior of different operating parameters of the simulated model in relation to the ethanol content in the fuel and the compression ratio.

- To analyze the behavior of CO, CO_2 and NO_X emissions after combustion and its change with respect to the percentage of ethanol and compression ratio.

1.6 Scopes and delimitations

1.6.1 Scopes and Delimitation

The project was carried out in the internal combustion engines laboratory of the Federal University of Santa Catarina, Campus Joinville through an agreement with the Francisco de Paula Santander University.

In this work the operation of a representative system of a four-cylinder internal combustion spark ignition engine working at 2500 rpm was simulated using the AVL BOOST software and varying the fuel, i.e., used five blends of ethanol-gasoline. The ethanol-gasoline blends used in the simulation were E0, E20, E40, E60 and E84, where each number represents the volumetric percentage of ethanol. The geometry, thermodynamic and other parameters of the elements that build the model used were obtained from the AVL BOOST software database and other research. The parameters of the combustion model (Vibe) used were taken from Yeliana's (2008) doctoral thesis. Likewise, those parameters not mentioned as variables in chapter 3 of the methodology will be taken as constants for all fuel mixtures used.

The analysis will focus on the variation of engine operating parameters and the formation of emissions due to combustion with respect to the change of ethanol content. The performance parameters analyzed were: effective torque, effective torque, specific fuel consumption (*isfc* and *bsfc*). The emissions considered were gasoline and unburned ethanol, CO_2, H_2O, CO, H_2, OH, H, NO, O_2, O and N_2, focusing the analysis on gases harmful to health and the environment.

1.6.2 Limitations

The main limitation in the development of the project was the time for taking geometric values of each component of the engine model, therefore, it was necessary to use a model proposed by the AVL BOOST software and also the geometry values given by it.

Similarly, the data of the combustion model used, Vibe, are from a Simple Vibe model and not for a Vibe model of two zones, which would allow a more detailed calculation of the species formed by the combustion, allowing a better analysis of emissions.

2. Reference Framework

2.1 Background

This section presents research conducted in the area of: BOOST's simulations, spark ignition internal combustion engines, use of ethanol as fuel, ethanol and gasoline blends and their effects and consequences. These works are considered relevant as antecedent to the present project.

2.1.1 International background.

Jaramillo, A. (Fabricio, 2015) conducted a study called: "Design and simulation of the hybrid operation between the hydrogen-fuel mixtures in an Otto cycle internal combustion engine using a program.

The present study, developed a theoretical analysis for the combustion of the hybridization of the hydrogen-hydrocarbon mixture, the hydrocarbon to select is gasoline however for reasons of ease of calculation the octane will be taken, in order to study hydrogen as an alternative energy source to gasoline, since the pollution levels of hydrogen combustion along with a fossil fuel may be low in proportion to the increase of hydrogen during combustion (pag 16).

Sanz, M (2017), conducted a study through AVL-BOOST for the "Optimization of the closing of the intake valve of an alternative internal combustion engine" the scope that may have the implementation of the Miller and Atkinson shekels in alternative internal combustion engines, this study was not conducted through a test bench, but through simulations conducted with AVL-BOOST software.

Yang, Roth, Dubin, Shafer, Hemming, Antkiewicz,... & Karavalakis (2019), conducted an experimental study entitled "Emissions from a flex fuel DGI vehicle operating on ethanol fuels show marked contrasts in chemical, physical and toxicological characteristics as a function of ethanol content". This study compared the emissions of total hydrocarbons, carbon monoxide CO, nitrogen oxides NO, non-methane hydrocarbons NMHC, and CO_2 for four fuels E10, E10 HA (blend with a higher fraction of aromatic at 36.7%), E30 and E78, both for cold ignition and hot ignition. It was evidenced that for E78 there were no significant changes among them, only E78 obtained a significant reduction in cold ignition with respect to E10 and E10HA. As for CO, the increase in ethanol reduced its emissions and no significant changes were found in NOx emissions. Volatile organic compounds VOCs were also analyzed and the only carbonyls detected were Formaldehyde and Acetaldehyde, which increase significantly with the increase in ethanol concentration and are greater for cold ignition than for hot ignition.

In the University of the Armed Forces of Ecuador was developed a "comparative study of power, torque and pollutant emissions in a spark ignition internal combustion engine of (MEP) with extra fuel, E5 and E10 to a height of 2700 M.S.N.M. "The tests of torque, power and emissions were carried out in the research center CCICEV of the National Polytechnic School where a dynamometer and a certified gas analyzer were used following the norm INEN 2203. Finding that for the E10 there are improvements in torque and power, but also greater emissions of CO, CO_2 and HC (Castelo, Cepeda, Bonilla, Acosta, Moreano, Almacaña,… & Villalba, 2017) .

Hernandez, Escobar, García, Gómez, Higareda and Olivares (2019) carried out an experimental study in which they calculated brake power and fuel consumption in an SI engine with different blends of hydrogen-ethanol, hydrogen-gasoline and ethanol-gasoline, from 0 to

100% concentration, as well as ethanol-gasoline-hydrogen. They determined that by adding

hydrogen to both ethanol and gasoline the power to the brake decreases. Additionally, it was

concluded that the maximum power was obtained with ethanol, followed by gasoline and finally

with hydrogen mixtures, but a higher fuel consumption was registered for ethanol, but by adding

up to 8% hydrogen to ethanol this consumption is reduced without losing power.

A project entitled "The impact of various ethanol-gasoline blends on particulates and

unregulated gaseous emissions characteristics from a spark ignition direct injection (SIDI)

passenger vehicle " was developed in the School of Mechanical Engineering of Korea University

together National Institute of Environmental Research, , (Dongyoung, Kwanhee, Cha-Lee,

Younsung, Jongtae & Simsoo, 2017) the effects of gasoline with ethanol on the emission of

hazardous pollutants and fuel economy in five mixtures were studied: E0, E10, E30, E50 and

E85, using a chassis dynamometer using the federal test procedure mode (FTP-75). It was

determined that an E85 blend consumed 29% more fuel than pure gasoline due to the low energy

content of ethanol, but produced a dramatic decrease in particulate emissions. Carbonyl

compound emissions from the partial oxidation of ethanol increased sharply as the ethanol

content increased, while volatile organic compound (VOC) emissions decreased considerably.

In the project "The effect of ethanol-gasoline blends on performance and exhaust

emissions of a spark ignition engine through exergy analysis" (Dogan et.al, 2005) different

ethanol-gasoline mixtures (E0, E10, E20, E30) were analyzed, the results showed a decrease of

CO, CO_2 and NOx without significant difference of power when increasing the ethanol content,

as well as, an increase in HC emissions due to the decrease of temperatures inside the cylinder.

A study entitled "Five years of formaldehyde and acetaldehyde monitoring in the Rio de

Janeiro downtown area and Brazil" (Machado, et al, 2010), presents a monitoring campaign that

was executed from March 2004 to February 2009 by sampling at early morning on every sunny Wednesday for a total of 183 samples, this study allowed to know the levels of aldehydes and formaldehydes in the city of Rio de Janeiro, being Brazil the country with greater use of ethanol-gasoline mixtures. The study showed a strong reduction in formaldehyde levels and a slight reduction in acetaldehydes, which was most likely attributed to the increased use of vehicles with the necessary technology for the proper combustion of ethanol.

The project called "Impact of alcohol–gasoline fuel blends on the performance and combustion characteristics of an SI engine" (Eyidogan, Ozsezen, Canakci & Trukan, 2010) developed at Kocaeli University of Turkey, it was carried out on a chassis dynamometer while running the vehicle at two different vehicle speeds (80 km/h and 100 km/h) and four different wheel powers (5, 10, 15 and 20 kW).

> "The results obtained from the use of alcohol–gasoline fuel blends were compared to those of gasoline fuel.
> The results indicated that when alcohol–gasoline fuel blends were used, the brake specific fuel consumption increased; cylinder gas pressure started to rise later than gasoline fuel. Almost in the all test conditions, the lowest peak heat release rate was obtained from the gasoline fuel use" (p. 2713).

An experimental project together with simulation in AVL BOOST was carried out by Cassiano, Ribau, Cavalcante, Oliveira & Silva (2016), this was titled "On-board monitoring and simulation of flex fuel vehicles in Brazil". Here a light-duty vehicle, the flex-fuel Nissan Versa equipped with a 1.6 liter engine and manual transmission was monitored in real operation, using five-gas analyzer for CO, HC (CH_4), NO_2, CO_2 and SO_2 in addition to dry systems.

> "The operating parameters registered in this vehicle were: vehicle speed, engine speed, fuel consumption, angle position of the throttle valve, cooling water, and oil and exhaust gas

temperatures. The measurements were performed using gasoline with 27%, and 100% ethanol blends (E27 and E100 respectively, where E27 is used in emission certification). The vehicle-experiment (driving pattern) was realized in an urban route in the Fortaleza City, Brazil, under typical traffic conditions. The analysis indicates that the average emission rates (kg/h) for CO are more than a factor of 10 higher to NO idling emissions. AVL CRUISE integrated with AVL BOOST software were used to model the vehicle and the flex-fuel engine in both certification driving cycles and real operation ones. Real operation data is used to validate the model" (Demostenes, Ribao, Cavalcante, Olivera, & Silva, C, 2016).

2.1.2 National background.

Buitrago (2014) completed the master's degree project "Evaluation of the environmental effects of gasoline, diesel, biodiesel and fuel ethanol in Colombia through life cycle analysis" at the National University. A Life Cycle Assessment (LCA) study for the production of gasoline, diesel, biodiesel and bioethanol in Colombia, using the free software OpenLCA (2018), was carried out. Concluding that:

"The results show that the current bioethanol production system shows a 79% reduction in GHG emissions compared to gasoline, while there is an 87% reduction in the Non-Renewable Energy Demand (bioethanol: 1.7E-2 kg CO_2eq/MJ and 1.8E-1 MJeq/MJ; gasoline: 8.3E-2 kg CO_2eq/MJ and 1.4 MJeq/MJ). On the other hand, current biodiesel production shows an 82% reduction in GHG emissions compared to fossil diesel and a 35% reduction in Non-Renewable Energy Demand (biodiesel: 1.6E-2 kg CO_2eq/MJ and 3.9E-1 MJeq/MJ; diesel: 8.9 kg CO_2eq/MJ and 6.0E-1 MJeq/MJ)" (p. IX).

2.2 Theorical Framework

2.2.1 History of internal combustion engine.

The invention and search for new knowledge has been linked to the history of man, the need for connection and cultural, academic and market exchanges led to the development of

different means of transport today, which according to Heywood (1988) saw its origin 1860 when for the first time the development of the first internal combustion engine was proposed using a mixture of coal gas and air by JJ E. Lenoir, who worked in two careers. The air was dragged into the chamber in the first half of the cycle, where the ignition occurred and expanded through the remaining run and then a second escape run (Stone, 2012). In 1867, Nicolaus Otto and Eugen Langen developed a combustion engine of the fuel-air charge early in the outward stroke to accelerate a free piston and rack assembly so its momentum would generate a vacuum in the cylinder (Heywood, 1988). As mentioned by Ferguson & Kirkpatrick (2016) later in 1872 Gegorfe Brayton commercialized a constant pressure MCI which was first used in a car and consisted of two cylinders, one compression and one expansion.

According to Ferguson & Kirkpatrick (2016), four years later in 1876 again Otto built the first single-cylinder four-stroke engine with a brake efficiency of 14%, this being the forerunner of modern engines, by 1890 he had sold at least 50,000 copies. In 1878 Sir Dugald Clerk invented the first two-stroke engine patented three years later, this consisted of a power cylinder and the other responsible for pumping air and fuel to the first cylinder. Then, Gottlieb Daimler was the first to make a patented high-speed engine in 1884, but in 1889 he commercialized his twin cylinder "V" engine more successfully (Stone, 2012). By 1885 Karl Benz (1844-1929) manufactured a two-stroke, spark-ignition engine capable of delivering 3.5 hp, which was ignited by means of an electric induction coil with a rotary switch operated by the engine and a spark plug (Ferguson & Kirkpatrick, 2016).

According to Stone (2012) in 18970, a compression ingestion engine was patented by Akroyd Stuart and Rudolf Diesel, but it was two years after the first one was built. With a compression ratio of 3 it provided an ignition of the fuel, it had a pre-chamber or vaporizer for

the fuel that was injected directly into the combustion chamber. It used light petroleum distillate or fuel oil as fuel, also had greater efficiency compared to other engines.

On the other hand the catalysts were introduced from the study on air pollution in 1940 by Prof. A J. Haagen-Smit, likewise, the noise produced was regulated in 1970 by vehicle noise legislation. The progress on ICE' scontinued its course to this day, it seeks to improve efficiency, power and reduce emissions, leading to the development of materials, fuel injection and fuels themselves (Heywood, 1988).

2.2.2 Classification of the internal combustion engines.

ICE's can be classified taking into account different characteristics, whether physical or functional. A classification refers to work cycles and according to Stone (2012) the main difference between a 2-stroke and a 4-stroke engine is the assumption of individual induction and exhaust races. On the other hand, there is the method used for the preparation of the fuel mixture: the carburetor works by admitting an air flow that is mixed with the necessary amount of fuel within the same carburetor; the injection port works by injecting the amount of fuel needed in or near the cylinder inlet port (Caton, 2016).

Another common classification is according to the ignition method: ignition by spark or forced and ignition by compression or spontaneous and according to Caton (2016) this is perhaps the highest classification of ICE's, since when defined, many other characteristics are fixed, such as the method of mixing the air-fuel, the type of fuel, among others.

There are other classifications as described by Ferguron & Kirkpatrick (2016) according to: their application, piston layout or basic design, type of fuel, ignition chamber design, load control method, valve arrangement and cooling method.

2.2.3 Thermodynamics cycles.

As it was previously mentioned, the type of ignition that the engine possesses will define the type of fuel it uses and in turn the thermodynamic cycle that defines the operation of the engine. On the other hand, Brunetti (2009) shows that in order to be able to model a real cycle from a theoretical one, different hypotheses must be raised such as: the fluid is air, there is no admission or escape, the expansion and compression processes are isentropic, combustion is replaced by a heat delivery (supply), heat is removed to return to the initial state and all processes are reversible.

2.2.3.1 Otto cycle.

This cycle is the one associated with the spark ignition engine and has the characteristic that the heat input into the engine is carried out at a constant volume (Florez, et.al, 2005). In Figure 1 the representation of the cycle is observed where: state 1 to 2 an isentropic compression is presented where work is entered into the system. Process 2-3 represents an addition of heat at a constant or isochoric volume. Subsequently, the process 3-4 shows an isentropic expansion where the system performs work and finally the process 4-1 where the heat is removed from the system, which would be equivalent to the process of exhaust of the gases.

Representation of Otto cycle in the *p, v* and *T*, s diagram
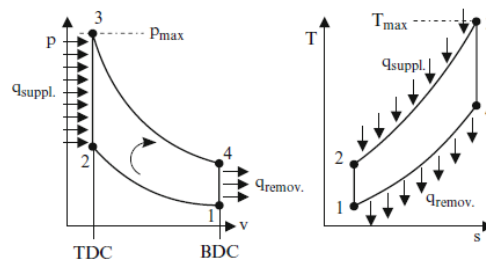
Figure 1 Representation of Otto cycle in the p, v and T, s diagram. Source. Merker, Schwarz & Teichman (2019)

2.2.3.2 Diesel cycle.

According to Florez, et. al. (2005), this cycle corresponds to compression ignition engines, and its main difference with the Otto cycle is based on the heat addition process, in this case it is introduced at constant pressure. Additionally, the Diesel cycle the compression ratio can be between 14 and 24, while in the Otto it is much smaller, from 6 to 10. The cycle is composed of four processes as seen in Figure 2: process 1-2 it is an adiabatic compression; between 2-3 there is an isobaric process where the heat input (equivalent to combustion) occurs; process 3-4 represents an isentropic expansion and finally process 4-1 shows a constant volume heat extraction (equivalent to exhaust).

According to Cengel & Boles (2012), in high-speed engines:

"The fuel starts its ignition at an advanced stage of the compression cycle and, consequently, part of the combustion takes place almost at a constant volume. The fuel injection continues until the piston reaches the upper dead center, and the combustion of the fuel keeps the pressure high until well into the expansion cycle. Thus, the entire combustion process can be better modeled as the combination of constant volume and constant pressure processes. The ideal cycle based on this concept is called the dual cycle" (p.505).
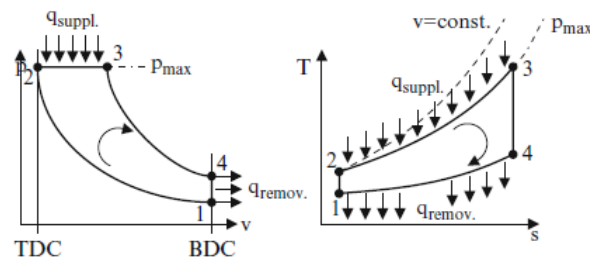
Figure 2 The Diesel cycle in the P-v and T-s diagram. Source. Merker, Schwarz & Teichman (2019).

Therefore, the Dual cycle can be modeled according to the amount of heat added in each process, becoming both the Otto cycle and the Diesel (See Figure 3).
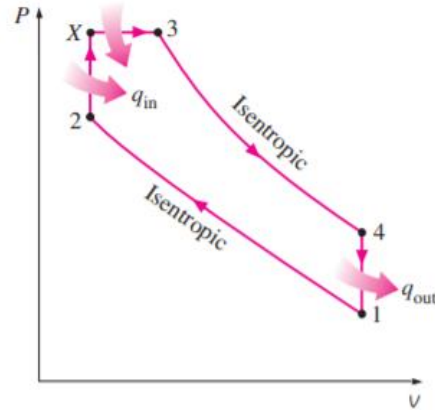
Figure 3 The Dual cycle in the p, v diagram. Source. Cengel & Boles (2012)

In general, comparing the three named cycles can show advantages and disadvantages of each of them. For the same compression ratio, the Otto cycle has the highest efficiency, followed by the Dual cycle and finally the Diesel cycle. On the other hand, for the same temperature at point 3, the maximum, the Diesel cycle has the highest efficiency, followed by the Dual and then the Otto.

2.2.4 Parameters of an internal combustion engine

2.2.4.1 Compression ratio

Thermal efficiency increases with the compression ratio, but is limited by knock for spark ignition engines and by the maximum pressure for the engine in general. The increase in thermal efficiency decreases at high compression ratio values due to increased friction (Caton, 2016).

The Figure 4 shows the distribution of energy as a function of the compression ratio, this shows that as the compression ratio increases the brake work, friction and heat transfer increases while exhaust energy decreases (Caton, 2016).

2.2.4.2 Mean Effective Pressure

According to Caton (2016), "the mean effective pressure is the average cylinder pressure that provides the equivalent work of the actual cycle" (p.15). This parameter is useful when

comparing two types of motors of different size as it gives a relative measure of the power for

the motor size. *mep* is calculated through the following expression (Caton, 2016):

$$mep = \frac{W}{V_d} \qquad (1)$$
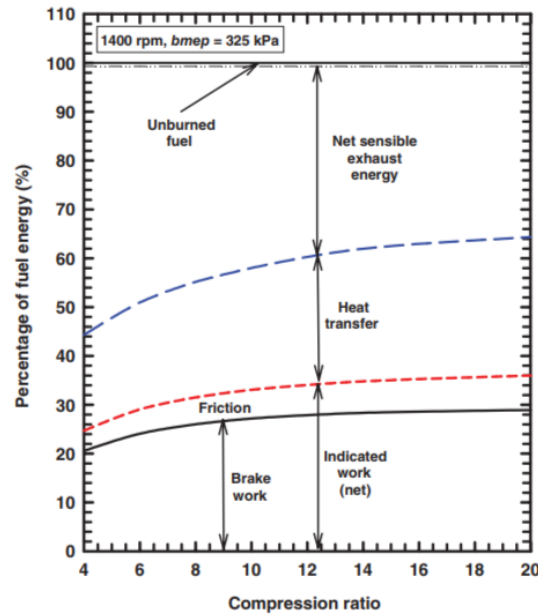
Figure 4. Distribution of the fuel energy as functions of compression ratio for a *bmep* of 325 kPa and 1400 rpm.

Source. Caton (2016)

Adicionalmente, la presión media efectiva puede nombrarse como presión media efectiva

el freno (*bmep*), se le asigna este nombre debido a que es la presión media efectiva calculada

usando la potencia al freno, la cual a su vez, es la potencia que es medida con un dynamometer

rotor en un test bed (Heywood, 1988)

2.2.4.4 Work

The work of a motor cycle is the area of the curve of a pressure-volume diagram as

shown in Equation 2. Where a positive work (output) and a negative work (input) or pumping

work is observed in Figure 5 (Caton, 2016).

$$W = \int p\, dV \quad (2)$$

The gross indicated work (W_{gross}) is the work associated with compression and expansion strokes, which is the work that the gases can deliver to the piston. On the other hand, the pumping work is that necessary to perform the intake and exhaust strokes, if this work is subtracted from the gross indicated work, the net indicate work ($W_{net\ ind}$) is obtained as shown in Equation 3 .
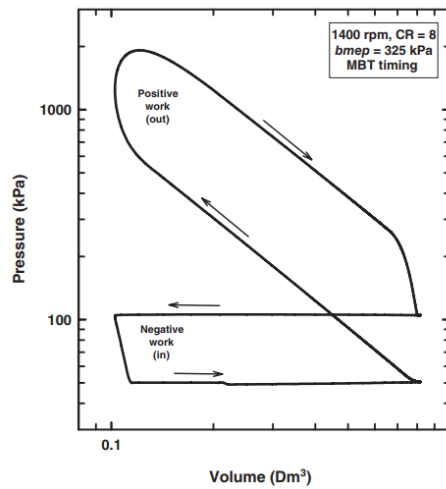
Figure 5. Cylinder pressure as a function of cylinder volume with the "work out" and the "work in". Source. Caton (2016).

Additionally, if the net indicate work is subtracted from the friction work (W_{frict}), which is the work lost by friction of components in the engine, the shaft work (W_{shaft}) is obtained as shown in Equation 4, also known as brake or delivered work (Caton, 2016).

$$W_{net\ ind} = W_{gross} - W_{pump} \quad (3)$$

$$W_{shaft} = W_{net\ ind} - W_{frict} \quad (4)$$

2.2.4.6 Specific fuel consumption

According to Colin, (quoted by Ferguson & Kirkpatrick, 2016), the specific fuel consumption is a comparative metric for the efficiency of converting the chemical energy of the fuel into work produced by the engine. Two types of specific consumptions are defined: brake (*bsfc*) and indicated (*isfc*), calculated by means affective pressure brake and indicated, respectively.

$$bsfc = \frac{\dot{m}_f}{\dot{W}_b}; \;\; isfc = \frac{m_f}{W_i} \qquad (5)$$

2.2.6 Combustion

2.2.6.1 Normal combustion

At the end of the compression period, a spark is generated between the sparking plug electrodes. This spark leads to a small flame nucleus that is propagated by the unburned mixture. Until the core reaches a scale the same size as the turbulence scale, the flame will not be enhanced by the turbulence. The first period comprises the initial laminar combustion and the transition period to a completely turbulent combustion, the "delay period", which is shown in the Figure 6 (Stone, 2012).
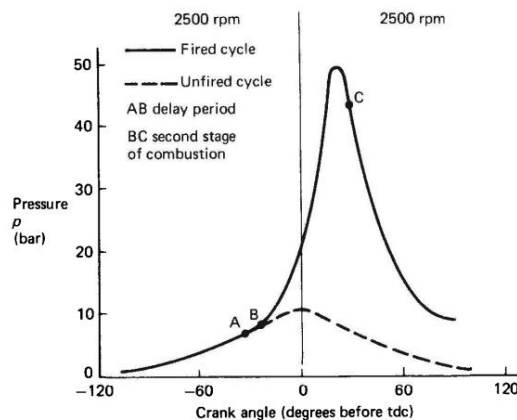
Figure 6. Hypothetical pressure diagram for a spark for a spark ignition engine. Source. Stone (2012).

The initial combustion period or delay period comprises between 5% and 10% of the fraction of burned mass and is mainly determined by the temperature, pressure and consumption of the mixture. Then, in the main combustion period, 5-95% or 10-90% of the mass is burned (Stone, 2012).

The final state of combustion the flame front is in greater contact with the walls of the chamber and the area of contact with the unburned mixture decreases, in this period the pressure of the cylinder begins to fall causing the unburned mixture to leave the holes (crevices), and some of the fuel absorbed by the oil is desabsorbed, this initiates its oxidation process but is usually not completed due to the opening time of the exhaust valve, which generates unburned hydrocarbon emissions (Stone, 2012).

2.2.6.2 Abnormal combustion

An abnormal combustion phenomenon is surface ignition caused by ignition of the mixture as a result of contact with hot surfaces, as well as the exhaust valve. Even if the engine has a cooling, mixing and ignition time the hot surfaces exist, mainly by build-up of combustion deposits or "coke" (Stone, 2012).

When surface ignition occurs before the flame arrives, pre-ignition occurs, which can cause self-ignition. Self-ignition occurs when a mixture of unburned gases is "trapped" between two flame fronts (normal and pre-ignition), this mass of unburned gases substantially increases their pressure and temperature causing a spontaneous ignition known as "knocking" (Stone, 2012).

The octane number represents the resistance of a fuel or an air-fuel mixture to be self-ignited, that is to say, to the presence of self-explosion in the engine, which is related to unwanted spontaneous combustion. Combustion is a process of radical reactions, so the speed of

combustion depends on the strength of the C-H bond, so the resistance to self-ignition varies

significantly with the size and structure of each hydrocarbon. Therefore, hydrocarbons with a

high self-ignition temperature have a higher resistance to self-ignition (Brunetti, 2012).

The higher the mix temperature, mix pressure and spark advance, the greater the

likelihood of self-ignition. On the other hand, if the mixture is slightly rich, (close to

stoichiometric), there is a greater probability of detonation and the greater the turbulence inside

the chamber, the lower the probability of self-igniting, since they reduce combustion time and

homogenize the mixture and temperature (Brunetti, 2012).

2.7 Vibe combustion model

In 1970 Vibe developed an expression considering the kinetics of reactions that relates

the amount of heat delivered to the total amount of heat, which is calculated with the mass of

fuel inside the cylinder and its lower heat capacity. (Merker, Schwarz, & Teichmann, 2012).

The Vibe function is used to approximate actual heat input values in engines. It is one of

the simplest models of combustion, this signals the amount of heat released with respect to the

angle of the crankshaft. It is represented by the following expressions (AVL, 2018):

$$\frac{dx}{d\alpha} = \frac{a}{\Delta\alpha_c} * (m + 1) * y^m \quad (7)$$

$$x = 1 - e^{-ay(m+1)} \quad (8)$$

$$dx = \frac{dQ}{Q} \quad (9)$$

$$y = \frac{\alpha - \alpha_0}{\Delta\alpha_c} \quad (10)$$

These parameters are mostly obtained using adjustments and statistical methods from

engine pressure curves obtained experimentally. On the other hand, useful graphs have also been

provided to estimate some of these parameters, such as the graph in the Figure 7, where the

duration of combustion is related to the parameter in the form "m". The shape parameter "m" indicates the mass burning characteristics. (AVL, 2018)

As for the start of combustion, it is determined according to the maximum pressure that the cylinder can withstand, fuel consumption and auto detonation in SI engines (AVL, 2018).

Parameter "a" defines whether the combustion is complete or not, that is, the parameter a refers to the efficiency of conversion of fuel into energy, for 99.9% its value is 6.9 decreasing significantly along with the decrease in the value of conversion efficiency as shown in Table 1 (Merker, Schwarz & Teichmann , 2009). The expression that allows the calculation of the value of "a" according to the conversion efficiency is shown in the Equation 11.

$$a = -\ln(1 - \eta_{conv,total}) \quad (11)$$
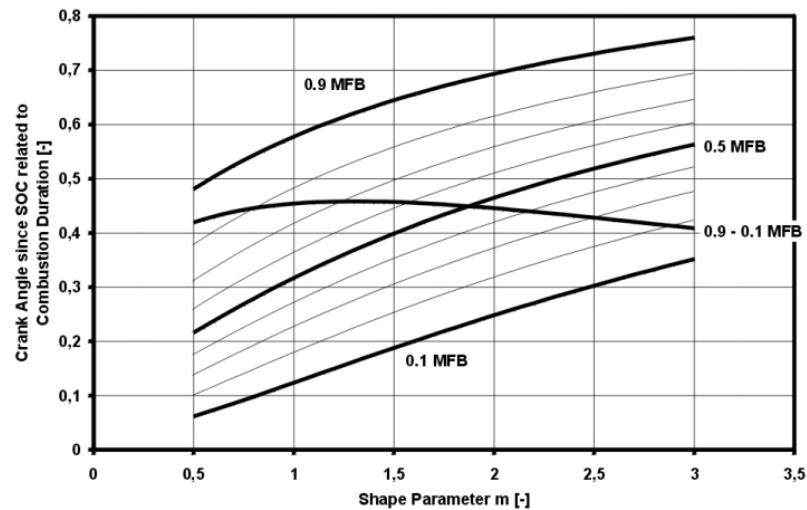
Figure 7.Crank Angle related to Combustion Duration. Source. AVL (2018)

Table 1

Parameter "a" of Vibe Function

$\eta_{conv,total}$	0.999	0.990	0.980	0.950
a	6.908	4.605	3.912	2.995

Source. Merker, Schwarz & Teichmann (2009).

2.7.2 Vibe function of two zones

In the two-zone Vibe model the combustion chamber is divided by two stop zones by a flame front, a first zone or "unburned zone" contains fresh air and unburned fuel, while the second zone or "burned zone" contains combustion products, fresh air and residual gas (Merker, Schwarz & Teichmann , 2009).

This model stands out in that it allows the calculation of NOx. The two zones are separated by the front of the flame, which could be a third zone, and since the chemical kinetic assumptions here are simple, no account is taken of the equilibrium equations in this third zone. . That is, energy and mass balances must be established for each burned zone and unburned zone separately.

Both zones have the same pressure, but different volumes, temperature, mass and λ. Both secondary oxidation and NOx formation occur in the flared gas zone, for which it is necessary to use reaction kinetics. As already mentioned above both zones are separated by the flame front which is assumed to be infinitely thin and without mass and it is in the flame front where primary oxidation occurs until the OHC components are in equilibrium (Merker, Schwarz & Teichmann , 2009).

Furthermore, it should be noted that the sum of the changes of the volumes of both zones must be equal to the change of the total volume within the cylinder, as well as the sum of the volumes of the zones must be equal to the volume of the total cylinder (AVL, 2018).

2.2.8 Stoichiometry

The stoichiometric quantity of an oxidant, in internal combustion engines: air, is the quantity necessary for the fuel to burn completely forming an ideal set of products. When there is a greater quantity of oxidant, it is said that the mixture is poor, and if on the contrary, there is

less quantity of oxidant with respect to stoichiometry, it is said that the mixture is rich (See Equation 14) (Turus, 2012).

The stoichiometric air-fuel ratio is represented as follows:

$$(A/F)_{stoic} = \left(\frac{m_{air}}{m_{fuel}}\right)_{stoic} \quad (12)$$

In order to classify fuel air mixtures into rich or poor in a general way (for all fuels) the equivalence ratio ϕ or λ is used. (Turus, 2012).

$$\phi = \lambda^{-1} = \frac{(A/F)_{stoic}}{(A/F)} \quad (13)$$

These equivalence ratios relate the stoichiometric air-fuel ratio of a fuel to the air-fuel ratio actually used, this parameter allows the control of internal combustion engine intake systems (Turus, 2012).

$$\begin{matrix} \phi < 1, \ \lambda > 1 & Fuel - lean \ mixture \\ \phi > 1, \ \lambda < 1 & Fuel - rich \ mixture \end{matrix} \quad (14)$$

2.2.9 The Arrhenius rate expression

In most reactions speed is dominated by collisions between atoms of two species that react to each other (second order), while others are dominated by rupture of links (first order). (Glassman, Yetter & Glumac, 2015) for a general second order reaction.

The interaction of the reagents of a reaction involves collisions between molecules of each reagents, but not all of these molecules, nor all collisions lead to the formation of reagents. According to Arrhenius, only molecules that possess a certain energy, to which is added the energy acquired in the collision, greater than an activation energy will react and lead to products. Arrhenius then postulated an expression for the constant speed of formation or destruction of chemical species (See Equation 15) (Glassman, Yetter & Glumac, 2015):

$$k = Ae^{(-E/RT)} \quad (15)$$

Where A is a pre-exponential kinetic factor, E is the Activation energy and $e^{(-E/RT)}$ the Boltzmann factor, which gives the fraction of all collisions that have a translational kinetic energy along the internuclear axis greater than E (Glassman, Yetter & Glumac, 2015).

2.2.10 Chemical equilibrium

The chemical equilibrium corresponds to an area of thermodynamics that represents physical-chemical characteristics of reaction systems, focusing on the quantities of related matter (Arshad, 2018).

When a fuel is burned at high temperatures, the combustion products obtained are not simply those determined by a general combustion reaction (Equation 16). During combustion, the main species (CO_2, H_2O, O_2 and N_2) are dissociated and form other secondary species (H_2, OH, CO, H, O, etc.), which are found at the end of combustion in different proportions according to temperature and pressure conditions (Turns, 2011)

$$CH_4 + 2O_2 \rightarrow CO_2 + 2H_2O \quad (16)$$
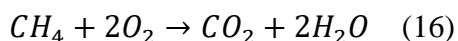
2.2.11 Chemical kinetics

Chemical kinetics is fundamental for the thermal study in engine cycles, for predicting the chemical delay of reactions and the improvement of the optimum spark point and for studying self-ignition (Arshad, 2018). It describes the composition and decomposition of chemical elements as a function of the time and speed at which each reaction occurs.

A chemical reaction can be directed forward (products) or backward (reagents), but it always seeks to reach equilibrium. The changes or direction in a macroscopic way will depend on the speed of each type of reaction (forward or backward), but although on this scale it is in equilibrium, on a microscopic level reactions may still be happening. Now, to determine the

speed of reactions must make use of chemical kinetics or reactions because it cannot be

determined only with "the balance". (Soustelle, 2011)

The Equation 17 determines the change in the concentration of a species, i.e., velocity

(Soustelle, 2011).

$$\frac{d[A_c]}{dt} = v_c\left(K_f[A_a]^{v_a}[A_b]^{v_b} - K_r[A_c]^{v_c}[A_d]^{v_d}\right) \quad (17)$$

The constants k are speed coefficients that are calculated experimentally and depend on

temperature (See Equation 18) (Soustelle, 2011).

$$k = AT^b exp\left[-\frac{E_A}{\tilde{R}T}\right] \quad (18)$$

If we suppose that the reaction is in equilibrium, the Equation 19 can be obtain for

determine an equilibrium constant (Soustelle, 2011).

$$\frac{K_f}{K_r} = \frac{[A_c]^{v_c}[A_d]^{v_d}}{[A_a]^{v_a}[A_b]^{v_b}} = K_c \quad (19)$$

This equilibrium constant in turn is related to the equilibrium constant defined in terms of

pressure according to the following equation, as it is also observed, these only depend on

temperature and not on the concentration of species, therefore, the expression can be used not

only for the state of equilibrium but in any state (See Equation 20) (Soustelle, 2011).

$$\frac{K_f}{K_r} = K_p \left(\frac{p^0}{\tilde{R}T}\right)^{\sum_i v_i} \quad (20)$$

The two major problems associated with kinetics are, first, the determination of the

reaction pathways that transform reactants into products, and second, the experimental

determination of the velocity constants of the different reactions involved (Soustelle, 2011).

2.2.12 Alcohols

Alcohols as fuels has been an alternative for certain countries with low oil resources or

with sources of material for their production. These have been used as additives to fossil fuels to

improve their octane number. In addition to the high octane number the alcohols have a high enthalpy of vaporization which allows to improve the volumetric efficiency but can cause starting problems. The disadvantage of the use of ethanol is the low energy density, approximately two thirds of that of oil and its miscibility with water (Stone, 2012).

There are different types of automotive alcohols, mainly those between 1 and 5 carbons (Brunetti, 2012):

- Methanol (CH_3OH)

- Ethanol (C_2H_5OH)

- Tert-butyl alcohol -TBA (C_4H_9OH)

- Acetone Butanol Ethanol Mix(ABE)

- Other alcohols such as iso-propanol, butane-1, iso-butanol, butanol-2, etc.

According to Brunetti (2012), compared to hydrocarbons, oxygenated fuels have a much higher flammability range, improving the cyclic dispersion of combustion in engines. Despite this advantage, they become easily flammable especially in very rich mixtures, becoming critical in terms of safety".

2.2.12.1 Ethanol

Ethanol of chemical formula C_2H_5OH (C_2H_6O) can be obtained from sugar, corn, beet, potato, etc., (10), is a biofuel used as a substitute for gasoline in spark ignition engines (National Petroleum Agency, 2019).

1st and 2nd generation ethanol can be produced, with 2nd generation plants being those that introduce cellulose pre-treatment and hydrolysis before starting fermentation. Brazil's National Petroleum Agency ANP (s.f.) states that using ethanol as a pure fuel or added to gasoline minimizes greenhouse gas emissions and energy dependence on oil.

There are currently two ways of using ethanol: anhydrous ethanol and hydrated ethanol, the first is blended with gasoline and the second can be used as finished fuel in Flex-fuel engines (National Petroleum Agency, 2019):

-Anhydrous ethanol, which is added to gasoline, contains a maximum content of 0.4% by volume of water (Brunetti, 2012).

- Hydrous ethanol is the one with the greatest amount of water and is used as a direct fuel in flex cars or alcohol. (Brunetti, 2012)

The octane number of ethanol may vary with respect to the percentage of water it contains, Figure 8, this variation is shown for methanol and ethanol.
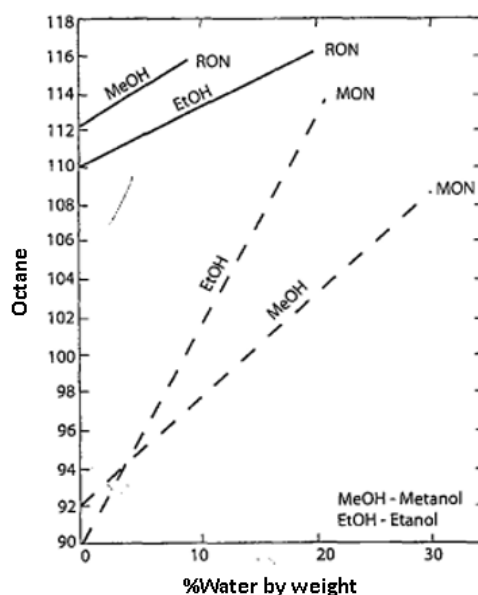
Figure 8. Variation of octane number with the presence of water. Source. Brunetti (2012)

On the other hand, hydrated ethanol should not be added to gasoline, since the presence of water can cause separation in two different phases, and as the density is higher, a mixture of more oxygenated water is concentrated in the bottom, which is problematic and unsuitable for engine operation. This occurs because hydrocarbons have low polarity, that is, their molecules

are symmetrical and without heteroatoms, making their electronic distribution homogeneous (Brunetti, 2012).

As for emissions, several studies have suggested that CO, HC and CO_2 emissions are reduced with the increase in ethanol, without showing decisive trends for NOx. But, despite the reduction of some emissions, it has been demonstrated that the higher ethanol content also leads to higher emissions of unburned ethanol, acetaldehyde and formaldehyde, these compounds being highly toxic and potentially carcinogenic, in addition to being precursors of ozone and peroxyacetyl nitrates.(Suarez, R., Clirotte, M., Arlitt, B., Nakatani, S., Hill, L., Winkler, K, … Astorga, C, 2012)

2.2.13 Exhaust gases

In an ideal combustion of a fuel the exhaust gases contain oxygen (O_2), nitrogen (N_2), carbon dioxide (CO_2) and steam (H_2O). However, for real combustion other gases are formed, such as: carbon monoxide (CO), unburned hydrocarbons (HC), hydrogen (H_2), nitrogen oxides (NOx) and solid particles. (Merker, Schwarz, & Teichmann, 2012).

The compounds formed by combustion, which are detrimental to human health, are called "pollutants". Although CO_2 contributes directly to the greenhouses effect, it is not considered a pollutant, since it is a product of the complete oxidation of a hydrocarbon, and the only way to reduce its emissions is by reducing consumption or altering the amount of carbon in a fuel (Merker, Schwarz, & Teichmann, 2012).

According to Merker, Schwarz, & Teichmann (2012) "In actuality however, combustion progresses under such air ratios at most until chemical equilibrium, i.e., always incompletely, even under ideal conditions" (p.193). This indicates that incomplete combustion gases will always be found even when sufficient oxygen is supplied. The formation of CO, HC and NOx

varies with the variation of the equivalent ratio λ, bearing in mind that the formation of CO and HC is favored by rich mixtures and the formation of NOx by the increase in temperature, as shown in Figure 9.
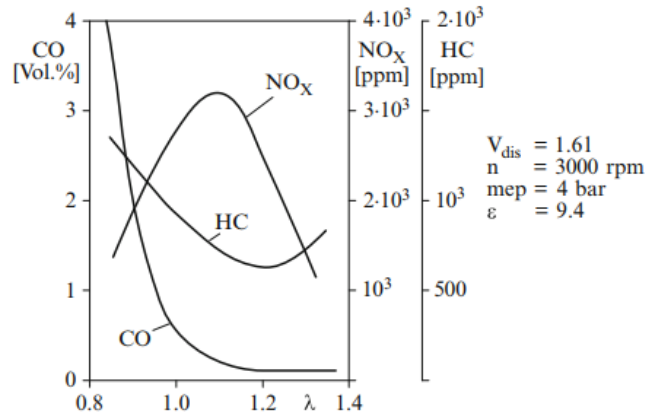
Figure 9. Pollutant formation as a function of the equivalence ratio. Source. Merker, Schwarz & Teichman (2012).

2.2.14 Emissions

2.2.14.1 Carbon Monoxide

The CO is an intermediate product of combustion. Theoretically for stoichiometric and poor mixtures CO is totally oxidized to CO_2, but for rich mixtures part of the CO formed comes out as exhaust gases (Merker, Schwarz, & Teichmann, 2012).

The reactions that dominate CO oxidation are shown in the Equation 21.

$$CO + OH \rightarrow CO_2 + H$$
$$CO + HO_2 \rightarrow CO_2 + OH \quad (21)$$
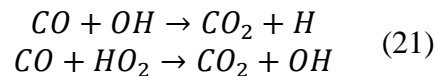
The first reaction is dominant in most conditions, which is dependent on the amount of OH radicals and its rate of reaction is slower than that of the reaction of these radicals with hydrocarbons. Due to this, it is necessary that all fuel and intermediate hydrocarbons are first oxidized for this reaction to occur. Additionally, the amount of CO decreases with the decrease of the equivalent ratio λ, due to the absence of O_2 (Merker, Schwarz, & Teichmann, 2012).

On the other hand, CO increases again for λ values greater than 1.4 due to low temperatures and incomplete combustion near the chamber wall. This demonstrates the dependence of CO oxidation on temperature (Merker, Schwarz, & Teichmann, 2012).

2.2.14.2 Carbon Dioxide

Carbon dioxide is a colorless and odorless gas, composed of a carbon atom and two oxygen, is part of the naturalization and is essential for life, it is not a toxic gas. As for engines, this gas is a product of the combustion processes of all fuels containing carbon, therefore, will always be present as a product of combustion.

The problem around carbon dioxide revolves around the excessive production of this, which increases the greenhouse effect, causing global warming. Much of the CO_2 production is attributed to the transport sector and the burning of fossil fuels. In 2008, 43% of CO_2 emissions from fuel combustion were produced from coal, 37% from oil and 20% from gas. (IEA STATISTICS)

According to NASA (2019), carbon dioxide (CO_2) is an important heat-trapping gas (greenhouse), which is released through human activities such as deforestation and the burning of fossil fuels, as well as natural processes such as respiration and volcanic eruptions. According to CO_2 observations made, in the 1950s, the annual rate of increase in CO_2 concentration was approximately 0.73 ppm per year, and from 2005 to 2014 the increase was approximately 2.11 ppm per year. Statistics also show that in the last 400,000 years, the concentration of CO_2 ranged from 200 ppm to 280 ppm (NASA, 2019).

2.2.14.3 Unburned Hydrocarbons

HC are formed in areas without combustion or with partial combustion, they are composed of several fuel components. Emissions of this type are regulated in a general way, i.e.,

the sum of all HC components is regulated, and their composition is not taken into account (Merker, Schwarz, & Teichmann, 2012).

To determine the sources of HC in an internal combustion engine it is necessary to take into account the type of engine (SI or CI), the type of injection and the characteristics of the mixture (Merker, Schwarz, & Teichmann, 2012).

In conventional SI engines, the most important sources of HC emissions are: flame extinguishing within crevices and excessively low flame speed; adsorption and desorption of the fuel in the oil film on the cylinder liner and in deposits on the combustion chamber walls; leakage of the fuel-air mixture through the closed outlet valve. Although certain HC formation routes are known, an accurate quantitative prediction of HC emissions in SI engines is not yet practical (Merker, Schwarz, & Teichmann, 2012).

2.2.14.4 Nitrogen Oxides

NO formation has been described mainly by the Zeldovich mechanism (Equation 23) which describes three reactions to NO formation. The first two equations for lean mixtures and the last equation should also be taken into account for rich mixtures and stoichiometric. Some of the most important factors influencing the formation of NO are temperature, the fuel air ratio. On the other hand, temperature and fuel air ratio cannot be treated as mutually independent and in adiabatic conditions when the fuel air ratio is close to or between 1 and 1.1 maximum NO production is reached (2). It has been identified that NO is produced by four mechanisms (Arshad, 2018):

- Thermal mechanism.

- Sudden, prompt or Fenimore mechanism.

- Mechanism due to N_2O intermediate.

- Mechanism due to the nitrogen content of the fuel (NO-fuel).

The first mechanism, NO thermal is formed in the post flame zone to more than 2000 K. The first mechanism, NO thermal is formed in the post flame zone to more than 2000 K. (Arshad, 2018). Multiple studies have defined that it is the thermal NO that has greater importance in the formation of NO (Hernandez, Escobar, García, Gómez, Higareda and Olivares, 2019).

The second mechanism is the prompt or Fenimore shown in the Equation 22, can occur in the front of the flame, due to the higher concentration of radicals O and OH. Species involving hydrocarbon compounds react with N_2 to form amines that then produce NO, this depends only slightly on temperature (Arshad, 2018).

$$
\begin{aligned}
O + N_2 &\Leftrightarrow NO + N \quad (k_1) \\
N + O_2 &\Leftrightarrow NO + O \quad (k_2) \qquad (22) \\
N + OH &\Leftrightarrow NO + H \quad (k_3)
\end{aligned}
$$
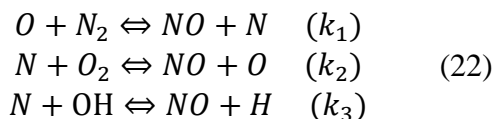
There are three ways in which thermal NOx is formed in the post-flame zone over 2000 K and one NO Prompt in the rich radical flame zone with temperatures of 2800 K and the NO fuel, which is oxidized from the N containing the fuel. Multiple studies have defined that it is the thermal NO that has greater importance, the second a secondary and the third can be ignored.

2.2.13.5 Carbonyl compounds

According to Merker, Schwarz, & Teichmann (2012) "Carbonyl compounds can harm the human organism by affecting it directly or via by-products formed in the atmosphere. They contribute, for example, towards the formation of ozone close to the ground (photochemical smog) in concert with nitrogen oxide"(p.200). The Figure 10 shows the carbonyl compounds detected.
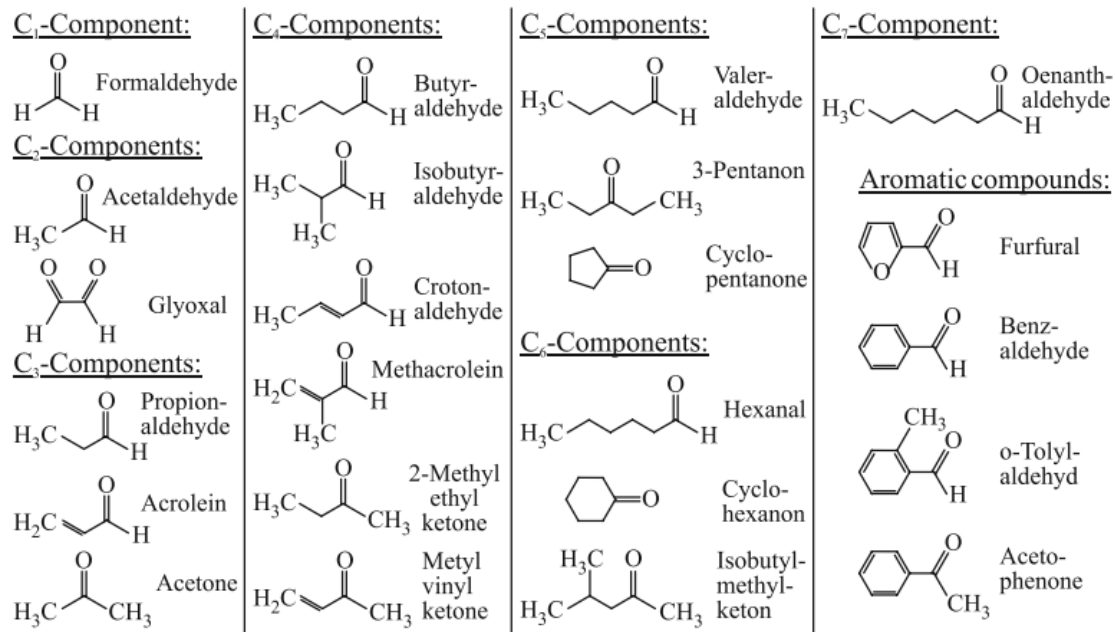
Figure 10. Detectable carbonyl compounds. Source. Merker, Schwarz, & Teichmann (2012)

2.2.15 Emissions of aldehydes in the combustion of ethanol

"Ethanol has a reaction lifetime of several days and the major products of its OH-initiated degradation is acetaldehyde. The OH-initiated degradation of acetaldehyde gives upon further reaction with NO_2 peroxy-acetyl nitrate (PAN). Other reactions of acetaldehyde give mainly formaldehyde and CO_2. All of acetaldehyde, formaldehyde and PAN have negative effects on human health (Fridell, Eugensson, Moldanova, Tang, Sjoberg & Forsberg, 2010).

Since the combustion of ethanol produces some different gases, it is necessary to know their emissions and the risks that their emissions have on health and the environment. In spite of this, since the aldehydes are unregulated pollutants, there is not much data on their emissions.

. Ethanol and its gasoline blends have received great attention as an alternative fuel due to the reduction of emissions and greenhouse gases and because it is produced from renewable sources. The problem with ethanol from the point of view of air quality is that during combustion aldehydes are produced, that having less energy than gasoline and diesel makes it necessary to

burn more and that in cold start conditions alcohols crack and form aldehydes. (Formaldehyde and acetaldehyde measurements in urban atmosphere). Impacted by the use of ethanol biofuel: Metropolitan Area of Sao Paulo (MASP, 2012-2013)

Only the gaseous aldehydes are considered pollutants of the atmosphere, these are formaldehyde (CH_2O) and acetaldehyde (C_2H_4O) and their emissions are high in the combustion of ethanol unlike gasoline because of the presence of the hydroxyl (OH) functional group (Barros & Sodré, 2016).

It can be considered that acetaldehyde is mainly formed in the intermediate phase of the post-flame oxidation of unburned ethanol, both in the combustion chamber and in the exhaust pipe, according to the reaction of Equation 23: (Barros & Sodré, 2016).

$$CH_3CH_2OH + O \rightarrow CH_3CHO + H_2O \quad (23)$$
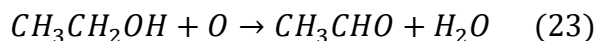
Another way of producing both acetaldehyde and formaldehyde is the oxidation of methane and ethane, respectively. Methane and ethane remain unburned gases due to the interruption of combustion by low temperatures or low oxygen concentrations (Barros & Sodré, 2016).

Equation 24 shows the formation of formaldehyde from methane and Equation 25 the formation of acetaldehyde from ethane (Barros & Sodré, 2016).

$$CH_4 + O_2 \rightarrow CH_2O + H_2O \quad (24)$$

$$C_2H_6 + O_2 \rightarrow C_2H_4O + H_2O \quad (25)$$
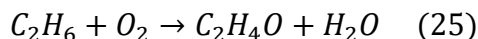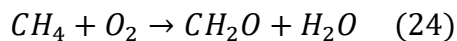
Moreover, "the aldehydes formed in the intermediate stages of the combustion process are immediately consumed by the flame front due to the high temperature attained in the combustion chamber" (Barros & Sodré, 2016).

Formaldehyde is the simplest compound in the aldehyde group and Fridell, Eugensson, Moldanova, Tang, Sjoberg & Forsberg (2010) describes that in 2006 IARC's Monograph 88 reported that there is enough information to conclude that formaldehyde is carcinogenic, due to evidence of high concentrations of nasopharyngeal cancer in industrial settings. However, this has not been confirmed by more recent research. He also cites OEHHA (1999), who uses a lifetime risk for cancer of 0.000006 per μg/m3 for formaldehyde, and US EPA (1999) a lifetime risk of 0.000013 per μg/m3 (Fridell, Eugensson, Moldanova, Tang, Sjoberg & Forsberg, 2010).

The aldehyde formation reactions start in the cylinder and propagate through the exhaust pipe. Various studies have led to conclude the risk of exposure to high concentrations of aldehydes. An increase in nasal tumors in rats and laryngeal tumors in hamsters was observed after inhalation of high concentrations of acetaldehyde. Moreover, "a few epidemiological studies of occupational exposure found associations but with a complex mixture of chemical and have not been used in the cancer risk assessment for acetaldehyde". This gas is considered as a human carcinogen potential by the US EPA (1999), IARC and OEHHA (Fridell, Eugensson, Moldanova, Tang, Sjoberg & Forsberg, 2010).

In more detail, Marinov (1999) developed a detailed chemical kinetic model for ethanol oxidation. In this it describes the multiple chemical reactions that happen during the combustion of ethanol together with the parameters of the Arrhenius equation, this model consists of 369 reactions and allows to know diverse sources from which acetaldehyde and formaldehyde are produced, as well as the reactions of these also.

2.2.16 Computer simulations

According to Hermann (1990), the computer simulation approach allows obtaining information on the behavior of complex systems, also providing standards that can be compared

with experimental models, thus allowing the evaluation of the validation of a model. Additionally, computer simulation can calculate and determine quantities that may be impossible or difficult to measure experimentally. Similarly, Caton (2016) comments that the simulation of the ICE was very basic and limited to computational resources and lack of knowledge, but over time, sophisticated tools used by various industries have been developed.

Therefore, it is possible to simulate the operation and operation of an ICE using computational tools, According to Merker, Schwarz & Teichman (2009), "The prerequisite for simulation are mechanical, thermodynamic, and chemical models for the description of technical processes, whereby the understanding of thermodynamics and of chemical reaction kinetics are an essential requirement for the modeling of Internal Combustion Engine processes." (p. 3) Figure 11 shows the fields of knowledge involved in a simulation process of an ICE.
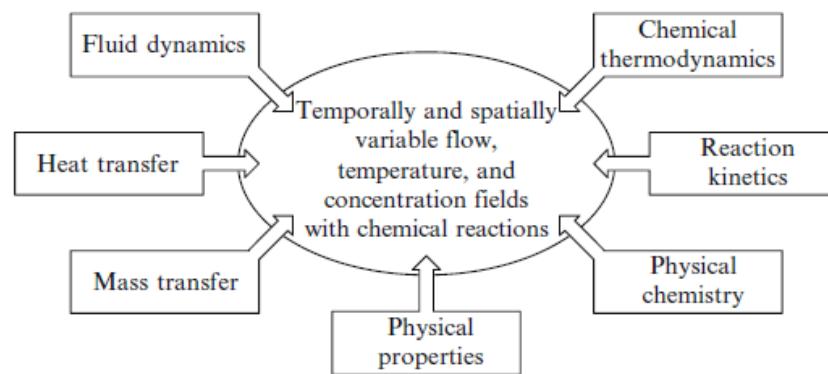
*Figure 11.*Area of knowledge important for process simulation. Source. Merker, Schwarz & Teichman (2009)

The first step is the construction of the model describing the technical processes. It is recommended that the global model be fragmented into partial processes. Additionally, models must meet certain requirements: The model must be formally correct, must describe reality as exactly as possible and The cost necessary for the solution of the model with respect to the

calculation time must be justifiable in the context of the setting of the task (Merker, Schwarz & Teichman, 2009).

2.2.16.1 Thermodynamic engine cycle simulations.

According to Caton (2016), one of the first thermodynamic cycle simulations was performed by Patterson and Van Wylen in 1960, which was a simulation for a spark-ignition engine that includes unburned and burned zones, progressive combustion, heat transfer, and flame propagation for uniform (homogeneous) charge engines. For the same year, McAulay and Krieger and Borman reported a thermodynamic simulation of a CI engine where the diesel combustion process was not fully described. Later in 1979 Heywood described a simulation using three zones for the combustion process. Subsequently, the development of the simulation was growing, the prediction of nitrogen oxide was improved and the importance of multiple zones in combustion was shown, as well as a transitory operation by Rakopolpulas and Giakoumis.

2.2.16.2 Quasi-dimensional thermodynamic engine cycle simulation.

These types of simulations do not have a spatial context, by using the geometric structure of the combustion chamber and using a flame propagation velocity and geometry, the flame may be identified and assigned a spatial location. These types of models assume a velocity of the laminar flame or may use a turbulent entrainment sub-model with a laminar burning process based on a characteristic length scale. The quasi-dimensional engine cycle simulation successfully predicts engine parameters (Caton, 2016).

2.2.16.3 Multi-dimensional simulations

These types of simulations have been developed in parallel with thermodynamic simulations, these are based on a set of partial differential conservation equations. He focuses his analysis on the dynamics of computational fluids, in addition to taking into account models of turdability, chemical reactions, heat transfer, fuels and boundary layer processes. Being a 3-dimensional model, the development of this is more complex. (Caton, 2016).

Each of the simulation categories has a field of action and its use depends on the results that want to be obtained and analyzed. According to Merker, Schwarz & Teichmann (2009),

"Quasi-dimensional models differ from zero-dimensional models, which simplify the combustion chamber as being ideally mixed at every point in time and are based on empirical approaches for the combustion rate. On the other hand, phenomenological combustion models differ from the CFD codes, in that we consciously do without an explicit solution of the turbulent three-dimensional flow field, which reduces the calculation time considerably. The calculation time for one engine revolution lies in the region of seconds in phenomenological models, while in CFD codes it takes hours or days." (P. 415).

2.2.16.4 Simulation software

As for the thermodynamic / quasi-dimensional simulations, the following software can be found:

Table 2

Simulation software 0-D and 1-D models

AV L Boost	AVL BOOST™ is a fully integrated IC engine simulation software. It delivers advanced models enabling accurate prediction of engine performance, tailpipe emissions and acoustics. (AVL, 2019)
GT-Power	GT-POWER is used to predict engine performance quantities such as power, torque, airflow, volumetric efficiency, fuel consumption, turbocharger

performance and matching, and pumping losses, etc. (GT- Power, 2019)

| Virtual Engine | It has two versions, both for two- and four-stroke engines (Virtualengine, s.f) |
| Wave | WAVE is a state-of-the-art 1D gas dynamics simulation tool. It enables performance and acoustic analyses to be performed for virtually any intake, combustion and exhaust system configuration (s.f.). |

Source. AVL, 2019; GT-Power, 2019; Virtualengine, s.f.; Ceveny & Gravante, s.f.

On the other hand, some software for multi-dimensional simulations and CDF are:

Table 3
Simulation software 3-D models and CFD

AVL FIRE	It simulates the prediction of fuel aerosols, ignition, combustion and engine emissions, as well as the adaptation of the components of exhaust gas after-treatment systems, but also the modeling of electrochemistry and thermal behavior of batteries and fuel cells. (AVL FIRE, 2019)
CFX (ANSYS, Inc.)	CFX is recognized for its outstanding accuracy, robustness and speed when simulating turbo machinery, such as pumps, fans, compressors and gas and hydraulic turbines (ANSYS, 2019)
FLUENT (ANSYS, Inc.)	Fluent software contains the broad, physical modeling capabilities needed to model flow, turbulence, heat transfer and reactions for industrial applications. These range from air flow over an aircraft wing to combustion in a furnace, etc. (ANSYS, 2019)
OpenFOAM	It is a free and open source CFD software, simulates from complex fluid flows involving chemical reactions, turbulence and heat transfer, to acoustics, solid mechanics and electromagnetism (OpenFOAM, 2019)
VECTIS	VECTIS is a fast and accurate C simulation tool to facilitate vehicle and engine development. It solves the 3D form of the Navier-Stokes equations using the finite volume method. It simulates the transport of mass, momentum, energy and other physical phenomena (Gravante, 2019)

Source. AVL, 2019; ANSYS, 2019; OpenFOAM, 2019 y Gravante, 2019.

2.2.17 History of ethanol

The sugar industry (ethanol producer) represents in Brazil a strong economic weight in generating employment, wealth and foreign exchange (Girardi, 2019).

Before 1970 ethanol was only a by-product of sugar cane, but from the creation of the National Alcohol Program (Proálcool) and the first oil crisis its production increased as far as Brazil (Schwingel, Viera, De Oliveira, Ziani, Coronel, 2018).

Later, in 1980, the price of oil fell again, subtracting the world's attention on biofuels, but by that time Brazil and the United States had their interest in the independence of oil and the environment, being the first countries to focus their attention on oxygenated fuels, unlike countries such as Japan and the European Union. The introduction of the electronic injection and the catalyst for the decade of 1990 reduced considerably the emissions of the transport sector and motivated to the use of the oxygenated fuels. On the other hand, since the 1980s scientists in the world warned about global warming, fossil fuels being one of the main causes, this concern focusing for example on the increase from 280 PPM before the Industrial Revolution to 380 by 2007 (Santos, 2019).

Based on these and more evidences, the 1992 Rio de Janeiro Climate Convention and the 1997 Kyoto Protocole were established, making the issue of environmental pollution official, establishing responsibilities for the signatory nations of the United Nations Framework Convention on Climate Change (Santos, 2019).

For the last few years, instability in oil prices and politics, linked to high pollution rates have given way to biofuels which have the responsibility of both reducing greenhouse gas emissions and replacing oil in terms of fuels.

The PROÁLCOOL program began in 1975, seeking to confront the oil crisis through the obligatory inclusion of ethanol in gasoline between 4% and 10%. Over the years, ethanol production has fallen and increased according to the market and above all the price of oil (Girardi, 2019).

The PROÁLCOOL program began in 1975, seeking to confront the oil crisis through the obligatory inclusion of ethanol in gasoline between 4% and 10%. Over the years, ethanol production has fallen and increased according to the market and, above all, the price of oil. (Girardi, 2019).

According to Bittencourt, Fontes, Campos (2012) Proálcool had as its objective the substitution of fuels derived from petroleum, mainly gasoline, through the increase of agro-energetic crops and the increase of industrial capacity in the country (Bittencourt, Olivera, Carvalho, 2012).

The first U.S. efforts to use ethanol date back to 1990, seeking to reduce dependence on fossil fuels. This led to the 1992 energy policy act, which established a mixture of 85% ethanol and 15% gasoline as an alternative fuel for transportation, and the Clean Air Amendment, which established that in certain urban areas car fuel must be oxygenated (Mitsutani, 2010).

For its part, the U.S. in 2005 focused great efforts and investment in the cultivation of corn for the manufacture of ethanol, becoming at present the largest producer, consumer and exporter of ethanol in the world despite having only an addition of 10% ethanol to gasoline to 27.5% of Brazil. "The United States and Brazil export on average between 5% and 10% of ethanol production and in 2014 represented 56.8% and 24.6% of world fuel production, respectively" (Girardi, 2019, p. 6).

According to the Renewable Energy Policy Network for the 21st Century (REN21), Brazil, USA and the EU are both the largest ethanol producers in the world with 85% of total annual production, as well as the largest consumers of it (Chawla, Lins, McCrone, Musolino, Riahi, Sawin, Sims,... & Sverrisson, 2014).

As can be seen in Figure 12, by 2016, the United States, Brazil, Holland and France accounted for 59.76% of world ethanol exports. Likewise, it is observed a growth of Brazil's participation in ethanol exports since 2003, which may be due to the intrinsic nature of the country's ethanol exports.
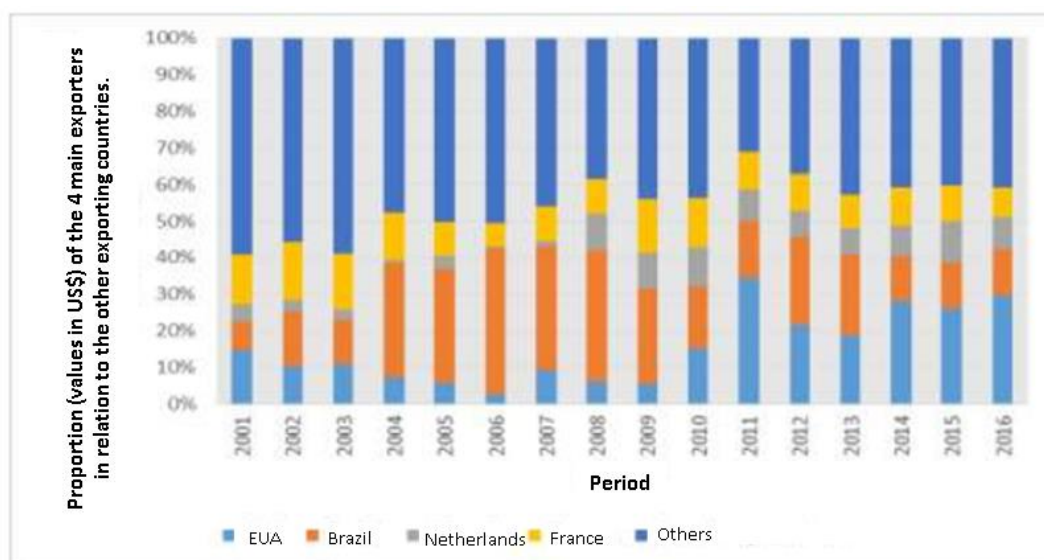
Figure 12. Proportion of 4 major exporters in relation to others exporting countries. Source. UN COMTRADE (2017)

The following are some of the advantages of using carburant alcohol as an additive to gasoline presented by Cardona C.: (Cardona, 2009)

- Reduction of carbon monoxide emissions.

- Less dependence on oil and/or gasoline imports.

- It favors the use of raw materials and renewable resources of the country as well as a large amount of ligo-cellulosic residues with potential for transformation into ethyl alcohol.

- Promotion of employment in depressed rural areas and benefits for the countryside.

It also has some disadvantages of its use:

- More expensive production than obtaining gasoline from petroleum.

- The vapor pressure of gasoline-ethanol blends is higher, so its volatility is greater, contributing to the formation of ozone and smog.

 - Formation of two phases due to the water contained in the gasoline.

- Possibility of corrosion in the engine elements due to the water content in the ethanol.

- Dependence of the sugar sector and indirectly on sugar prices.

- Possible increase in food prices manufactured from the same raw materials as ethanol.

- Increased emission of toxic compounds such as aldehydes compared to gasoline.

2.2.18 Ethanol in Colombia

The Colombian Federation of Biofuels announced the national demand for Ethanol during the last year in Colombia, observing variations, being the month of June 2019 where it was least consumed as shown in Figure 13 (Ministry of Mines and Energy, 2019).
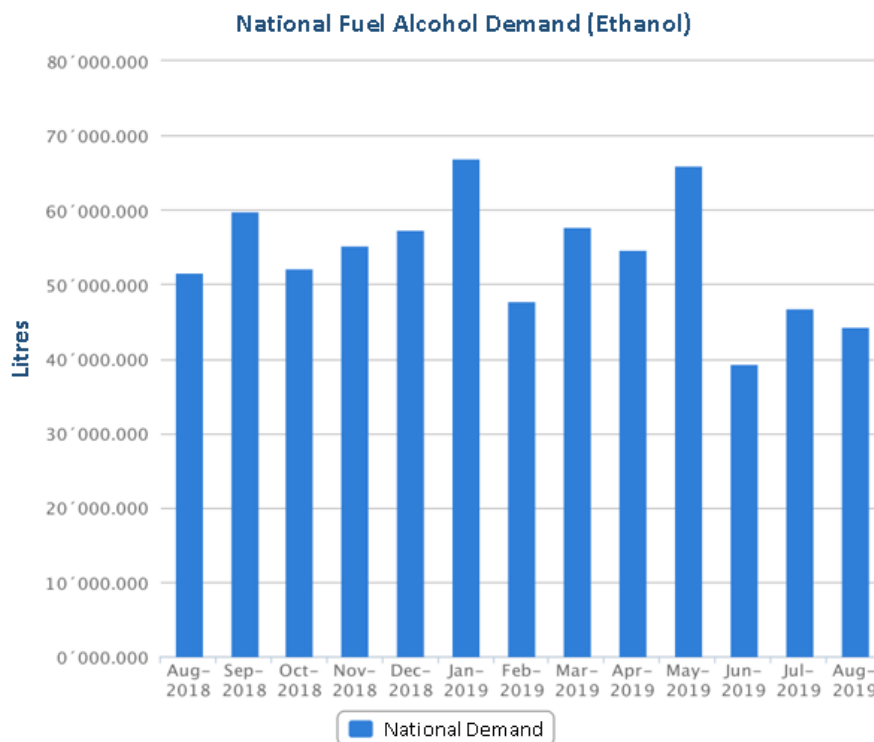
Figure 13. National fuel alcohol demand in Colombia. Source. Ministry of Mines and Energy (2019)

Since 2001, Colombia promoted the use and production of biofuels, starting with Law 693 of 2001, which promoted the use of carburant alcohol as an additive to gasoline, following with Law 939 of 2004, which encouraged the use of biodiesel. (Congress of the Republic of Colombia, 2019) Within Law 693 different principles for the use of biofuels were enunciated, which are according to Serrato and Lesmes (2016):

- Environmental sustainability

- Improved fuel quality

 - Agro-industrial development

- Generation of employment

- Agricultural Development

- Energy Supply

In August 2018, Semana magazine presents a brief description of the use of ethanol in Colombia as a biofuel, which at the beginning was 8%, rising to 10% from 2018, being even lower compared to other countries such as Brazil and the United States. This low percentage is still due to the limitations of national agricultural and industrial production, despite having seven bioethanol distilleries with 30.000 barrels produced daily. Additionally, in 2014 ethanol imports were authorized when the national supply was not sufficient, but by 2017 free imports were authorized with the argument of not giving rise to shortages, bringing discontent of national producers, which claim to be at a disadvantage against such imports, generating a fall in national production (Semana, 2018).

More recently, in February 2019, the Colombian Association of Motor Vehicles (Andemos) proposed to sell voluntary blends of biofuels in the country. In a document addressed to the president of the republic, it is recommended to continue offering mandatory mixtures of 10% ethanol, in order not to affect the vehicle fleet of Colombia, which is not established to work with biofuels and since this is the maximum proportion recommended by the International Organization of Manufacturers of Motor Vehicles (OICA). The recommendation of voluntary mixtures aims to promote and introduce new technologies that adapt to the new requirements of mixtures. Among others, one recommendation that stands out is to seek to implement a program of assurance and quality control of biofuels, since these are more prone to degrade in the supply chain (El Nuevo Siglo, 2019).

In order to develop the ethanol market in Colombia, different measures must be implemented that are supported by the national government, including the introduction of Flex automobiles, since these allow higher ethanol-gasoline blends, justified by their social, environmental and energy independence content.

2.2.19 Boost Theory

2.2.19.1 General Species Transport

General Species Transport is a model for the calculation of the Transport the composition of the gas by means an arbitrary number of species that is defined directly by the user.

Seven species should be defined as a minimum, such as: Fuel, O_2, N_2, CO_2, H_2O, CO, H_2. For each species a conservation equation (mass fraction) is solved in each of the elements of the model.

Species are assumed to be ideal gases, the single species standard state thermodynamic are calculated by polynomial fits (NASA polynomials).

Specific heat at constant pressure is shown in the Equation 26.

$$\frac{Cp_k}{R} = \sum_{m=1}^{M} a_{mk} T^{(m-1)} \quad (26)$$

From these, the following are calculated: the standard state enthalpy and the standard state entropy (See Equations 27, 28, 29 and 30)

$$H_K = \int_0^T Cp_k \, dT \quad (27)$$

$$\frac{H_k}{RT} = \sum_{m=1}^{M} \frac{a_{mk} T^{(m-1)}}{m} + \frac{a_{M+1,k}}{T} \quad (28)$$

$$S_k = \int_0^T \frac{Cp_k}{T} \, dT \quad (29)$$

$$\frac{S_k}{R} = a_{1k} \ln T + \sum_{m=2}^{M} \frac{a_{mk} T^{(m-1)}}{m-1} + a_{m+2,k} \quad (30)$$

For ideal gas mixtures, BOOST takes the same approach presented by Heywood, where the composition of an ideal gas mixture is expressed in terms of the partial pressure, parts by volume, mass fraction and mole fraction.

Mass and molar fraction (See Equation 31).

$$\frac{p_i}{p} = \frac{V_i}{V} = x_i \frac{M}{M_i} = \tilde{x}_i \quad (31)$$

Internal energy, enthalpy and entropy (See Equation 32)

$$u = \sum_i x_i u_i \qquad h = \sum_i x_i h_i \qquad s = \sum_i x_i s_i \qquad (32)$$

Molecular weight (See Equation 33)

$$M = \frac{1}{n} \sum_i n_i M_i = \sum_i \tilde{x}_i M_i \quad (33)$$

2.2.19.2 Cylinder

The thermodynamic state within the cylinder is calculated by applying the first law of thermodynamics, while the variation in mass is calculated by a mass balance. Equation 34 and 35 shown the first law and the mass balance:

$$\frac{d(m_c \cdot u)}{d\propto} = -p_c \cdot \frac{dV}{d\propto} + \frac{dQ_F}{d\propto} - \sum \frac{dQ_w}{d\propto} - h_{BB} \cdot \frac{dm_{BB}}{d\propto} + \sum \frac{dm_i}{d\propto} \cdot h_i - \sum \frac{dm_e}{d\propto} \cdot h - q_{ev} \cdot f$$

$$\cdot \frac{dm_e}{dt} \quad (34)$$

$$\frac{d_{mc}}{d\propto} = \sum \frac{dm_i}{d\propto} - \sum \frac{dm_e}{d\propto} - \frac{dm_{BB}}{d\propto} + \frac{dm_{ev}}{dt} \quad (35)$$

The mass flows entering or leaving through the ports are calculated with the equation isentropic orifice flow (Equation 36) under consideration of the flow efficiencies of the ports determined on the steady state flow test rig.

$$\frac{d_m}{dt} = A_{eff} \cdot p_{o1} \cdot \sqrt{\frac{2}{R_o \cdot T_{o1}}} \cdot \psi \quad (36)$$

$$\psi = \sqrt{\frac{k}{k-1} \cdot \left[\left(\frac{p_2}{p_{o1}} \right)^{\frac{2}{k}} - \left(\frac{p_2}{p_{o1}} \right)^{\frac{k+1}{k}} \right]} \quad (37)$$

$$A_{cff} = \mu\sigma \cdot \frac{d_{vi}^2 \cdot \pi}{4} \quad (38)$$

2.2.19.3 Scavenging model

"A perfect mixing model is usually used for four-stroke engines. This means that the composition of the exhaust gases is the mean composition of the gases in the cylinder, and also that the energy content of the exhaust gases is equivalent to the mean energy content of the gases in the cylinder" (AVL,2018). In this case the change of the air purity over crank angle can be calculated from Equation 39:

$$\frac{dR}{d\alpha} = \frac{1}{m_c} \cdot (1 - R) \cdot \frac{dm_i}{d\alpha} \quad (39)$$

2.2.19.4 Piston Motion

The movement of the piston as a function of the angle of the crank, taking a standard crank train is described with Equation 40 based on the geometry shown in Figure 14.
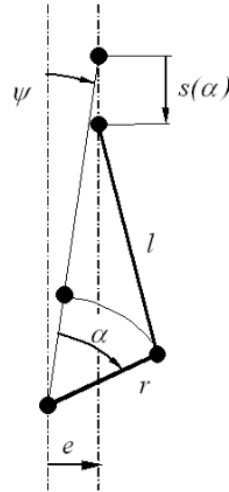
Figure 14. Standard Crank Train. Source. AVL (2018)

$$s = (r + l) \cdot \cos\psi - r \cdot cos(\psi + \propto) - l \cdot \sqrt{1 - \left(\frac{r}{l} \cdot sin(\psi + \propto) - \frac{e}{l}\right)^2} \quad (40)$$

$$\psi = \arcsin\left(\frac{e}{r + l}\right) \quad (41)$$

2.2.19.5 Scaling Factor

This factor is used as a way that the total effective flow area of all considered valves is obtained (See Equations 42 and 43). This modeling is preferred as it requires fewer elements and is therefore less complicated and more efficient.

$$A_{eff} = f_{sc} \cdot \alpha \cdot \frac{d_{pi}^2 \cdot \pi}{4} \quad (42)$$

$$f_{sc} = \frac{n_v \cdot d_{vi}^2}{d_{pi^2}} \quad (43)$$

2.2.19.6 Heat Transfer

For heat transfer the cylinder head, the piston and the cylinder liner, the following

equation is used the Equation 44 and the Equation 45 shows the liner temperature.

$$Q_{wi} = A_i \cdot \alpha_w \cdot (T_c - T_{wi}) \quad (44)$$

$$T_L = T_{L,TDC} \cdot \frac{1 - e^{-c \cdot x}}{x \cdot c} \quad (45)$$

$$c = \ln\left(\frac{T_{L,TDC}}{T_{L,BDC}}\right) \quad (46)$$

For the calculation of the heat transfer coefficient, the Woschni 1978 model is used. This

model is summarized in the Equations 47 and 48.

$$\alpha_w = 130 \cdot D^{-0.2} \cdot p_c^{-0.8} \cdot T_c^{-0.53} \cdot \left\{ c_1 \cdot c_m + c_2 \frac{V_D T_{c,1}}{p_{c,1} V_{c,1}} (p_c - p_{c,o}) \right\}^{0.8} \quad (47)$$

Where c_1=2.28+0.308c_u/c_m and c_2=0.00324 for DI engines.

In the process of gas exchange it is necessary to consider heat transfer due to the high

heat transfer coefficients and temperature in the region of the valves and valve seats. For this, a

modified heat transfer model Zapf. This model is show in the Equations 48, 49 and 50.

$$T_d = (T_u - T_w) \cdot e^{\left(-A_w \frac{\alpha_p}{\dot{m} \cdot C_p}\right)} + T_w \quad (48)$$

The heat transfer coefficient, α_p, depends on the direction of the flow (in or out of the

cylinder) (See Equations 49 and 50)

$$\alpha_p = [C_4 + C_3 + T_u - C_6 \cdot T_u^2] \cdot T_u^{0.44} \cdot \dot{m}^{0.5} \cdot d_{vi}^{-1.5} \cdot \left[1 - 0.797 \cdot \frac{h_v}{d_{vi}}\right] \quad (49)$$

$$\alpha_p = [C_7 + C_8 + T_u - C_9 \cdot T_u^2] \cdot T_u^{0.33} \cdot \dot{m}^{0.68} \cdot d_{vi}^{-1.68} \cdot \left[1 - 0.765 \cdot \frac{h_v}{d_{vi}}\right] \quad (50)$$

The constants used in the Equations 49 and 50 are contains in the Table 4.

Table 4

Constants used in the formulation of the Woschni heat transfer model

Exhaust Valve		Intake Valve	
C_4	1.2809	C_7	1.5132
C_5	7.0451×10^{-4}	C_8	7.1625×10^{-4}
C_6	4.8035×10^{-7}	C_9	5.3719×10^{-7}

Source. AVL (2018).

2.2.19.7 NOx Formation Model

The NOx formation model implemented in BOOST™ is based on Pattas and Haefner.

The following 6 reactions (based on Zeldovich mechanism) are taken into account:

Table 5

Reactions of the NOx formation mechanism

R1	$\mathbf{N_2 + O = NO + N}$
R2	$O_2 + N = NO + O$
R3	$N + OH = NO + H$
R4	$N_2O + O = NO + NO$
R5	$O_2 + N_2 = N_2O + O$
R6	$OH + N_2 = N_2O + H$

Source. AVL (2018).

The concentration of N_2O is calculated according to Equation 51.

$$c_{N2O} = 1.1802 \cdot 10^{-6} \cdot T^{0.6125} \cdot e^{\left(\frac{9471.6}{T}\right)} \cdot c_{N2} \cdot \sqrt{po_2} \quad (51)$$

The final rate of NO production/destruction in [mole/cm^{3}s] is calculated for the Equation 52.

$$r_{NO} = C_{PostProcMult} \cdot C_{KineticMult} \cdot 2.0 \cdot (1 - \alpha^2) \cdot \left(\frac{r_1}{1 + \alpha \cdot AK_2} + \frac{r_1}{1 + AK_1} \right) \quad (52)$$

$$\propto = \frac{c_{NO,act}}{c_{NO,equ}} \cdot \frac{1}{C_{KineticMult}} \qquad AK_2 = \frac{r_1}{r_2 + r_3} \qquad AK_4 = \frac{r_4}{r_5 + r_6} \quad (53)$$

2.2.19.8 CO Formation

The CO formation model implemented in BOOST™ is based on Onorati et al (2001). The reactions are in the Table 6 are taken into account.

Table 6

Reactions of the CO formation mechanism

R1	**CO + OH = CO₂ + H**
R2	CO + O₂ = CO₂ + O

Source. AVL (2018).

The final rate of CO production/destruction in [mole/cm^{3}s] is calculated for the Equation 54.

$$r_{CO} = C_{Const} \cdot (r_1 + r_2) \cdot (1 - \alpha) \quad (54)$$

$$\propto = \frac{C_{CO,act}}{C_{CO,equ}}$$

2.2.19.9 Wall temperature

The cycle averaged wall temperatures influence the wall heat losses during the high pressure cycle and thus the efficiency of the engine. During the gas exchange, the heat transfer from the cylinder walls heats the fresh charge and lowers the volumetric efficiency of the engine. The energy balance between the heat flux from the working gas in the cylinder to the cooling medium determines the wall temperatures. The 1D heat conduction equation is solved using the

average heat flux over one cycle as boundary condition at the combustion chamber side and the

heat transfer to the cooling medium on the outside. (See Equation 55)

$$\frac{dT}{dt} = \frac{\lambda}{\rho c} \cdot \frac{d^2T}{dx^2} \quad (55)$$

The mathematical formulation of the boundary conditions are shown in the equation 56

and 57:

$$q_{in} = -\lambda \frac{dT}{dx} \quad (56)$$

$$q_{out} = \propto_{CM} \cdot (T_{WO} - T_{CM}) \quad (57)$$

2.2.19.10 Plenum

The calculation of the gas conditions in a plenum is very similar to the simulation of the

gas exchange process of a cylinder, here the first law is as the Equation 58.

$$\frac{d(m_{pl} \cdot u)}{d\alpha} = -p_{pl} \cdot \frac{dV}{d\alpha} - \sum \frac{dQ_w}{d\alpha} + \sum \frac{dm_i}{d\alpha} \cdot h_i - \sum \frac{dm_e}{d\alpha} \cdot h_e + \frac{dQ_{reac}}{d\alpha} \quad (58)$$

2.2.19.11 System Boundary

The flow at the end of a pipe is calculated from the pressure in the pipe, the ambient

pressure and the effective flow area at the pipe end. Based on the quasi steady-state equation for

orifice flow the flow conditions at the end of the pipe can be calculated for the Equation 59.

$$\dot{m} = \propto \cdot p_0 \cdot \sqrt{\frac{2}{R \cdot T_0}} \cdot \sqrt{\frac{k}{k-1} \cdot \left[\left(\frac{p}{p_o}\right)^{\frac{2}{k}} - \left(\frac{p}{p_o}\right)^{\frac{k+1}{k}} \right]} \quad (59)$$

$$\frac{p_k}{p_0} = \left(\frac{2}{k+1}\right)^{\frac{k}{k-1}} \quad (60)$$

2.2.19.11 Restriction

The simulation of the flow through a flow restriction (and a rotary valve) is based on the energy

equation, the continuity equation, and the formulae for the isentropic change of state (See

Equation 61).

$$\dot{m} = \propto \cdot A_{geo} \cdot p_{o1} \cdot \sqrt{\frac{2}{R_o \cdot T_{o1}}} \cdot \psi \quad (61)$$

$$\psi = \sqrt{\frac{k}{k-1} \cdot \left[\left(\frac{p_2}{p_{o1}} \right)^{\frac{2}{k}} - \left(\frac{p_2}{p_{o1}} \right)^{\frac{k+1}{k}} \right]} \quad (62)$$

2.3 Conceptual Framework

Auto ignition: Self-ignition is the process by which flammable liquid vapors are able to

extract enough energy from the environment to self-ignite without the presence of a spark or

flame. The self-ignition capability of a flammable liquid is characterized by the self- ignition

temperature of the liquid (Zink, 2011).

Spark Ignition: Spark ignition is a process in each cycle using a spark plug. The spark

plug produces an electrical discharge between two electrons, which ignites the displaced air-fuel

mixture (Pulkrabek, 1997).

Mixture: A mixture is a combination of two or more substances in which the substances

retain their characteristic properties, e.g. air-fuel mixtures used in ICMs. The mixtures do not

have a constant composition, since they depend on the conditions of the environment. (Chang &

College, 2002).

Internal combustion engine (ICM): A machine whose purpose is to produce

mechanical power from the chemical energy contained in a fuel, this energy is extracted from the

fuel by a combustion process, which is initiated by a spark or by specific conditions of temperature and heat in a chamber. (Heywood, 1988).

Bottom dead center (BDC): Indicates the lower point of the piston stroke, i.e., where the combustion chamber volume is maximum (Heywood, 1988).

Top dead center (TDC): Indicates the upper point of the piston stroke, i.e., where the combustion chamber volume is minimized (Heywood, 1988).

Pollutants: Are solid particles or gases, mostly from human activities or natural phenomena that pollute the atmospheric air. (Ministério de Meio Ambiente, 2015).

Biomass: Biomass is organic matter originated in biological processes with the capacity to be used as an energy source, being able to be agricultural or forestry (Association of Renewable Energy Companies, 2018. (National Geographic, 2019, pag. 5).

Vehicle Flex-Fuel: "Flexible fuel vehicles (FFVs) have an internal combustion engine and are capable of operating on gasoline and any blend of gasoline and ethanol up to 83%. (Deparment of Energy, s.f).

Biofuel: These fuels come from renewable sources such as biomass, when burned they emit less carbon dioxide and other pollutants. These are some of the main renewable energies currently in use, mainly in the transport sector. They are blended with existing fuels such as gasoline and diesel as an effective form of emission reduction (Biofuels, n.d.).

Greenhouse Effect: The greenhouse effect is the way heat is trapped near the Earth's surface by greenhouse gases, thereby increasing the temperature of the planet and generating an imbalance that affects all ecosystems and living conditions. Some of the gases that cause this effect are: carbon dioxide, methane and nitrous oxides (NASA, 2019).

VOCs: Volatile organic compounds, or VOCs are organic chemical compounds whose composition makes it possible for them to evaporate under normal indoor atmospheric conditions of temperature and pressure" (United States Environmental Protection Agency, 2017).

2.4 Contextual Framework

2.4.1 Identification of the institution: Federal University of Santa Catarina (UFSC).

It is a free public university and has campuses in four other municipalities: Araranguá, Curitibanos, Joinville and Blumenau. The camps were instituted with resources from the Program of Support to Restructuring Plans and Expansion of Federal Universities (Reunion), from the Ministry of Education (MEC), in a process of interiorization of the University for other regions in Santa Catarina. (UFSC, 2019).

Its commitment to excellence and solidarity makes it reach high levels of qualification, participating in the construction of a more just and democratic society. At the University of World ranking 2018 Times Higher Education, a British consultant in the field of higher education, the UFSC is the only state to be included in the ranking and appears as Brazil's 16 in the list. (UFSC, 2019).

The University Ranking Sheet (RUF), 2017 edition, which evaluated 195 institutions in the country, UFSC emerged as the sixth best university in the country. Among the federal universities of Brazil, the UFSC is the 4th placed, and the 2nd best university in the Southern Region.

And according to the General Course Index of the Evaluated Institution (CIG), published by the Ministry of Education in 2017, the UFSC is the sixth best federal university in the country, and seventh in the overall ranking. The IGC of 4.0747 points out of five possible places

the Santa Catarina institution among the universities considered of excellence by the MEC.

(UFSC, 2019).

Starting in the 1980s, the institution began to invest intensely in the expansion of

postgraduate studies and research, in addition to supporting the creation of technology centers in

the state of Santa Catarina and developing a series of extension projects aimed at society.

(UFSC, 2019).

2.4.2 Internal Combustion Engine Laboratory LABMCI

The Laboratory of Internal Combustion Engines – LABMCI, at Federal University of Santa

Catarina – Joinville Campus, started its activities in the first half of 2014. The focus of LABMCI

is directed to teaching and research activities in several disciplines of Engineering courses of

Mobility Engineering Department of the Joinville Technological Center – CTJ/UFSC. LABMCI

also carries out extension activities, involving different projects and funding sources such as the

CNPq and PETROBRAS (LABMCI, 2019).

The LABMCI supports the development and accomplishment of undergraduate and graduate

thesis involving the following areas (LABMCI, 2019):

- Internal combustion engines

- Vehicle aerodynamics

- Applied Computational Fluid Dynamics

- Combustion Chemical kinetics and Fuel formulation

2.5 Legal framework current legislation

The legal regulations in force regarding the use of ethanol and ethanol-gasoline blends in Colombia are presented below.

RESOLUTION 40185 OF 27 FEBRUARY 2019: "By which e establishes the percentage of fuel alcohol mixture in the current and extra motor gasoline at national level (E10)".

From March 1, 2018, mixtures of ten percent (10%) of carburant alcohol with ninety percent (90%) of current and extra fossil motor gasoline, called E-10 and EX-10, must be distributed in all municipalities and departments that currently consume oxygenated fuels under the national biofuels policy (Ministry of Mines and Energy, 2019).

RESOLUTION 1962 OF SEPTEMBER 25, 2017: "For which the greenhouse gas emissions inventory quotient indicator limit for anhydrous ethanol denatured fuel is issued and other provisions are adopted".

ARTICLE 1.- OBJECT - Establish the limit of the quotient indicator associated with the greenhouse gas emissions inventory of the product Ethanol Anhydrous Denatured fuel, in order to protect the environment (Ministry of Environment and Sustainable Development, 2017).

RESOLUTION 0789 OF 20 MAY 2016. "By which Resolution 898 of 1995 is modified in relation to the parameters and quality requirements of the Anhydrous Ethanol Fuel and Anhydrous Ethanol Denatured Fuel used as an oxygenating component of gasoline and other provisions are dictated".

The purpose of this Resolution is to establish the parameters and quality requirements of anhydrous ethanol, fuel and anhydrous ethanol, fuel and anhydrous ethanol, denatured fuel, using as an oxygenating component of gasoline, for use in the Colombian territory, with the objective

of protecting the environment and improving the quality of liquid fuels. The above, within the framework of the Air Pollution Prevention and Control Policy that seeks to minimize the generation of polluting emissions and noise into the atmosphere, as well as to reduce the impacts on public health (Ministry of Environment and Sustainable Development, and Ministry of Mines and Energy, 2016).

3 Methodology

This chapter will show in detail the characteristics of the model of a spark ignition internal combustion engine simulated in AVL-BOOST. Likewise, each of the parameters used to define the model will be described, such as: geometry, properties, and initial conditions, among others. In addition, the simplifications and estimates made throughout the process will be defined, together with their respective justification.

Similarly, throughout the development of this methodology will be presented the definitions of each parameter and formulas and procedures used by AVL-BOOST software for the calculation of results. It should be noted that this information will be obtained directly from the same software in the "Documentation" module.

In addition, a practical guide to BOOST model development, simulation and data post-processing is presented in Appendix A.

3.1 Model design

The engine model used was taken from the AVL-BOOST database. This model represents and contains the main components of a four-cylinder spark ignition engine, as well as an appropriate relationship between them.

Figure 15 shows the model used, as stated above has four cylinders (C1, C2, C3 and C4) with a multipoint and indirect fuel injection type (I1, I2, I3 and I4). It contains one plenum (P2)

which represents the intake manifold and two plenums (PL3 and PL4) representing the exhaust

manifold. On the other hand, at the air inlet there is an air filter (CL1) and at the end of the

model there is a catalyst (CAT1). The boundaries, i.e., the inlet and outlet of engine gases, are

represented by Systems boundaries (SB1 and SB2). In addition to the above, the model contains:

pipes joining the above mentioned elements, joints between pipes, restrictions representing

cross-sectional changes and various measurement points.
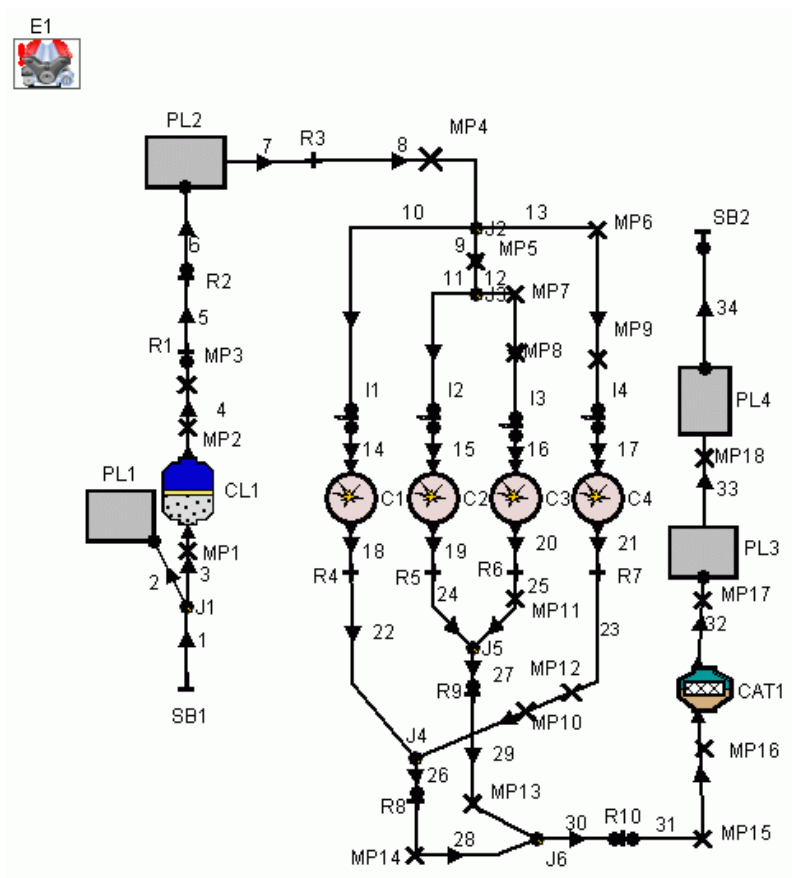
*Figure 15.*Model of engine 0-D. Source. AVL (2018)

   Table 7 shows the elements that make up the proposed model, its representative symbol in

AVL-BOOST and the quantity. Thus, each of them will be defined more broadly below.

Table 7

Elements that make up the simulated engine model.

Element	Symbol	Quantity	Figure
Cylinder	C	4	
Engine	E	1	
Air cleaner	CL	1	
Catalyst	CAT	1	
Injector	I	4	
System boundaries	SB	2	
Plenum	PL	4	
Junction	J	6	
Restriction	R	10	
Measuring point	MP	18	
Pipe	Numbers	34	

Adapted from AVL (2018).

3.2 Simulation Control

In this section the general entry data is aggregated, these must be specified first than the other data of any element. It consists of different sub-groups where the type of simulation, transport species, convergence controls, initialization sets, among others, are defined.

3.2. 1 Simulation Task

This subgroup selects the tasks or types of simulation required.

The "Cycle simulation" option is selected as it is this type of simulation that is of interest for the present project.

3.2. 2 Cycle Simulation

In transport species we select "general", this allows us to define at least seven species and for each of them a conservation equation (mass fraction) is solved in each one of the elements of the model. The general species transport unlike classic species allow to calculate the mass fraction of emissions at the end of high pressure, which is essential for emissions analysis.

A limit of 100 cycles is defined for the simulation. Since, it is estimated that with this number of cycles the solution will reach a convergence value before finishing the simulation process.

Similarly, the control convergence allows to establish a control of the convergence of the simulation, that is to say, to define an evaluative criterion where the simulation is concluded, with satisfactory results. Table 8 summarizes the income data in this section.

Table 8

Cycle Simulation Data

Species Transport	General
Simulation interval	
End of simulation	100 cycles
Convergence control	Activate
Spatial pipe discretization	
Average cell size	30 mm

Adapted from AVL (2018).

3.2.3 General Species Setup

How the general species transport was selected in the sub-group folder Cycle Simulation, this option is enable in the tree for add the input data necessary.

The species set defines the chemical species that the software will analyze during and at the end of the combustion process. Species that enter the cylinder (fuels and air components) and some intermediate species formed during combustion and the exhaust gas components are add here.

The species taken into account for this project were:

- Gasoline
- Ethanol
- O_2
- N_2
- CO_2
- H_2O
- CO
- H_2
- O
- OH

- H
- HO_2
- H_2O_2
- N
- NO
- N_2O
- CH_2O
- CH_3HCO
- C_2H_4O1-2
- CH_3

- HCO
- CH_2OH
- CH_3O
- CH_3OH
- C_2H
- C_2H_2
- C_2H_3
- CH_2CO

The fuel species set section defines the number of fuel components with which the engine will be simulated. The mass fractions and density of each components fuel are added here.

As the project is based on the analysis of performance parameters and emissions varying for different blends of ethanol-gasoline, it is in this section where the composition of the fuels simulated is defined. The Fuel Species were ethanol and gasoline with a density of 790 kg/m^3 and 720 kg/m^3 respectively.

The values of the densities were taken from (Yeliana, Cooney, Worm, Michalek & Naber, 2008), because from this research the combustion model data was taken, which will be discussed later.

The blends used for the simulations were E0, E20, E40, E60 and E84, where the letter "E" indicate that the ethanol is the additive and the numerical value represents the volumetric percentage of ethanol. This format is the most used way in the definition of ethanol- gasoline blends.

Blends were defined from volumetric percentage. So, calculate the mass fraction of each of the fuels in each mixture is necessary. For conversion from volume fraction to mass fraction the Equation 24 was used.

$$x_{m,i} = \frac{m_i}{\sum m_i} = \frac{\rho_i V_i}{\sum \rho_i V_i} \quad (24)$$

Finally, taking into account the proposed blends and the density of each fuel, the mass fractions were calculated and presented in Table 9.

Table 9
Mass composition of worked ethanol-gasoline blends

BLEND	GASOLINE $\rho = 720$ kg/m^3 x_m	ETHANOL $\rho = 790$ kg/m^3
E0	1	0
E20	0.7850	0.2150
E40	0.5778	0.4222
E60	0.3783	0.6217
E84	0.1481	0.8519

Adapted from AVL (2018).

As it was mentioned in the theoretical development of the project, ethanol combustion produces acetaldehyde and formaldehyde emissions, toxic gases, and in order to capture the formation of these gases, in the species set were added certain species that are not in the AVL-BOOST database, so it was necessary to modify it, adding the missing species according to the format specified in the software. The information of the properties of the added species were taken from available database at literature (CRECK Modeling Group). Hence, the modified database was entered by activating the "User Database" option and specifying the corresponding file.

3.2.3.1 Fuel Properties

The BOOST gas properties tool is a utility that allows know gas property data for an arbitrary mixture of fuel components. The BOOST database contains the properties of gasoline and ethanol as well as the enthalpy/ entropy polynomial coefficients.

This tool specifies each of the fuel mixtures used in liquid volume fraction based, and evaluates the lower heating value and stoichiometric A/F-Ratio. The properties of the fuels are presented in Appendix B. Similarly, the characteristics of each blend are shown in the Table 10.

Table 10
Properties of the blends used.

BLENDS	Lower Heating Value	Stoichiometric A/F-Ratio
	kJ/kg	[-]
E0	43529.29	14.6005
E20	40133.37	13.3946
E40	36864.56	12.2339
E60	33715.88	11.1159
E84	30086.88	9.8272

Adapted from AVL (2018).

3.2.3.2 Initialization

In this section three set of fuel-air mixture properties were defined, as shown in the Table 11. These initialization sets was used in other elements of the mode.

Set 1 represents environmental conditions of the gas, with an almost zero equivalence ratio in order to ensure that only air enters. Set 2 shows slightly higher temperature conditions, fuel vapor content and maintains the air equivalence ratio close to zero. The last set, set 3, has very high temperature values, is composed only of combustion products and an equivalent stoichiometric air ratio was specified (Table 11). The initialization set was used like this: set 1 for plenums and pipes before the injectors and the elements SB1 and SB2; set 2 for the pipes between injector and cylinder; set 3 for the plenums and pipes after cylinder.

Table 11
Initialization sets

Set	Pressure bar	Temp °C	Fuel Vapor	Combustion Products	Air Equivalence Ratio
1	1	30.85	0	0	0.00145
2	0.95	66.85	0.07	0	0.00145
3	1.5	216.85	0	1	1

Adapted from AVL (2018).

3.2.3.3 Convergence Control

The convergence control defined one convergence criterion where the calculation stops and the input data is shown in the Table 12. When the variation of the cycle average values of the selected parameter in the selected element over the last three consecutive cycles is less than a prescribed threshold (tolerance). On the other hand the number of convergence cycles can be defined, here was used three convergence cycles.

As an element of convergence control, the cylinder was selected, of which the IMEP with a value of 2500 Pa was set as the control parameter for all.

3.2.4 Restart Control

It is selected "No" for restart simulation, to order the calculation starts with the initial values specified in the model.

The "use most recent restart file" option was active in the case of a restart. So, the program checks for the most recent files and takes the stores conditions for the initialization.

To save restart data at regular crank must be specified the Specific Interval option and defined this interval.

Then, specific interval from the restart file saving interval pull-down menu was selected and entered 720 deg for saving interval.

3.2.5 Output Control

The saving interval is defined as the increment for which the traces results should be output, here was defined every 5 deg of crankshaft rotation.

The transients data can be written against the end of cycle time or the engine cycle number. The cycles was preferred in this project.

In addition, to calculate data such as delivery ratio, volumetric efficiency and others related to ambient conditions, the reference conditions are required. Typical ambient pressure and temperature values were set as 1 bar of pressure and 24.85 °C for temperature.

3.3 Engine

Engine was simulated in steady state, i.e., the velocity is kept constant, which was estimated at 2500 rpm, since it is a common average rotation speed. In addition, the cycle type, which is four-stroke, was selected.

3.3.1 Cylinder/ RPE-Rotor Setup

The section Cylinder/RPE-Rotor Setup defines the firing angle of each cylinder. The ignition dynamic of each cylinder consists of actuating a cylinder every 180 degrees of rotation of the crankshaft. The firing order of the cylinders is: cylinder 1, cylinder 3, cylinder 4 and cylinder 2. The firiging angle for each cylinder can be consult in the Table 1E.

Identical Cylinders option is activated, since cylinders of the same characteristics was used, allowing only data to be entered to one of the cylinders, and the others to be configured identically.

3.3.2 Engine Friction

"Engine friction adversely affects the maximum work output and fuel economy characteristics of an engine and directly accounts for much of the difference in fuel consumption between cold and full-warm engine operation. For the calculation of the brake mean effective pressure (*bmep*) and the brake specific fuel consumption (*bsfc*), the specification of friction mean effective pressure (*fmep*) over engine speed and engine load is required" (AVL, 2018).

The method to specify the *fmep* was as function of engine load, represented by the *bmep*, and the engine speed.

In this case, two sets of values were specified that defined the behavior of *fmep* according to rotation (See Figure 16).

Based on Figure 16 and know that the engine speed is of 2500 rpm, the *fmep* that was read was 111 kPa, and this value has influence on the Pressure, torque and power.
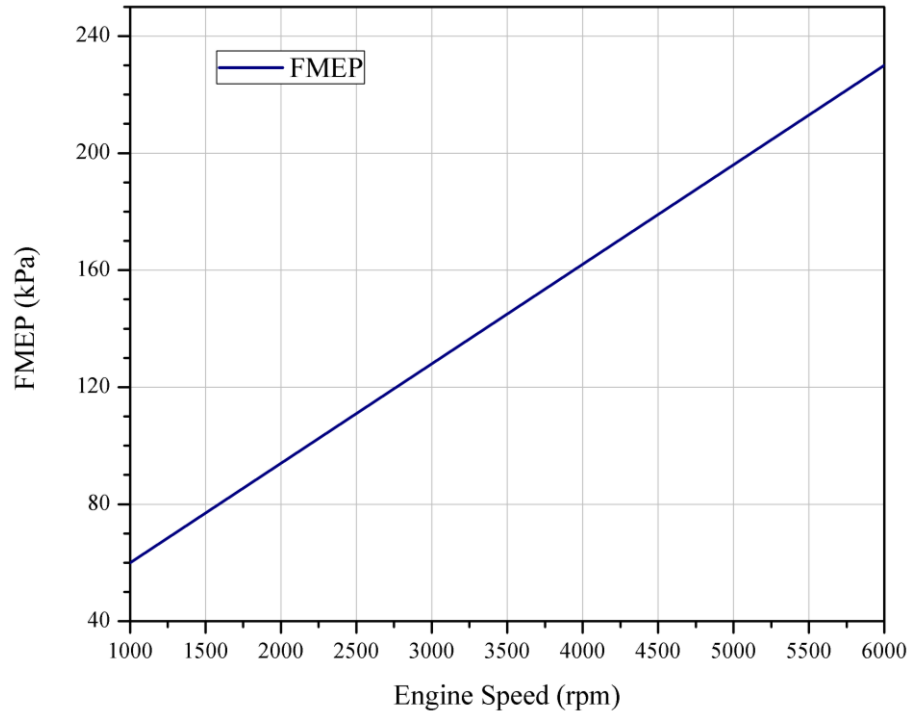
Figure 16. Friction Mean Effect Pressure. Soruce. AVL (2018)

3.4 Cylinder

"The specifications for the cylinders cover the basic dimensions of the cylinder and the crank train (bore, stroke, compression ratio, conrod length, piston pin offset, firing order), plus information on the combustion characteristics, heat transfer, scavenging process and the valve/port specifications for the attached pipes. Furthermore, initial conditions for the calculation in the cylinder must be specified" (AVL, 2018).

The four cylinders contained in the model will be defined in the same way, being only necessary to define the input data of one of them. To define this element, geometry, initialization, combustion model, heat transfer model and specifications on valve sizes and movements were entered.

3.4.1 General

Geometry data such as bore, stroke and con-rod length are obtained from BOOST. Also, it is established that the blow by gap will be null and the scavenge model as perfect mixing.

The Perfect mixing model is the standard scavenging model recommended by BOOST for simulation of 4-stroke engines. In this model the gas flowing into the cylinder is mixed immediately with the cylinder contents and gas leaving the cylinder has the same composition as the mixture in the cylinder.

For the determination of the compression ratio, it was taken into account that flex fuel vehicles are adapted to work with different ethanol-gasoline mixtures (including greater than 10%), which is why the compression ratio was estimated taking into account different commercial models of Flex Fuel cars of equal displacement to that defined with the geometry parameters.

According to the study "New advances in flex-fuel technology" carried out in São Paulo, Brazil, it is shown that with the passage of time, the compression ratio in Flex engines has been increasing (See Table 12). For the year 2009, the compression ratio is generally between 11 and 13. (Joshep, 2009).

Table 12
Characteristics of the Flex Fuel vehicle generations

Generation	Market entry	Engine compression ratio	Power gain with ethanol	Torque gain with ethanol	Mileage loss with ethanol	Cold start with gasoline
1st	2003	10.1-10.8	2.1%	2.1%	25%-35%	Yes
2nd	2006	10.8-13.0	4.4%	3.2%	25%-35%	Yes
3rd	2008	11.0-13.0	5.6%	9.3%	25%-30%	Yes
4th	2009	11.0-13.0	5.6%	9.3%	25%-30%	No

Source. Joseph Jr., H, (2009).

In addition, the technical data sheets of several Flex Fuel automobiles marketed in Brazil were consulted (Appendix C), with the aim of knowing characteristics such as the compression ratio that commercial cars have.

The revision of commercial cars was made focusing on cars with the same cylinder capacity of the engine model taken. The calculation of the cylinder capacity of the model presented, was made taking into account the data of bore, stroke and number of cylinders in the following way:

$$B = 8.6 \; cm \; ; \quad L = 8.6 \; cm \; ; \quad Ncilindros = 4$$

$$V/cilindro = \frac{\pi}{4}(8.6 \; cm)^2(8.6 \; cm) = 499.56 \; cm^3$$

$$V = 499.56 \; cm^3 * 4 = 1998.24 \; cm^3$$

Hence, it is a 2.0 L engine, which works with gasoline ethanol mixture and taking into account the above mentioned information and Appendix C. A consistent and acceptable value of the compression to work ratio of 11:1 can be established.

On the other hand, the compression ratio will be varied. Four values will be taken: 11, 12.5, 13 and 14. The above, in order to compare the behavior of the different performance and operating parameters of the engine with respect to this parameter. According to Heywood's book, for the use of gasoline, the maximum compression ratio without self-ignition is 12. Therefore, although the program performs numerical simulations for the pure gasoline mixture (E0), the values for E0 with compression ratios of 12.5, 13 and 14 will not be taken into account for the analyses, since they do not represent real performances.

The input data to the "general" section is shown in Table 13.

Table 13

General/ Cylinder

Bore	86 mm
Stroke	86 mm
Compression ratio	10.5
Con-rod Length	143.5 mm
Piston pin offset	0 mm
Effective Blow by Gap	0 mm
Mean crankcase press	1 bar
Scavenge model	Perfect mixing

Adapted from AVL (2018).

3.4.2 Initialization

The gas conditions ordered in this section are those you will have at the end of the high

pressure at the exhaust valve opening. These conditions of pressure, temperature and initial gas

composition are shown in the Table 2E.

3.4.3 Combustion

Among the different approaches proposed by BOOST, a heat release model was selected:

vibe simple, where the total heat released during the combustion is calculated from the amount of

fuel which is burned in the cylinder and the lower heating value of the fuel. This combustion

model was presented theoretically in section 2.2.

The type of preparation of the air-fuel mixture is external, i.e., the fuel is fed to the intake

system and the total heat supply is calculated from the amount of fuel in the cylinder at intake

valve closing.

Finally, the temperature was specified as 25 °C.

3.4.3.1 Vibe Model

The vibe combustion model was defined in the section of the theoretical framework and

as observed in Eq. 7, it is necessary to define the parameters m, a, the duration of combustion

and the angle of initiation of combustion. These data must be determined experimentally

according to the type of fuel used and for the present work the data were taken from the project

of (Yeliana, Cooney, Worm, Michalek & Naber, 2008) there an experimental determination is

made by different methods of the parameters of vibe and the most exact method is selected,

where the values were taken.

Table 14 shows the data used for the vibe function for each ethanol-gasoline blend (E0,

E20, E40, E60, and E84). On the other hand, it is observed that from the vibe input data the

software automatically makes a graphical representation of the vibe function for the burned mass

fraction (*mfb*) and the heat release rate (*ROHR*) as a function of the crankshaft rotation angle.

Table 14
Function Vibe data

Blend	α	Δα	a	m
E0	-10	40	2.3	2.75
E20	-10	40	2.3	2.95
E40	-10	40	2.3	2.90
E60	-10	40	2.3	2.91
E84	-10	40	2.3	2.84

Adapted from AVL (2018).

The graphs of vibe's function for *mbf* and *ROHR* are presented in Figures 17 and 18.

Figure 17 shows the slight variation present in the vibe curves, but even so, these curves are able

to predict the difference in heat release within the cylinder using each of the mixtures presented,

this is shown too in the Figure 18.
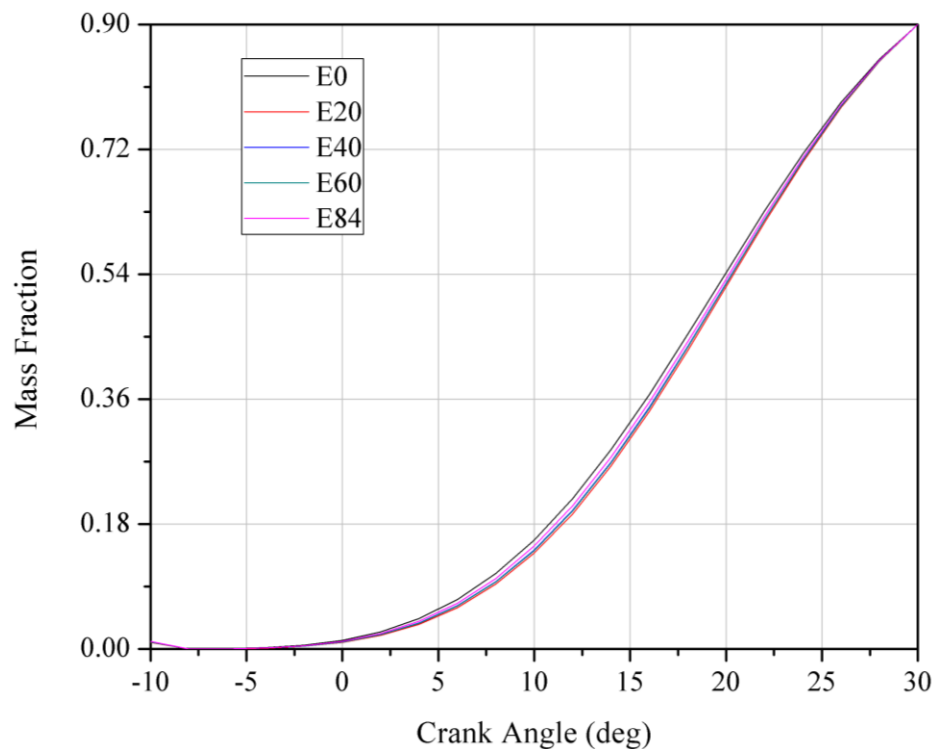
*Figure 17.*Comparison of the fraction curves of burned mass defined by the Vibe function for mixtures E0, E20, E40, E60 and E84. Source. AVL (2018).
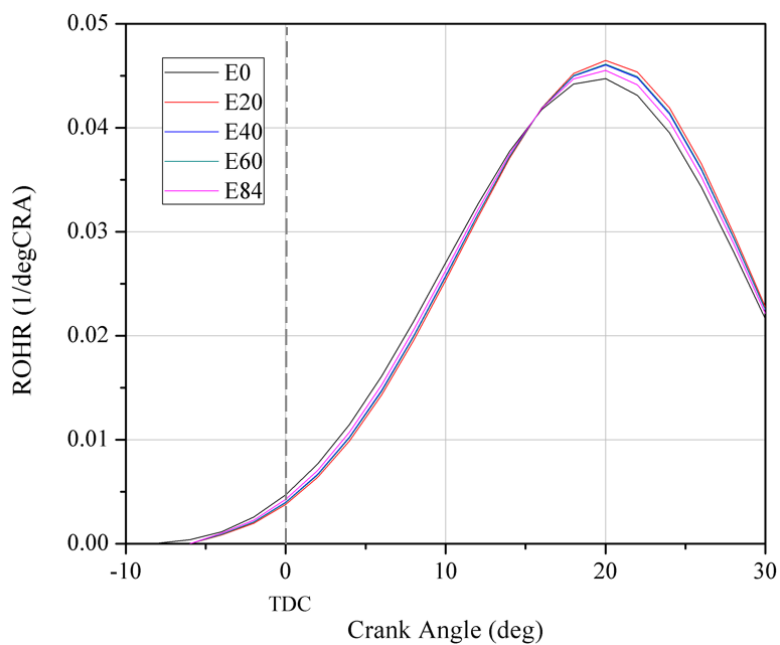
Figure 18. Comparison of the Rate of Heat Release defined by the Vibe function for mixtures E0, E20, E40, E60 and E84. Source. AVL (2018)

3.4.4 Heat Transfer

Heat transfer in the cylinder is taken into account for: piston, cylinder head and Liner. For these, the surface area and wall temperature of each must be specified. For the wall temperature of the liner the temperatures in TDC and BDC of the piston were specified. The above data were taken from the BOOST database.

The head calibration factor was defined as 1, i.e., it was decided to take the heat transfer values given by the program without increasing or decreasing them.

For the type of combustion system "DI" was selected, direct injection is recommended by BOOST for gasoline engines.

For the heat transfer in the ports the modified Zapf model was selected, it will be considered only heat transfer in the exhaust port, since it is in this one where greater temperatures are presented, the heat transfer in the port of admission can be simplified considering that the temperatures in average are not significant.

Table 3E shows the input data for the heat transfer section, which shows the type of ports, surface area and temperature of the wall and calibration factor of: piston, cylinder head and liner.

3.4.5 Valve Port Specifications

The ports connected to the cylinder must be controlled by an element: by the valve or by the piston. BOOST specifies that the control by the piston is only for 2-stroke engines, therefore the port control by the valve is selected.

The above can be consulted in Table 4E where they are shown: the pipe specifies connected to each port (intake and exhaust) of the cylinder; the type of port control, which will be for all will be by means of the valve; the surface area of the ports of escape and the temperature of the wall of the ports.

3.4.5.1 Intake and Exhaust

Each Port must be classified if it is intake or exhaust for the calculation of the mass flow rate. Since the control of the ports is by the valve, the inner valve seat diameter must be specified for the calculation of the heat transfer coefficient in the port and for the conversion of normalized valve lift to effective elevation. The inner valve seat diameter are shown in Table 15. The valve clearance was taken to be zero.

Because the program interprets the specified flow coefficients of the ports are related to the cross-section of the pipe attached to the cylinder and the port area has a different cross section, it is necessary to use a scaling factor to achieve the correct effective flow areas. The scaling factor was calculated with Equation 43 as follows:

$$f_{sc_{intake}} = \frac{1 * (43.84 \; mm)^2}{(33.5 \; mm)^2} = 1.712$$

The lifting curve of the valve defines the opening moment and the duration of the opening of each valve. The number of points or increments must be specified to give the elevation data. This curve will define the behavior of the valves and interfere with the efficiency of the motor.

To consider particular pressure losses resulting from multi-dimensional flow phenomena which cannot be directly predicted by the program, BOOST™ requires the specification of flow coefficients of the ports. The flow coefficients are defined as the ratio between the actual mass flow and the loss-free isentropic mass flow for the same stagnation pressure and the same pressure ratio. These, must be specified according to the valve lift and allow the calculation of the real mass flow from the isentropic mass flow calculated with the isentropic flow equations presented in the theoretical framework. Additionally, a pressure ratio of 1 was specified and the flow coefficients data were given according to the effective valve lift.

This lift curve and flow coefficient curve function was taken from the BOOST database, and when entered its graphical representation is automatically generated as shown in Figure 19. The flow coefficient and lift curves data for the intake and exhaust valves are shown in Appendix D.

Table 15

Intake and Exhaust Valve Data

PARAMETERS	INTAKE VALVE	EXHAUST VALVE
Inner valve seat diameter	43.84 mm	37.77 mm
Valve clearance	0 mm	0 mm
Scaling Factor for Eff. Flow Area	1.712	1.242
Specification		
Valve opening	340 deg	130 deg
Cam length	270 deg	260 deg
Increment	10 deg	10 deg
Manipulation		
Valve opening	340 deg	130 deg
Cam length	270 deg	260 deg

Adapted from AVL (2018).

The inner valve seat diameter values are specified because it was established that the port is controlled by the valve, this allows the calculation of the heat transfer coefficient of the port wall, in this case for the exhaust valve, as well as the conversion of the standard elevation of the valve to an effective elevation of the valve.
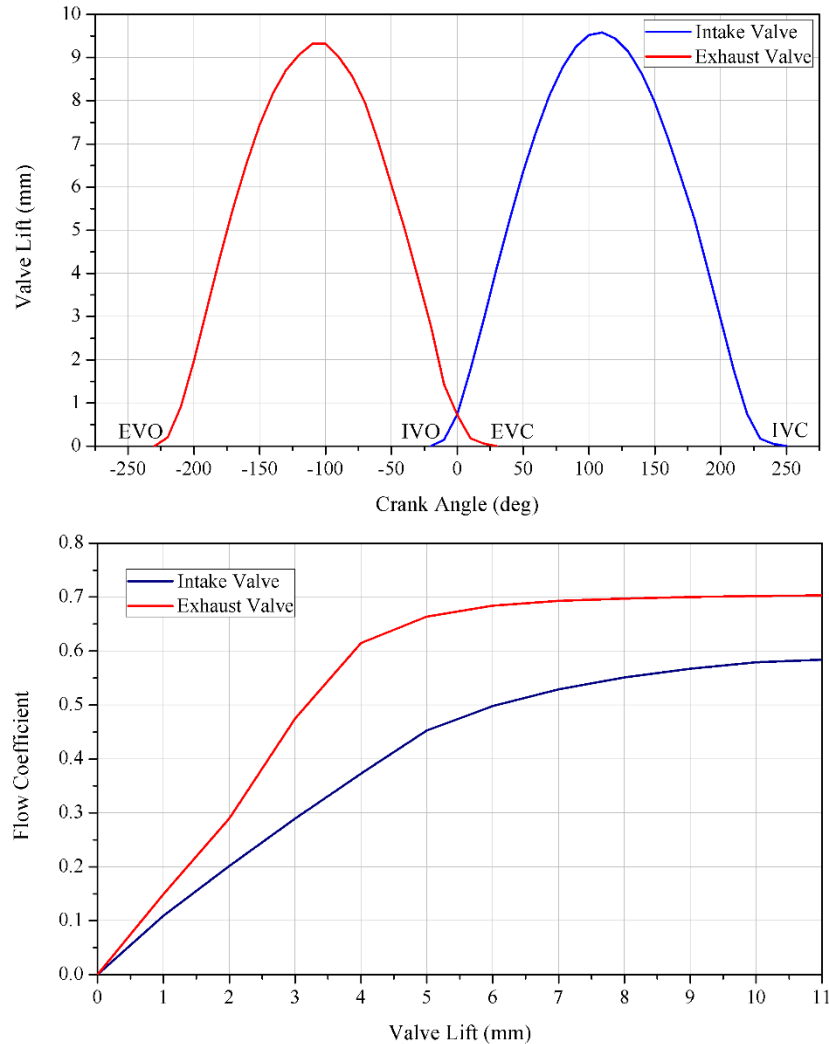
Figure 19.Valve Lift Curve and Flow Coefficient Curve/ Cylinder. Source. AVL *(2018).*

Inlet valve opening (IVO) occurs 20 deg before top center (BTC), this point does not have a great influence on the engine performance but it must be ensured that it happens before the TC to avoid an early pressure drop in the intake stroke. Inlet valve closing (IVC) occurs 70 degree after bottom center in order to provide a superior filling time, although if the intake conditions and pressure differences are not correct it can cause backflow. Exhaust valve opening occurs 30 degree before the bottom center (BC), i.e., even during the expansion stroke, in order to reduce the cylinder pressure and help to expel the exhaust gases. Exhaust valve closing (EVC)

occurs 30 degree after top center, the closing happens sufficiently later to guarantee the total exit

of the gases. Late EVC favors high power at the expense of low-speed torque and idling. Then, it

is observed that there is a crossing of 50 degree valves.

3.5 Air Cleaner

"BOOST ™ automatically creates a more refined calculation model of the plenum-pipe-

plenum type (See Figure 20) for the air filter. This is used to model the dynamic performance of

the air filter gas, as well as the pressure drop over the air filter, depending on actual flow

conditions".(BOOST)

The input data necessary to define the air filter geometry are: total volume, inlet collector

volume, outlet collector volume and length of filter element, these volumes are shown in Figure

21 and the data are taken from BOOST which represents a typical air cleaner.
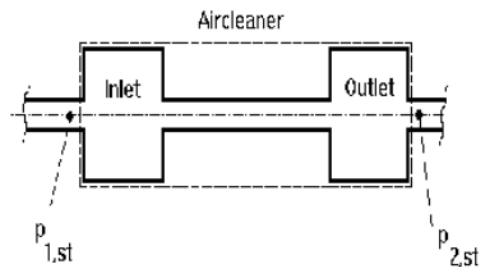
Figure 20. Air Cleaner design. Source. AVL (2018).

To specify the friction, was choose the target pressure drop option. This was considered a

more complete friction model approach, since it takes into account reference mass flow, the

target pressure drop (defined as the static pressure difference at the inlet and the outlet pipe

attachment) at the reference mass flow and the inlet air conditions (temperature and pressure).

All of the above parameters are presented in Table 1F. Additionally, Table 1F shows the volume

for the input and output collector, as well as the length of filter element.

Finally, it is necessary to determine the flow coefficients for the pipes attached to the inlet and outlet of the filter, giving a value of 1 for all of them.

3.6 Catalyst

"As for the air cleaner, BOOST™ automatically creates a more refined calculation model of the catalyst. This is used to model the gas dynamic performance of the catalyst as well as the pressure drop over the catalyst depending on the actual flow conditions" (AVL, 2018).

3.6.1 General

As it was not part of the study of this project, the catalyst was taken without chemical reactions, that is to say, the program will take the catalyst as a flow element where only data on geometry and friction are necessary. Therefore, in order to define this element, geometrical data was entered, type specification, friction data and flow coefficients.

La Table 1F provide the monolith volume and length and, the inlet and outlet collector volume.

3.6.2 Type Specification

The type of catalyst influences the calculation of pressure losses, in this project a general catalyst was taken, as this is the standard model. To define it, the open frontal area (OFA) input was specified as 1, that is, the entire area is taken and the hydraulic diameter option was selected, which was specified as 116.53 mm, this according to BOOST data and the value of the geometrical surface area is calculated automatically (See Table 2E).

3.6.3 Friction

There are two types of specifications for the catalyst friction model, the target pressure drop and friction coefficient, in this case, like the air filter, the target pressure drop model is selected.

To define the target pressure drop, the values for inlet mass flow, inlet temperature, inlet pressure and target pressure drop were entered in the Table 3E, these values are within the typical ranges.

3.6.4 Flow Coefficients

The flow coefficents allow to consider the resistances of the particular flows in the input and output of the catalyst, this value can be given as a constant or as a function of time, in degrees crank angle or pressure difference at the pipe attachment. To define the flow coefficients of the catalyst fixed values of 1 for all connections.

3.7 Injector

The intermittent method is selected as the injection method.As the simulated engine is MPFI, each injector is referred to the corresponding cylinder and the injection angle is given and it is said that this will be done in EOI. In addition, it is necessary to specify the duration rate and specifications of fuel film formation and evaporation specification, this values are shown in the Table 16 and was taken from BOOST database.

Table 16

Injector General Data

Injectio Method	Intermittent
Reference cylinder	cylinder 1/ cylinder 2/ cylinder 3/ cylinder 4
Injection angle (ref to FTDC)	540 deg

Eoi	Active
Injector Rater/Duration settings	Rate
Delivery rate	0.012 kg/s
Fuel Film Formation and Evaporation Specification	
Fuel film thickness	0.03 mm
Fuel film liquid density	750 kg/m^3
Fraction of Fuel in Wallfilm	0.001
Film-wall Temperature taken from	Measuring point 19
Evaporation multiplier	1
Shape multiplier	1

Adapted from AVL (2018).

When intermittent injection method was selected, the distillation curve had to be added, whose data can be consult in the Table 1H.

For the mass flow specification a "Ratio Control" was chosen, since in this method the control of fuel supply is carried out according to the A/F ratio and since the injector model is for injection nozzle, it is necessary to establish a reference point, where the program measures the air flow and, together with the A/F ratio, establishes the amount of fuel to be injected. In this project, the selected point is the MP2, which is located at the outlet of the air filter. On the other hand, since this flow goes directly to the four cylinders, the air percentage for each must be specified, which is 25% (See Table 2H).

In the simulation, the evaporation heat was taken into account and the species injected were only fuels, that is, those that were entered in the "simulation control" section, that is, ethanol and gasoline. In addition, the fuel inlet temperature must be added, the evaporation heat and the heat from wall, and this data is show in Table 3H.

The flow coefficients are necessary to consider the particular pressure losses of multidimensional flow phenomena, in any case, these coefficients represent the relationship

between the real mass flow and the isentropic mass flow at the same stagnation pressure and at the same pressure ratio. For this case, the flow coefficients are at 0.95 (See Table 4H).

3.8 System Boundary

The System boundary is the model's connection to the outside environment, so it allows the environmental conditions to be defined either constantly or as a function of time or angle.

The proposed model contains two system boundary, one for the air inlet and one for the outlet. The following describes the input data required to define these two elements.

3.8.1 General

A standard border type was selected for both SB1 and SB2, this model is the default setting for a system boundary and here no special feature are used.

3.8.2 Boundary Condition

For the sub-group folder, local boundary conditions were established (See Table 17). For both elements (SB1 and SB2) the pressure was set almost at atmospheric pressure, the temperature in SB1 was determined much lower than the temperature in SB2, because the exhaust gases are at a higher temperature. The value of the A/F ratio was determined high for SB1 indicating that only air enters through this element and as 1 for SB2, due to the fact that a stoichiometric mixture is taken.

Table 17
Boundary Condition Data

	Pressure (bar)	Gas Temp. (°C)	Fuel Vapor	Combustion Products	Ratio Type	Ratio Value
SB1	0.995	30.85	0	0	A/F Ratio	10000
SB2	0.995	676.85	0	1	Air Eq. Ratio	1

Adapted from AVL (2018).

3.8.3 Flow Coefficients

The flow coefficients in the joints with the pipes were defined with a value of 0.95 for SB1 and according to BOOST recommendations when air flows into a very large volume, e.g. the environment, flow coefficients of 1 according to BOOST recommendations when air flows into a very large volume, e.g. the environment, flow coefficients of 1.

3.9 Plenum

The plenum 1, is considered as a volume for pressure fluctuation attenuation along the admission duct, plenum 2 represents the volume of the intake manifold and plenums 3 and 4 represent the engine muffler system. These must be defined by entering their volume, initialization type and set, and the respective flow coefficients.

3.9.1 General

In this sub-group folder the way in which the geometry of the plenum will be defined is selected, in this case, it will be directly entering the volume. The Table 1I show the volume in liters of each plenum.

3.9.2 Initialization

The initialization will be done in a global way and choosing one of the sets defined in the "simulation control" section (See Table 1I).

3.9.3 Flow Coefficients

This section defines the input and output flow coefficients of each connection of the element with the corresponding pipe, i.e., it should be remembered that these coefficients must be less than 1 (See Table 1I)

The initialization was performed global in order to assign an initialization set already defined in the "Simulation Control" section. "The reduced flow coefficients at the attached Pipe

4 accounts for the flow losses of the opened throttle. The throttle is not explicitly modeled in this work". (AVL, 2018)

3.10 Junctions

The types of junctions available are: constant pressure, constant static pressure and refined model, according to the type selected, the characteristics of the junctions are defined.

Most joints were defined with the refined model, as it takes into account the geometry of the joint (ratio of areas and angle between pipes) and calculates the distribution of mass flows. For this model it is necessary to specify the angle between each of the pipes, i.e. having three pipes connected to the joint, three angles must be specified. The input data was taken from BOOST data base and this was obtained by means of a stable state flow test bench and these were represented in the Table J1

Only the joint separating the inlet airflow to the cylinders is defined by the constant pressure model, since the same amount of air must flow through each pipe. For the constant pressure model flow coefficients are required for each flow path in every possible flow pattern (See Table J1).

3.11 Restrictions

The model presented has ten restrictions, which are described by two flow coefficients one "one way" and one "back". On the other hand, it also allows to apply the Karal's end correction, which is an extreme correction that allows multidimensional effects to be taken into account. But for this simulation it will not be activated.

The flow coefficients of the restrictions depend largely on the design details of the restriction (control valve, orifice, flow separation, sudden diameter change, etc.). For cross

section changes, BOOST recommends a value of 1 for expansions, for reductions BOOST provides a table which allows the calculation of the coefficient of friction.

The restriction data was taken from BOOST and this is shown in the Table 2J.

3.12 Pipes

The BOOST pipe model takes a one-dimensional flow that is analyzed by equations that take into account the time delay caused by the propagation of pressure waves or the same flow. As for the heat transfer coefficient of the walls, it is calculated with the Reynolds analogy, and this is multiplied by a heat transfer factor that allows the user to define its quantity.

All the elements of the engine model are connected by pipes, these conduct the different gases inside the engine and some data must be defined, such as: length, diameter (constant or variable), friction coefficient (constant or variable), heat transfer factor, temperature and initialization set. The model has 34 pipes and the Table 1K shows the relevant values to enter in the setup of each one of them and Table 2K shows the data of those parameters defined by "table".

The coefficients of friction depend on the material and diameter of the pipe, BOOST provides a table that allows the calculation of this factor, for various materials and diameters. The heat transfer factor is defined as 1.0, i.e., the heat transfer values calculated by the program are not modified.

The pipes that are before the injector are initialized with set 1, because this characterizes its thermodynamic conditions, once the injector has passed, the addition of fuel changes the conditions and these pipes are initialized with set 2. For the pipes through which the combustion gases pass, the temperature and pressure are higher, therefore, they are initialized with set 3.

The values for length, diameter, wall temperature and bending radius (some pipes) are taken from BOOST.

3.13 Measuring Point

"The measuring points allow the user to access flow data and gas conditions over the crankshaft angle at a given location in a pipeline." (AVL, 2008). The output extent can be: standard or extended and depending on your selection different data are available. For standard output the following are available: pressure, flow rate, temperature, Mach number and mass flow rates. For extended output the above data are available in addition to: stagnation pressure, stagnation temperature, enthalpy flow, fuel concentration, concentration of combustion products, fuel flow and flow of combustion products.

In order to define the measuring points, the distance from the upstream end of the pipe in millimeters and the type of output extent must be specified, which for all measuring points is "standard". The input data is shown in the Table 1L.

The location of the measuring point was carried out an arbitrary way, that is, where you want to know values.

3.14 Reference Point for Volumetric Efficiency

For the calculation of the air supply ratio and the volumetric efficiency with the conditions of the intake manifold a reference point must be selected, this can be either a plenum or a measuring point, that are located before the injector and cylinder. For this simulation, the reference Point is the Measuring Point 2.

4. Results

This section shows the results obtained in the simulation of the SI combustion engine model using the AVL BOOST software, as presented above, the model was simulated with five ethanol-gasoline blends (E0, E20, E40, E60, E84). In addition, each mix was simulated with different compression ratios (11, 12.5, 13, and 14). From the results provided by the software, the behavior of different engine performance parameters was analyzed, such as: torque, power, specific consumption, among others. Parameters were also analyzed according to the crank angle and how they change according to alcohol content and compression ratio.

As for the use of the E0 mixture, which is pure gasoline, special care must be taken with regard to its self-ignition limits. For spark ignition engines the compression ratio must be between 8 and 12 (Heywood, 1988), in order not to present abnormal combustion, i.e., knocking. Therefore, the results given by the software for the E0 mixture in compression ratios of 12.5, 13 and 14, will not be taken into account in the analysis as these do not represent possible operating values. Additionally, it is recommended through future studies, to determine the convenience of using mixtures such as E20 at high compression ratios of 13 or 14, due to their high gasoline content.

4.1 Performance Parameters

Torque and power decrease with ethanol content, but increase with respect to the compression ratio as is shown in the Figure 21 and 22.
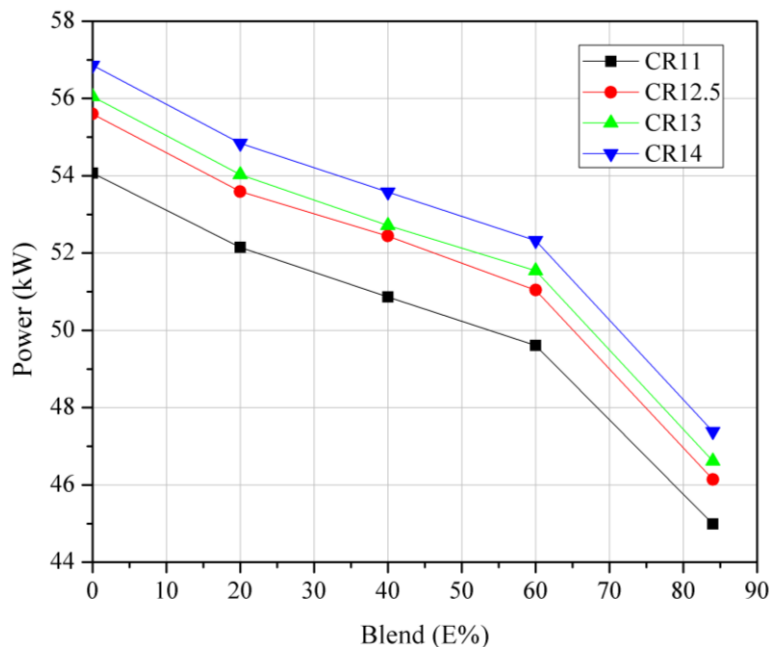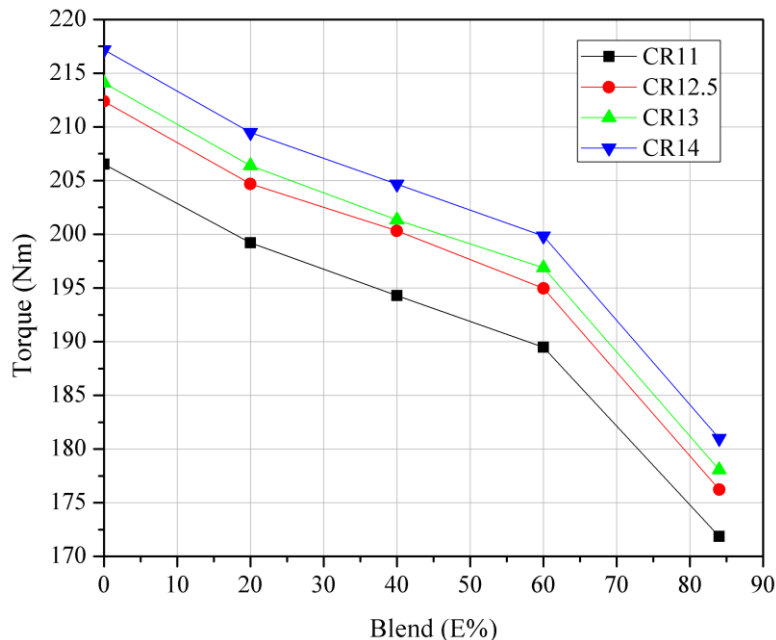
Figure 21. Comparison of the power obtained for each compression ratio in different ethanol-gasoline blends.

For pure gasoline with CR of 11 values of 206.53 Nm of torque and 54 kW of power were obtained. These can be achieved by using a mixture of E20 at a higher compression ratio of 12.5 or even obtaining very close values with the E40 mixture at a compression ratio of 14. The above shows that fossil fuels can achieve performance parameters as long as they are burned under proper operating conditions.

For CR11 the power and torque drop between E0 and E84 mixtures is 17%, which is considered significant in terms of performance, therefore it is recommended not to use mixtures with high alcohol content in engines with low compression ratios.

The torque and power gain for E84 to CR14 versus CR11 was 5.3%. According to Figures 21 and 22, it is observed that the mixture E60 to CR 14 presents performance values only 3% below pure gasoline, despite its high ethanol content.
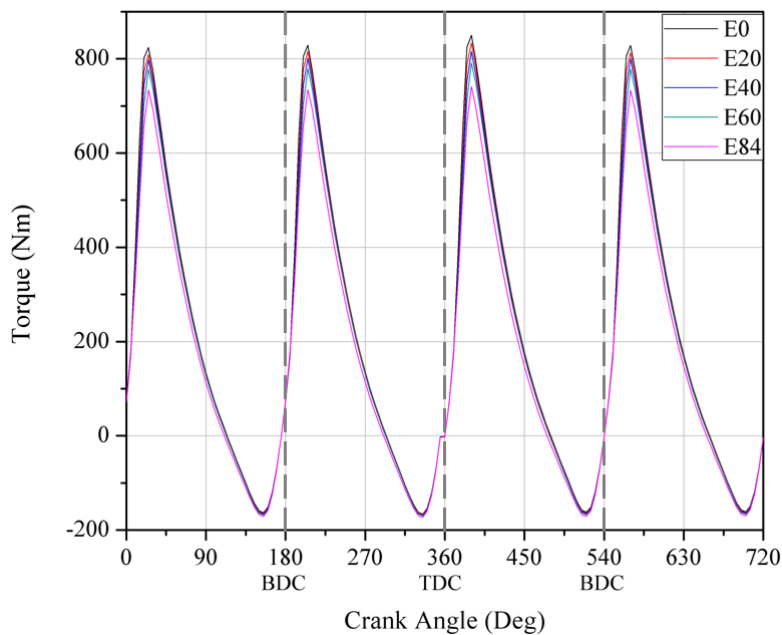
*Figure 22.*Comparison of the torque obtained for each compression ratio in different ethanol-gasoline blends.

The traces for torque using a compression ratio of 11 are shown in Figure 23. The four peaks in the graph represent the moments where each of the four cylinders reached maximum torque. As stated above, the torque generated for the E84 mixture is less than for the E0 mixture. In addition, small changes in the torque peaks can be observed, achieving the highest values in cylinder 2 since it is the third to be activated.

Similarly, the lower peaks of the curve also present small differences, here it is observed that they present negative values of torque. These negative torque values occur when the compensation masses in the engine are acting to complete the crankshaft rotation generally throughout the working pumping period.

The variation in the torque peaks for each of the cylinders is due to the difference in air intake to each cylinder through the intake manifold and therefore the amount of fuel injected, ie,

each cylinder will always present curves with variations with respect to the other cylinders as well, as variations with respect to itself but in different time.


Figure 23. Torque behavior according to crank angle in Cylinder 1 using compression ratio of 11.

Figures 24 and 25 show the specific fuel consumption indicated and the brake, the *isfc* being lower than the *bsfc* and showing the same behavior. There is a direct proportional relation with the ethanol content and inversely proportional with the increase of the compression relation.
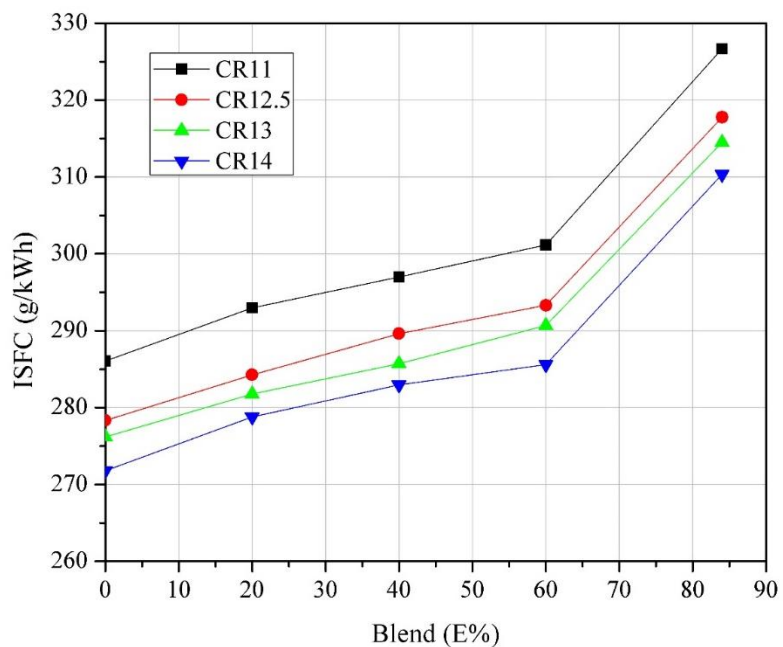
Figure 24. Comparison of indicated specific fuel consumption (ISFC) obtained for each compression ratio in different ethanol-gasoline blends.

The most favorable consumptions for all CR used were obtained for pure gasoline, this is because ethanol has a lower calorific value than gasoline, requiring greater use of fuel. But as mentioned above, gasoline cannot be used with high compression ratios, it is observed that the BSFC value for gasoline with RC11 is comparable for blends: E20 with CR 12.5, E40 with CR13 and E84 with 14. This shows that when using the appropriate compression ratio, it is possible to maintain the specific consumption of fuel, being able to have even lower consumption values.
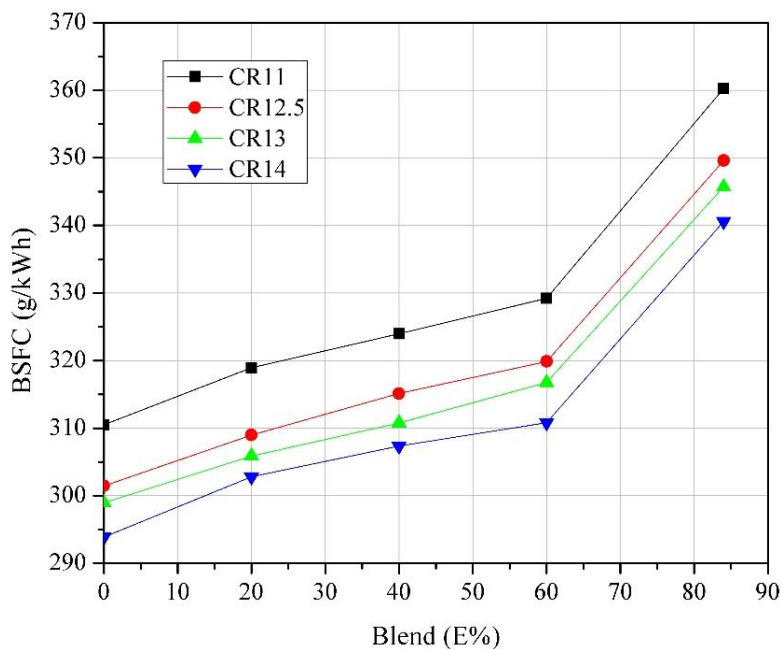
*Figure 25.*Comparison of brake specific fuel consumption (BSFC) obtained for each compression ratio in different ethanol-gasoline blends.

The *bsfc* at RC11 between pure gasoline and E84 increased by 16%, but when using E84 at a compression ratio greater than 14, the increase was only 9.7%. In terms of economy, it is known that in both Colombia and Brazil the price of ethanol is lower than that of gasoline, which could compensate for the increase in fuel consumption.

Specific fuel consumption increased with the increase in the percentage of ethanol, observing a steeper slope in the graph between E60 and E84. The E84 blend obtained a specific indicated fuel consumption 14.2% higher than E0.

4.2 Mass

Figure 26 shows the behavior of the exhaust gas composition when the exhaust valve is opened with respect to the ethanol content in the fuel used. These data were taken for the simulation carried out using a compression ratio of 11, it is therefore intuited that the behavior shown with respect to the ethanol content is maintained for the other compression ratios used.

For the composition of the combustion gases in OE the software gave values for 12 species bur in the Figure 26 only seven species are shown, the more important and which the software gave values. As expected, N_2 is in greater proportion to the other species, increasing with the ethanol content except for E84 where there was a slight decrease.

For the gasoline species, less unburned gasoline is found in the E84 mixture. The species content: ethanol, H_2O and NO increase with the ethanol content. On the other hand, CO_2 increases with ethanol content, but decreases for E84. On the other hand, CO decreases considerably.
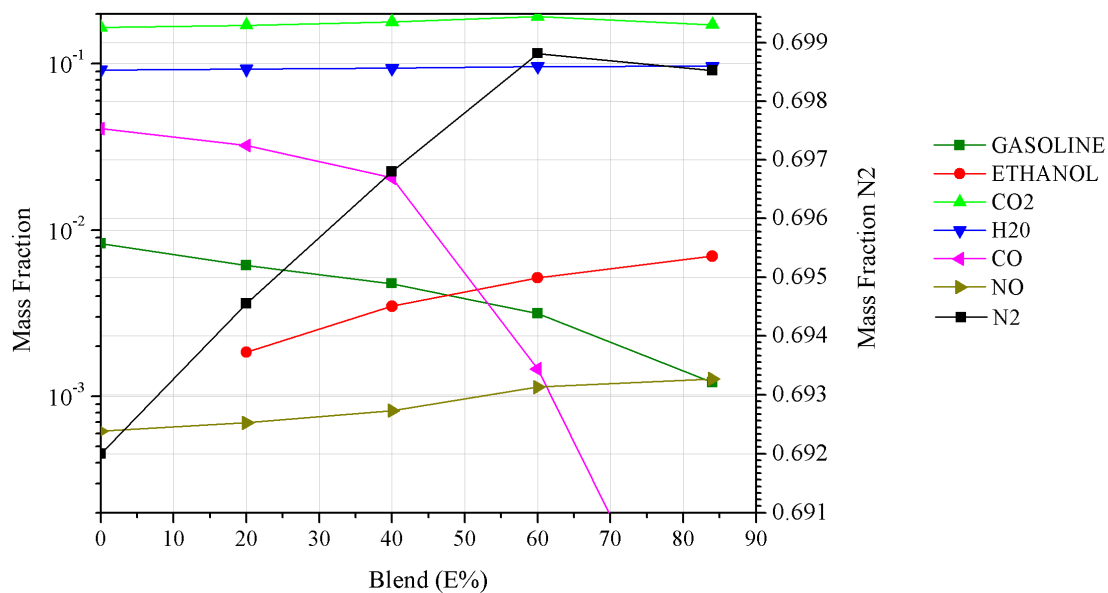
Figure 26. Composition of the combustion gases in OE.

The CO fraction decreased using E84 with respect to gasoline by 99.97%, which represents a quite significant decrease. Conversely, there was an almost fourfold (3.8 times) increase in unburned ethanol for E84 over E20, increasing the likelihood of formation of toxic

emissions such as aldehydes from this unburned ethanol. The increased ethanol content in E84 also led to a 106 per cent increase in NO production over E0.

For the species formaldehyde and acetaldehyde AVL BOOST does not manage to capture their formation. This is because the calculations made by the program are based on chemical equilibrium. In order to capture the formation of formaldehydes and acetaldehydes it would be necessary to use chemical kinetics, which is not part of the development of the project. Therefore, no data were obtained for these two pollutants.

Figure 27 shows the amount of mass contained within cylinder 1 for simulations performed with a compression ratio of 11 for mixtures E0, E20, E40, E60 and E84 with respect to the crank angle.

For cylinder 1 the intake stroke starts at 0 degrees. Figure 27 (a) shows and increase in the mass inside the cylinder from 0 degrees to 180 degrees, i.e., to the TDC. Subsequently, there is a decrease in mass, this is because the inlet valve is open up to 250 degrees (70 deg after BTC).

The decrease in mass in the cylinder is due to backflow into the intake, this shows that the engine's intake system is not correct for the speed regime at which the engine is being simulated, because it fails to take advantage of the RAM effect. In 195 degrees the greater amount of mass is presented inside the cylinder, that is to say 15 degrees of the final point of the admission race. Approximately 5% of the mass inside the cylinder decreases due to backflow.

The mass remains constant from 250 degrees to 490 degrees where the exhaust valve begins to open and the combustion gases begin to exit the cylinder. There is a slight increase in the amount of mass in the cylinder around 625 degrees, where the exhaust valve begins to

descend. Subsequently the mass continues descending, but without reaching zero, this small amount of mass is the residual gases of the cylinder.

On the other hand, Figure 27 (b) shows the difference between the amount of mass that is trapped in the cylinder, with a greater amount of mass for mixture E0 and less for mixture E84, with a difference of approximately 2.5×10^{-5} kg. The behavior of the mass for all curves with CR 11 is the same.

In Figure 28 the curves for the mass inside the cylinder 1 are shown for a mixture E0 and diverse compression ratios, this graph describes the same behavior as that of Figure 27, therefore, it is shown in order to determine the behavior of this parameter according to the compression ratio. It is observed that there was only a 1% decrease in the mass trapped between the curve for CR11 and CR14.

Figure 29 shows the variation in the composition of the combustion gases at the moment of opening of the exhaust valve (EVO) for each of the mixtures used and for each compression ratio, most do not present a significant variation in terms of mass fraction. The six species considered in Figure 26 were plotted.

Figure 29 (a) shows the mass fraction for gasoline, it is observed that with respect to the compression ratio there were no variations, while a decrease of the unburned gasoline fraction is shown with the increase of the ethanol content. This decrease in unburned gasoline from approximately 0.0082 to 0.0012, which is represented as unburned hydrocarbons is beneficial to the environment, as these are an important source of pollution forming toxic gases for both the environment and public health, as shown in section 2.2.
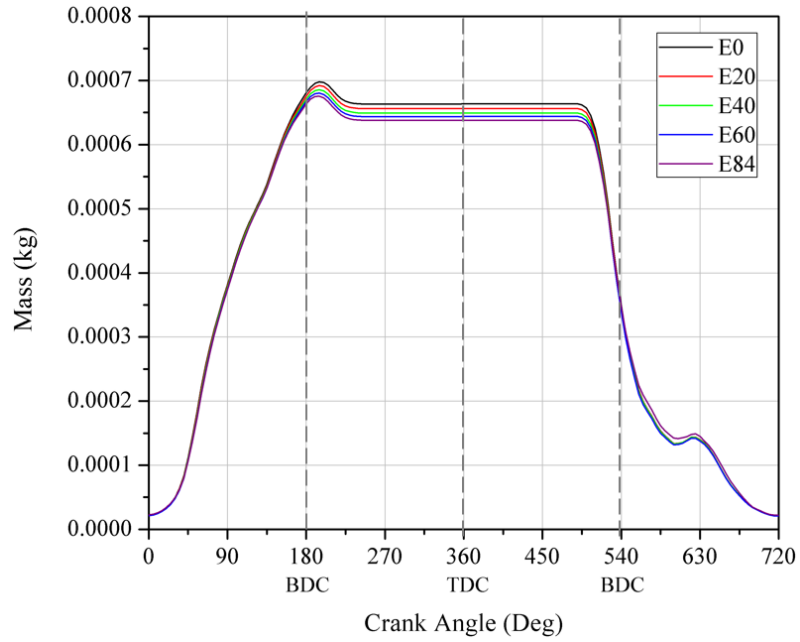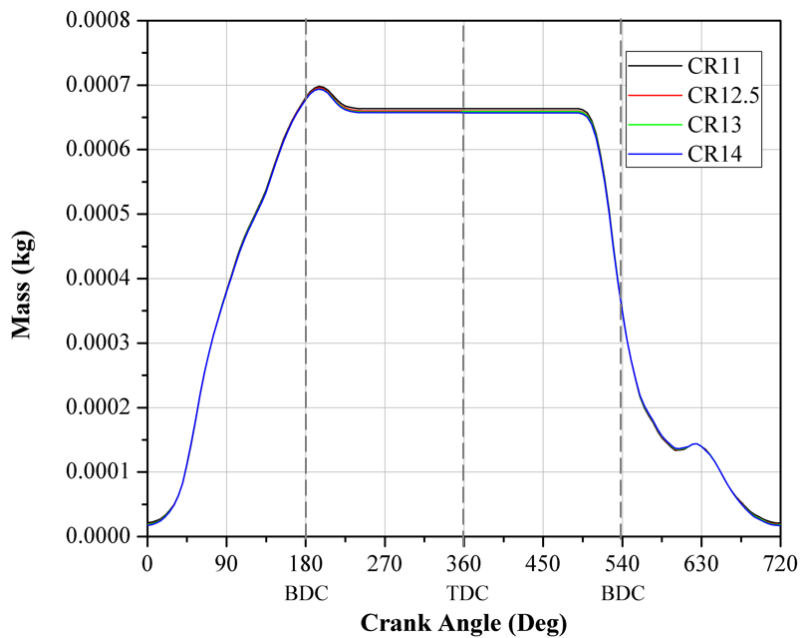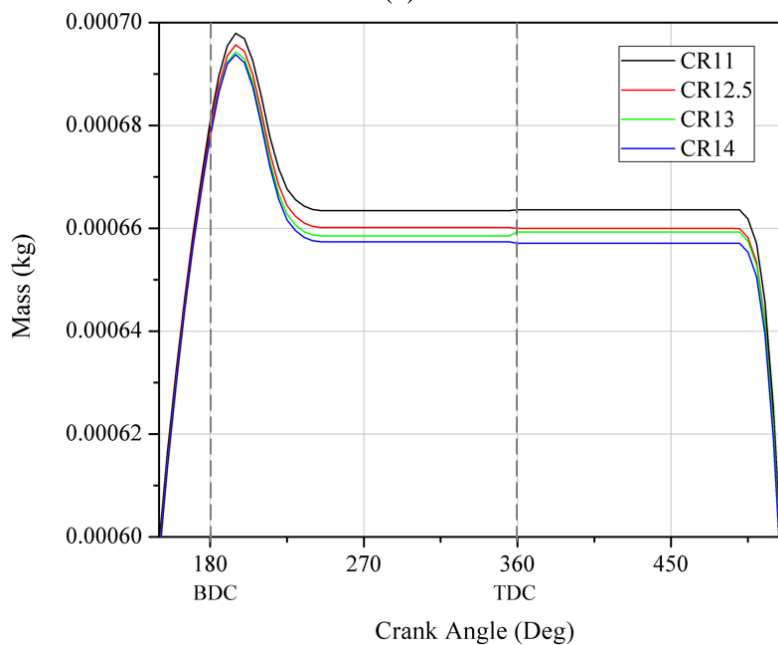
(a)
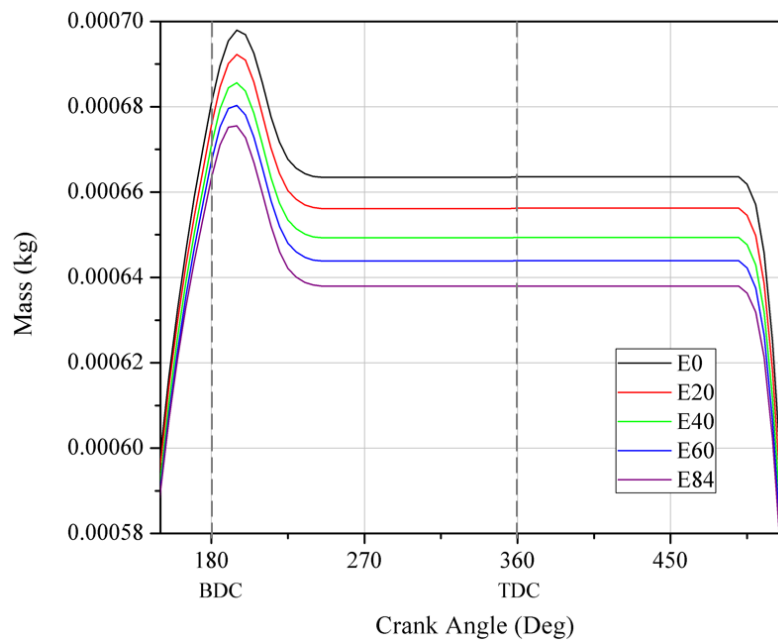
(b)

Figure 27. Mass inside Cylinder 1 at a compression ratio of 11, (a) From 0-720 Deg. (b) From 150-550 Deg.

Figure 28.Mass inside Cylinder 1 using an E0 blend, (a) From 0-720 Deg. (b) From 150-550 Deg.

Indeed, as the ethanol content of the fuel increases, the mass fraction of unburned ethanol increases by 3.8 times for the E84 mixture compared to the E20 mixture. Increasing the amount of unburned ethanol in the combustion gases leaving the cylinder allows typical combustion

emissions of this type of fuel such as formaldehydes and acetaldehydes to be generated, which can continue to form in the exhaust pipes and exit into the atmosphere. It is known that this type of emissions are toxic becoming carcinogenic to humans. On the other hand, it is observed in Figure 29 (b) that there are no variations for the mass fraction of ethanol for a mixture at different compression ratios.

Figure 29 (c) shows the variation of the NO mass fraction for the simulations performed. It is observed that for E0 and E20 mixtures there are no significant variations in the compression ratio, but for the other mixtures a small difference is evident. This fraction increases with respect to the alcohol content and decreases with respect to the compression ratios. The largest mass fraction of NO is presented for CR11 in mixture E84 with 0.00128.

Figure 29 (d) shows that for mixture E0 the mass fraction of CO is approximately 0.04, while for mixture E84 this value falls almost to zero. This is due to the low carbon content of ethanol, therefore, all carbon reacts in a complete combustion, not leading to the formation of CO, which is a toxic gas, also decreasing pollution.

As for the mass fraction of H_2O, there are no variations with respect to the compression ratio and it is increasing with the ethanol content in the fuel, except between mixtures E60 and E84, where it is almost constant. The mass fraction difference between mixtures E0 and E84 is 0.0049.
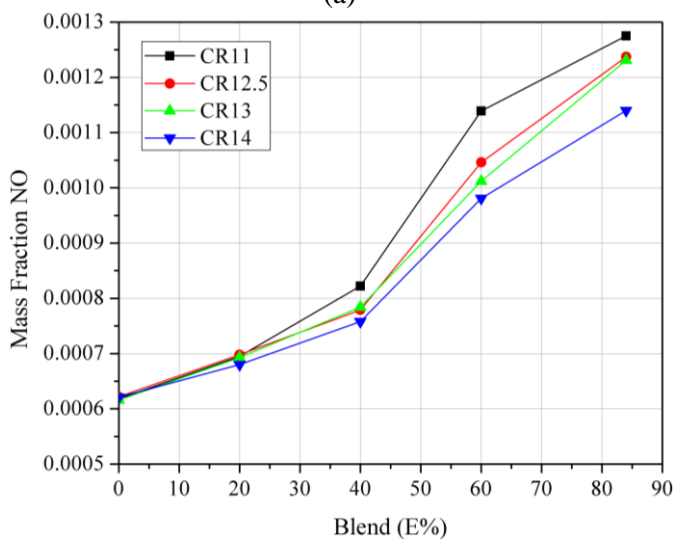
CO_2 is one of the most regulated pollutants currently, hence the importance of its analysis. Figure 29 (f) shows that the mass fraction increases with the ethanol content up to the E60 mixture, for the E84 mixture there is a fall in its value.
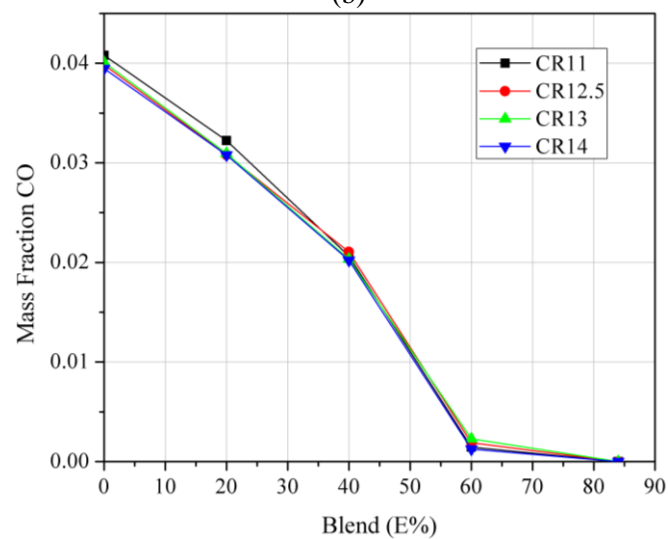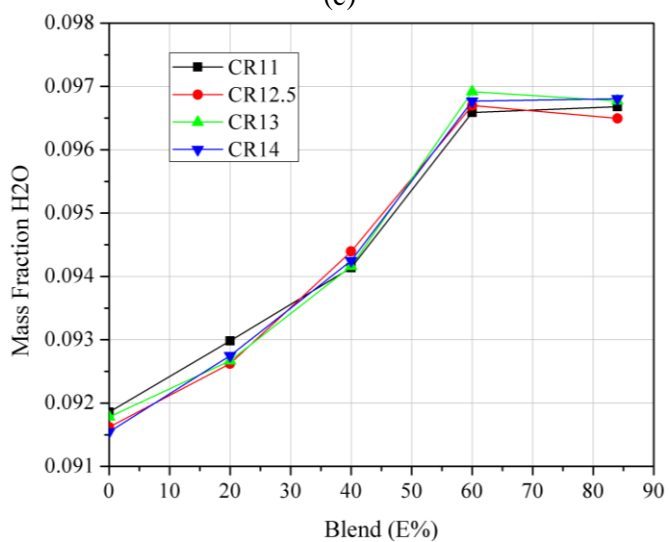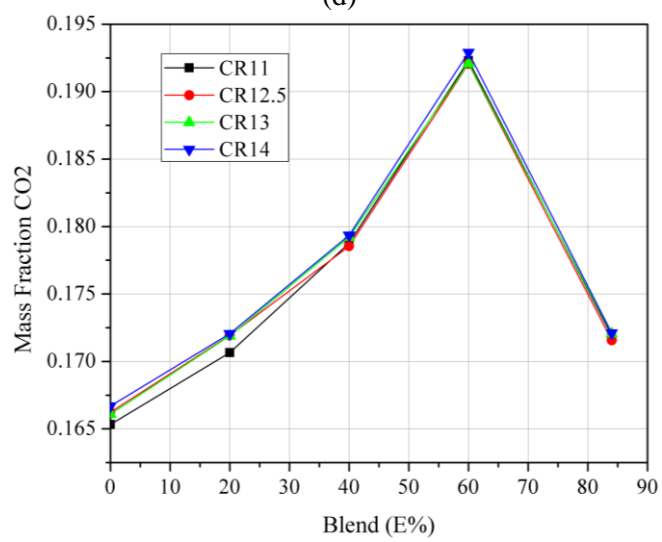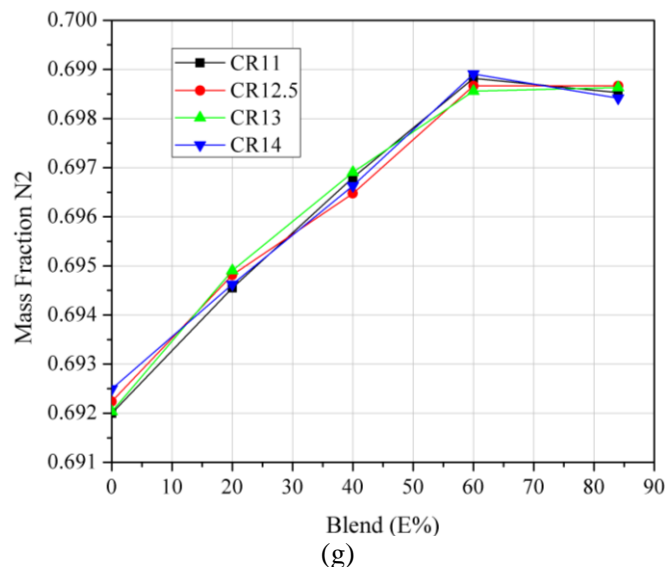
(a)

(b)

(c)

(d)

(e)

(f)

(g)
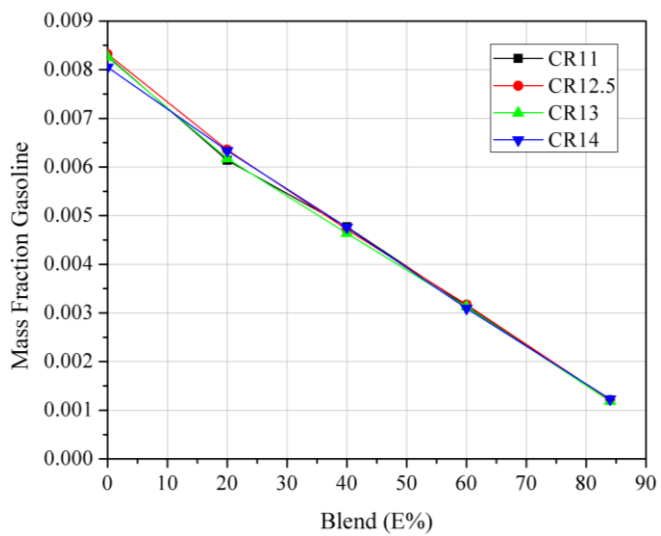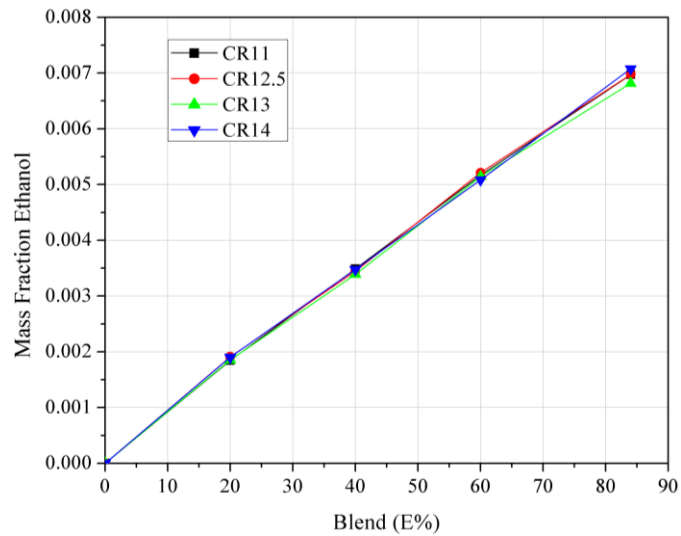
Figure 29. Mass fraction of combustion gases at the end of the high pressure cycle. (a) Gasoline. (b) Ethanol. (c) NO. (d) CO. (e) H_2O. (f) CO_2. (g) N_2.

As the ethanol content in the fuel increases, consumption increases and therefore it becomes necessary to increase the amount of air that must enter the cylinder to achieve a stoichiometric mixture, therefore, as the amount of air increases, the proportion of N_2 in the combustion gases increases, the increase of this species in the cylinder also increases the generation of pollutants of nitrogen oxides. The increase in the mass fraction of N_2 for E84 with respect to E0 was only 1%.

Figure 30 shows the behavior of the mass fractions of the species with respect to the crank angle for a mixture E20 simulated at a compression ratio of 11. In this figure it is observed that the point of inflection or change in behavior occurs around the combustion process, certain species increase their proportion, others decrease and others are created. Species such as O_2, gasoline, N_2, and ethanol decrease because these are the species that react to generate combustion, with the exception of N_2, which decreases its proportion because from this nitrogen oxides are generated, this fraction of mass is represented on the secondary axis of the graph. CO_2, H_2O and CO

increase, as they are the general products of a complete and incomplete combustion reaction for CO. Other species such as NO, HO_2, OH, among others in very small proportions are created during combustion.
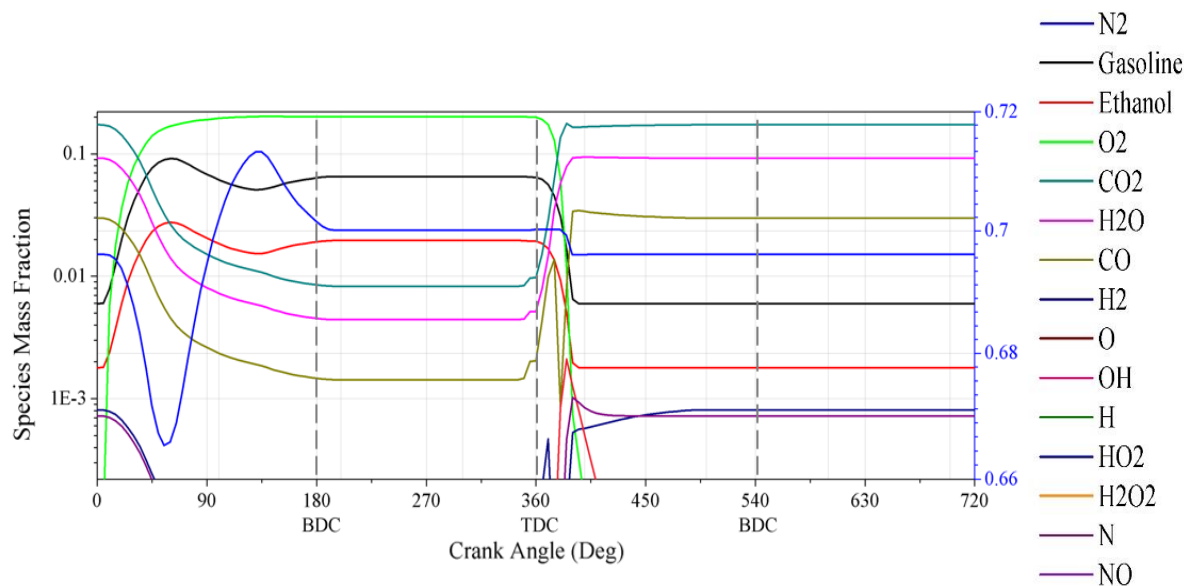
Figure 30. Behavior of chemical species as a function of the crank angle for the E20 mixture at a compression ratio of 11.

4.3 Pressure Curves

The pressure curves were taken from cylinder 1, BOOST takes the TDC at $0°$, but for a better visualization of the data, the TDC was moved to $360°$. The graph shows the pressure traces for the five ethanol-gasoline blends with respect to the degrees of rotation.

The pressure curves show the behavior of the pressure as a function of the crank angle. When the engine is run without combustion there is an increase in pressure due to the same movement of the piston inside the cylinder, and when combustion occurs, the pressure inside the cylinder increases considerably.

In Figures 31, 32 and 33 it can be observed that the pressure starts to increase in the compression stroke (after 180 deg) and a small peak occurs in the 360 deg curves, this is observed because the combustion has not yet developed before reaching the TDC. Shortly thereafter, already in the expansion race, the combustion causes the pressure to increase to its highest point to fall again.
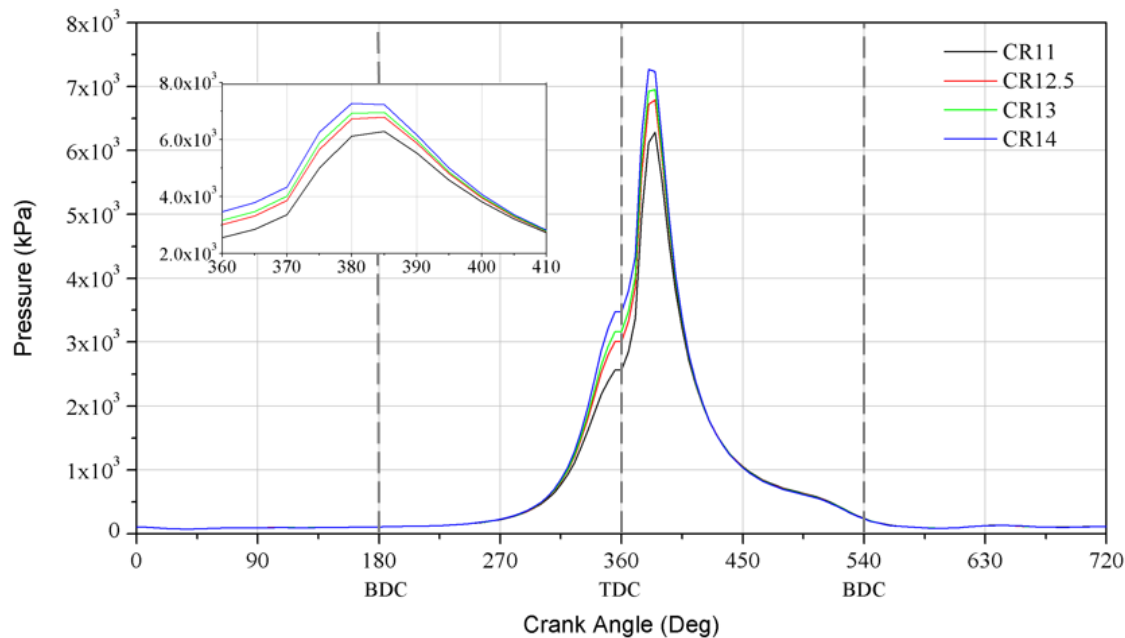
(a)
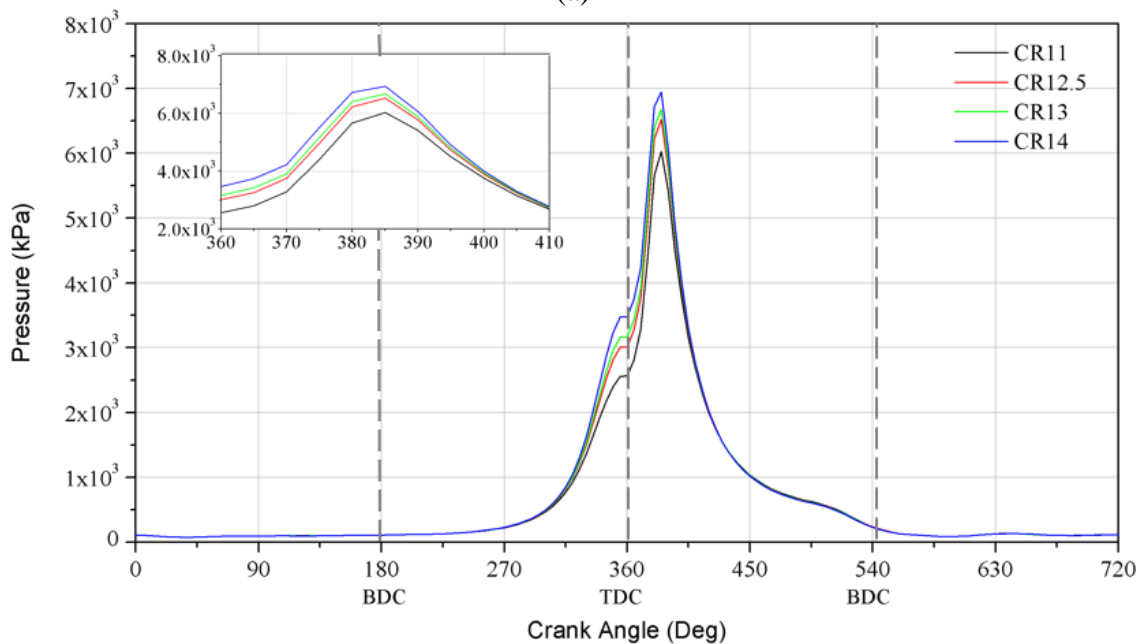
(b)

Figure 31. Pressure curves for (a) blend E0 (b) blend E20.
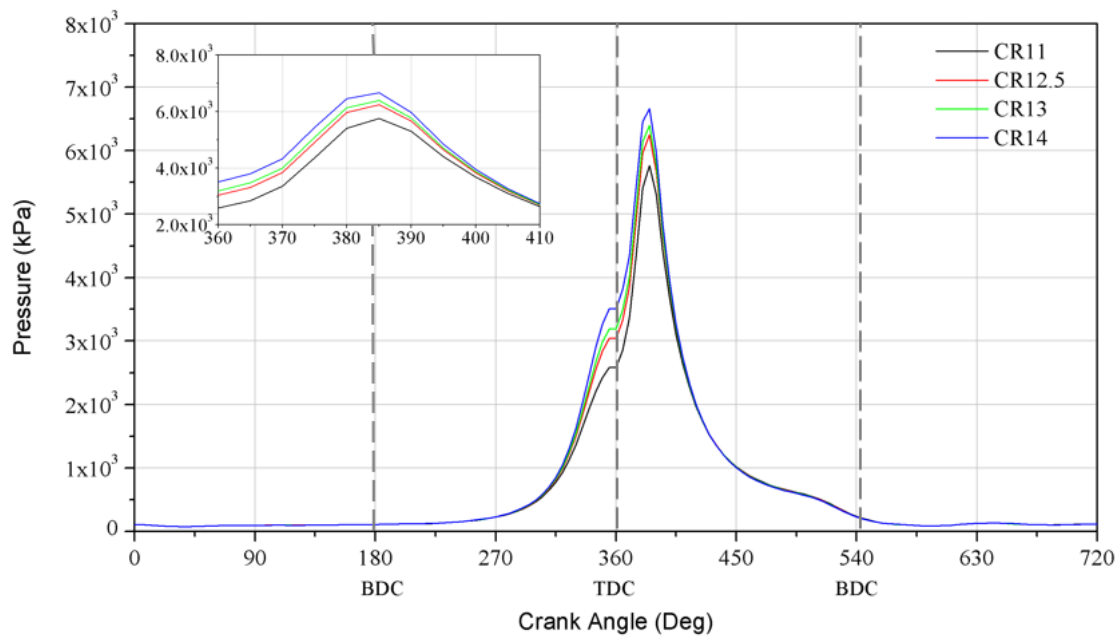
(a)
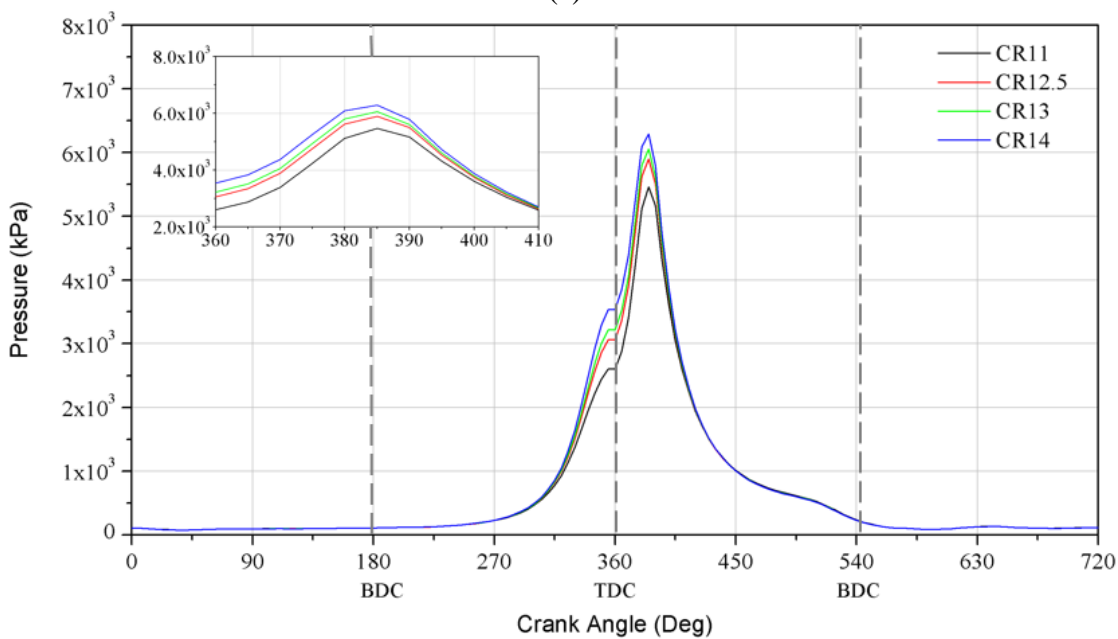
(b)

Figure 32. Pressure curves for (a) blend E40 (b) blend E60.

The fact that the maximum pressure peak due to combustion occurs in the expansion stroke shows that the operation of the engine is not optimal. Therefore, it is desirable to set the start of the spark at an angle that achieves the maximum possible torque (MBT).

It is also observed that in all ethanol and gasoline blends, the pressure curve was higher for higher compression ratios, which makes sense, as higher compression ratios lead to higher operating pressures.
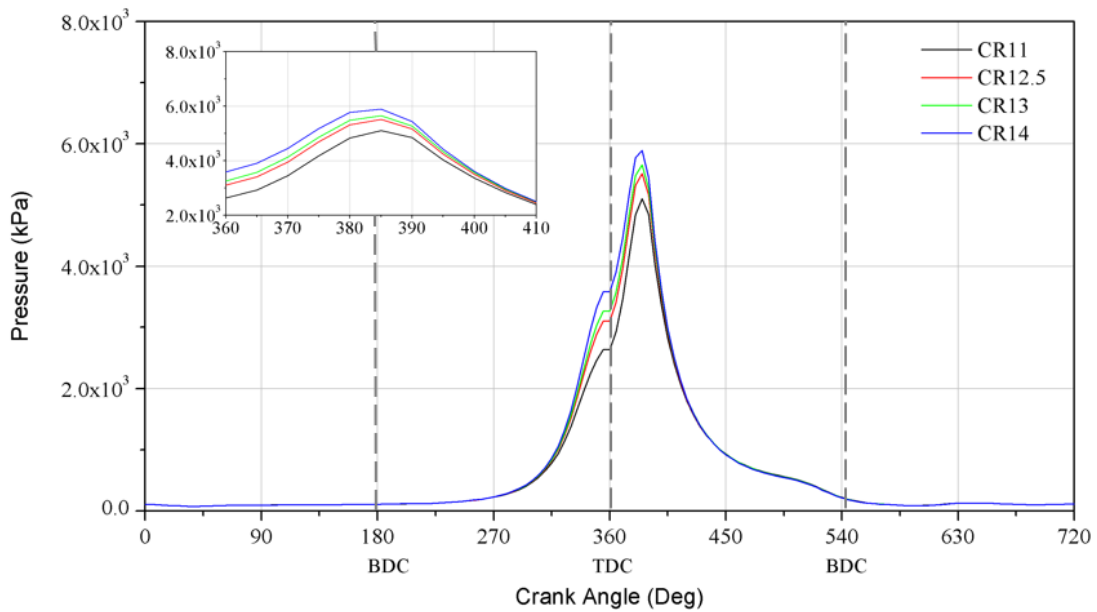
Figure 33. Pressure curves for blend E84. Source.

Figure 34 shows the highest pressure values achieved for each simulation, i.e., the pressure peaks shown in Figures 25, 26, 27, 28 and 29. For a compression ratio of 11 (in which gasoline achieves normal combustion), the pressure drop for E84 with respect to pure gasoline was 19.5%, while the pressure drop for E84 but using a compression ratio of 14 is 6.8%.
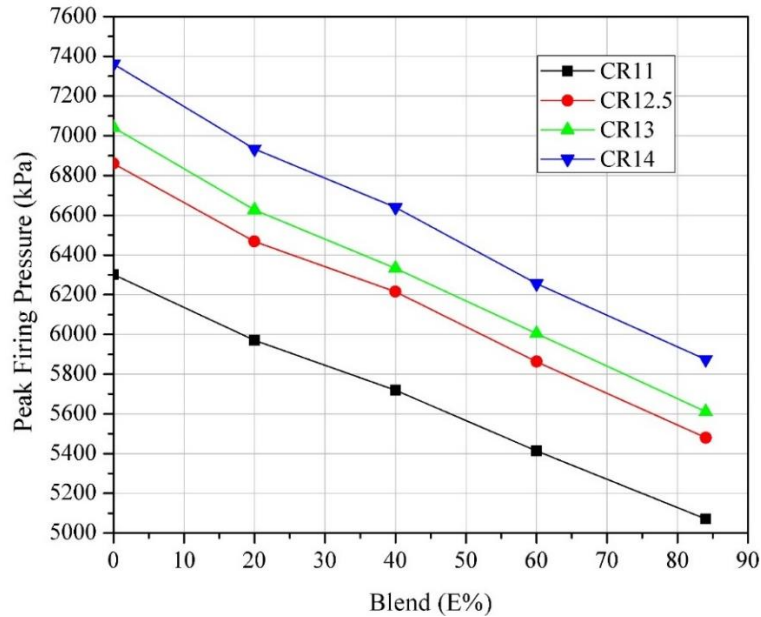
Figure 34. Peak Firing Pressure for each blend of ethanol-gasoline.

For each simulated compression ratio, the pressure peak decreased with increasing ethanol content following a linear slope function between -14 and -17.5, this is also due to the decrease in the calorific capacity of the mixtures. On the other hand, from Figure 34 it can be appreciated the importance of handling the adequate compression ratio, since gasoline with ethanol increases its octane rating allowing higher compression ratios and thus obtaining higher pressure and therefore torque values. For E20 the difference between CR11 and CR14 was 16% which is significant.

As for the angle after TDC where peak pressure occurs, it increases 1.97 deg from E0 to E84 for CR11, which also evidences the decrease in pressure. On the other hand, the maximum peak pressure decreases with the increase of the compression ratio between 1 and 1.5 deg (See Figure 35).
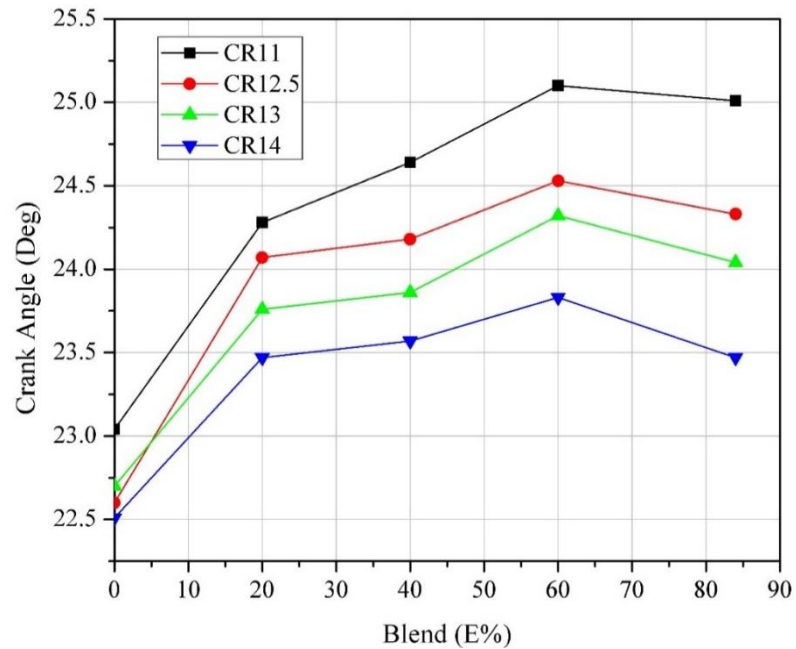
Figure 35. Crank angle after TDC where pressure peak occurs.

The P-V diagram was made for the simulations of E0 at a compression ratio of 11 and E84 at a compression ratio of 14. The curves of Figure 36 show the typical behavior for the Otto cycle, identifying each of the processes (intake, exhaust, compression, combustion and expansion), where the combustion process is performed almost at constant volume. It is observed that the area of the curve for E0 is a little larger than for E84 although it reaches values of smaller volumes, due to the higher compression ratio.
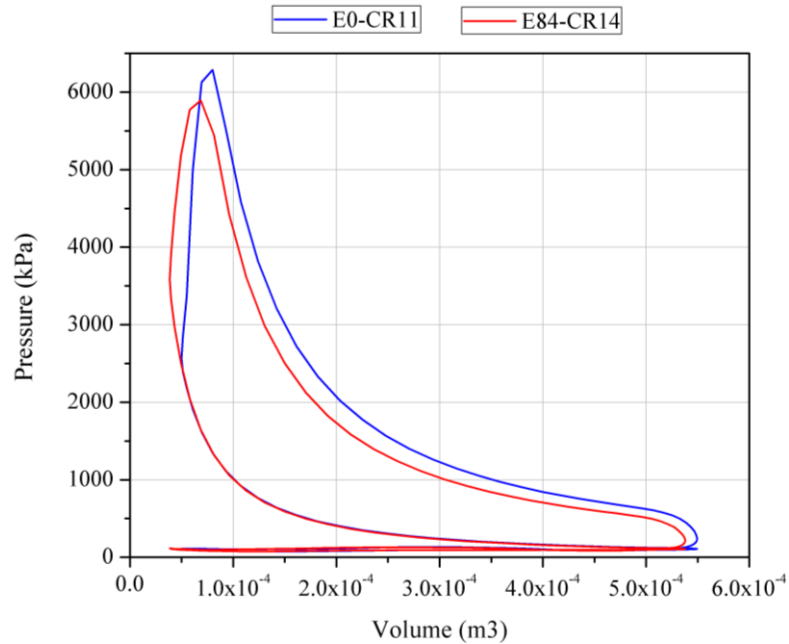
Figure 36. PV diagram for mixture E0 to RC11 and E84 to RC14.

4.3 Efficiencies

Mechanical efficiency is the ratio of the brake power delivered by the engine to the indicated power, where the brake power is equal to the difference between the indicated power and the brake power. It can be seen in Figure 37 that mechanical efficiency decreases as the ethanol content in the fuel increases, and since the friction power for this case was taken as a constant for all simulations, this decrease in efficiency is due to a decrease in the indicated power.

Also, it is observed that the behavior with respect to the compression ratio is that, as the compression ratio increases, the mechanical efficiency and therefore the indicated power also increase.
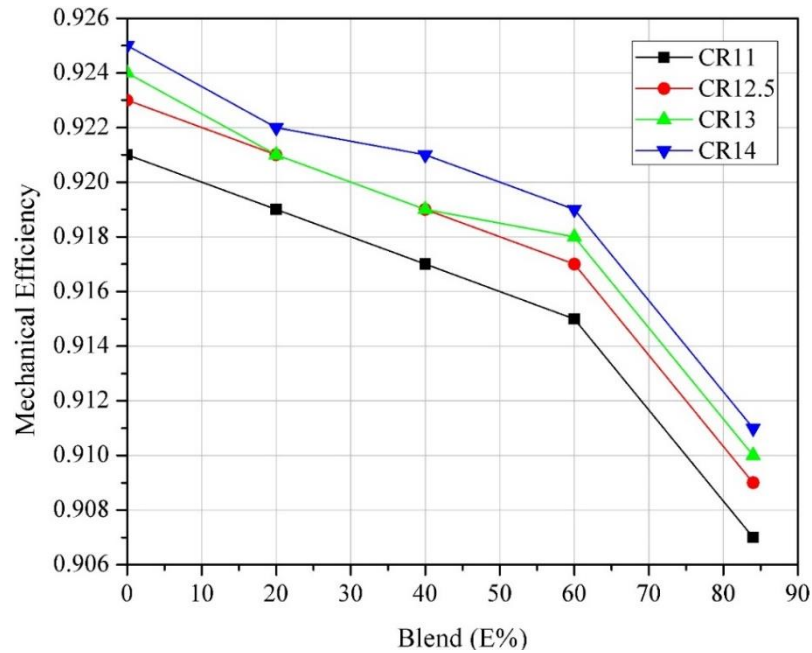
*Figure 37.*Mechanical Efficiency for each blend of ethanol-gasoline.

There is a drop in mechanical efficiency of about 1.5% when using a mixture of E84 versus pure gasoline for each CR. On the other hand, by increasing the compression ratio for the E84 blend from 11 to 14, a gain of less than 1% was achieved.

This shows that the mechanical efficiency does not suffer significant changes either with the variation of the compression ratio, nor with the variation of the ethanol content and since this depends on the friction power, which depends on the rotation speed of the engine, there could be changes when varying the rpm at which the model was simulated, but these changes are not part of this project.

AVL-BOOST defines fuel conversion or indicated efficiency by the Equation 63, since it relates the work done on the energy released by a mass of fuel.

$$n_T = \frac{\int_{CD} p_c dV}{m_{C,FV} \cdot H_u} \quad (63)$$

The overall performance of the fuel conversion efficiency is to increase along with the ethanol content and the compression ratio. It is observed that the values of this efficiency are between 29% and 38%. The efficiency increase indicated for E84 with respect to pure gasoline in RC11 is 27%. On the other hand, the increase for E84 using an RC14 over an RC11 is 5%.
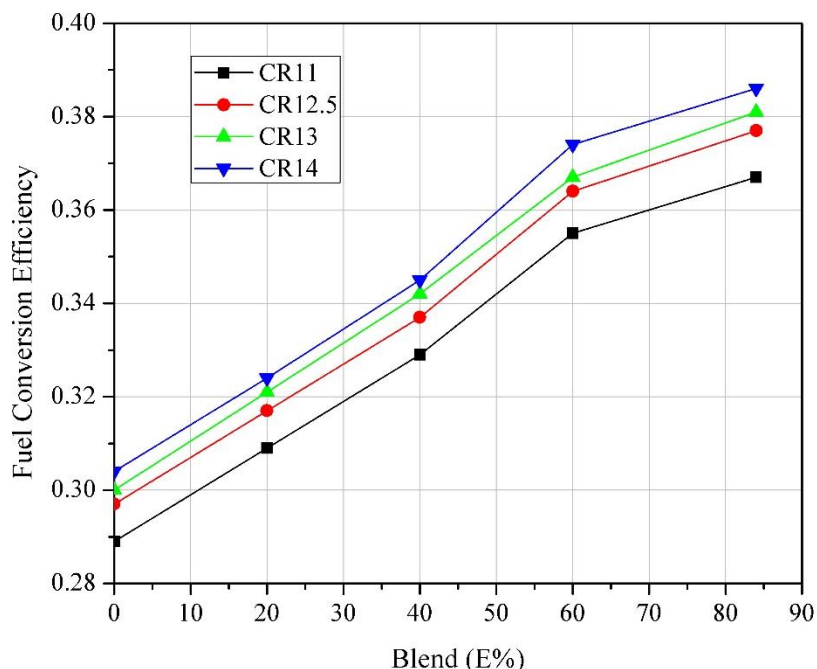
*Figure 38.*Fuel Conversion Efficiency for each blend of ethanol-gasoline.

Because in any combustion process the exhaust gases will have both complete combustion products and incomplete combustion products, the total chemical energy of the fuel cannot be released into the engine during combustion, and this is what measures combustion efficiency, the ratio of the energy released to the total chemical energy contained in the fuel.

By looking at Figure 39 it is determined that for all simulations for compression ratios of 11, 12.5 and 13 the combustion efficiency was the same, i.e., the proportion of the chemical energy released and the total fuel was equivalent. For the compression ratios of 11 the difference in efficiency between E0 is only 3%. On the other hand, the efficiency for simulations at a

compression ratio of 14, although not exactly the same, are very close and the differences are below 0.2%.
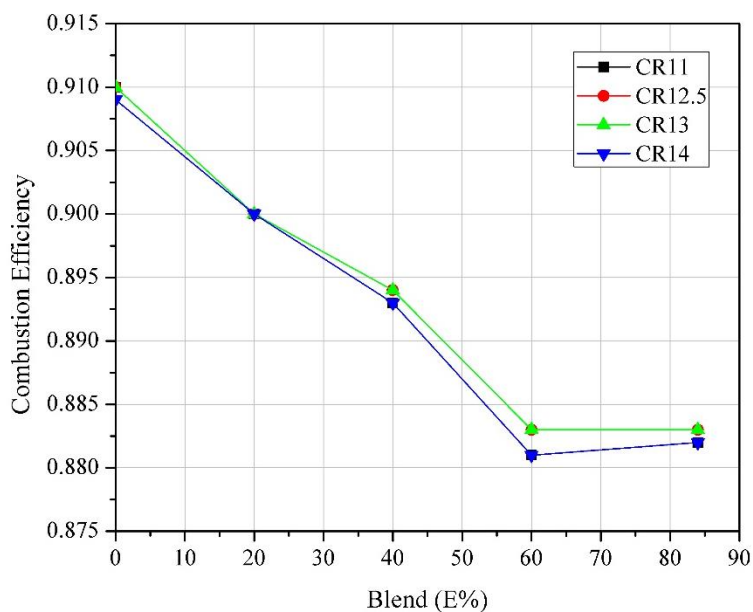
*Figure 39.*Volumetric Efficiency for each blend of ethanol-gasoline.

Figure 40 is presented by way of illustration, since this efficiency represents, in a single efficiency value, the fuel conversion and combustion efficiencies.
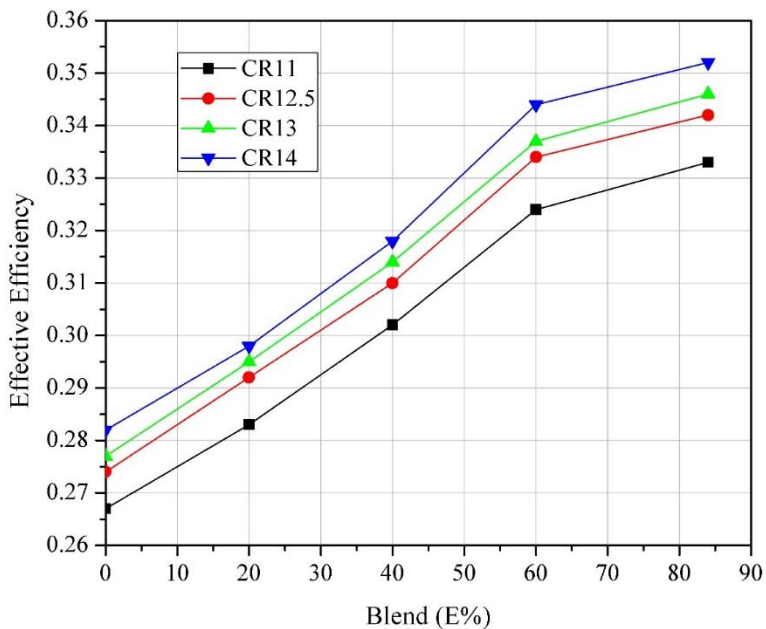
Figure 40. Effective Efficiency for each blend of ethanol-gasoline.

Thermal efficiency is defined as the relationship between the works done by a machine on the amount of heat entering the system as shown in Equation 64. Therefore, in order to calculate the thermal efficiency of the motor, the work performed for each simulation must be calculated from the effective power (Figure 21) and the heat released obtained from BOOST under the name effective released energy.

$$\eta_t = \frac{W}{Q_{Release}} \quad (64)$$

The power values obtained are given per cycle. A cycle is comprised of 720 degrees, i.e., two revolutions of the crankshaft. And, knowing that the engine has a speed of 2500 rpm it is possible to know the time in seconds for 1 cycle.

$$t = \frac{2\ rev}{2500\ rpm * \frac{1\ min}{60\ s}} = 0.048\ s$$

Then, the work is equal to the product between power and time. Table 18 presents the data for the work and Table 19 presents the values of the effective heat released.

Table 18

Work per cycle for each simulation

	Work kJ			
	11	12.5	13	14
E0	2.60	2.67	2.69	2.73
E20	2.50	2.57	2.59	2.63
E40	2.44	2.52	2.53	2.57
E60	2.38	2.45	2.47	2.51
E84	2.16	2.21	2.24	2.27

.

Table 19

Effective Released Energy for each simulation.

	Effective Released Energy (kJ)			
	11	**12.5**	**13**	**14**
E0	6.54485	6.56193	6.55935	6.56389
E20	6.41344	6.42616	6.42545	6.44066
E40	6.34156	6.36254	6.35279	6.37247
E60	6.24372	6.25165	6.26312	6.27358
E84	5.59532	5.58226	5.5954	5.60441

The thermal efficiency presented in Table 20 and Figure 41 is calculated from the data shown above.

Table 20

Thermal Efficiency for each simulation

	Thermal Efficiency			
	11	**12.5**	**13**	**14**
E0	0.40	0.41	0.41	0.42
E20	0.39	0.40	0.40	0.41
E40	0.38	0.40	0.40	0.40
E60	0.38	0.39	0.39	0.40
E84	0.39	0.40	0.40	0.41

The Figure 42 shows a decrease in thermal efficiency with the increase of ethanol up to the E60 mixture for the same compression ratio, i.e., the same engine used with different ethane and gasoline fuels is less efficient for the fuel with lower calorific value. For the E84 mixture a different behavior was observed, because the thermal efficiency increased, that is to say, the

engine took better advantage of the heat delivered by the fuel, in numerical terms the increase took place because, although both the work and the released energy decreased with respect to the previous mixture, the decrease of the heat was in a greater proportion than that of the work, and since the thermal efficiency had an inverse proportional relation to the released heat, higher values of thermal efficiency were presented. For all compression ratios the thermal efficiency between E0 and E60 fell by approximately 1.5% and increased by only 0.5% between E60 and E84.
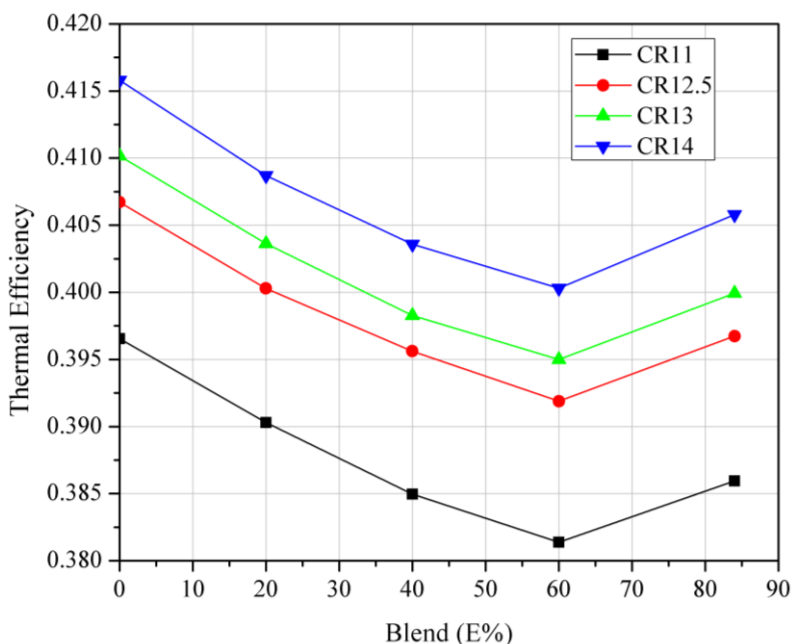
Figure 41. Thermal efficiency.

The thermal efficiency of an ideal Otto engine is given as a function of the compression ratio as shown in Equation 65. This equation shows that the higher the compression ratio the greater the thermal efficiency in the ideal Otto cycle. Therefore, it is this same behavior that is observed in the calculated thermal efficiency, which increases by about 5% for CR14 with respect to CR11.

$$\eta_t = 1 - \frac{1}{r_c^{\gamma-1}} \quad (65)$$

4.4 Heat Transfer

AVL BOOST calculates the temperature from the energy conservation equation (first law of thermodynamics), together with the gas equation. Therefore, the temperature at each angle of the crankshaft depends on factors such as: entering fuel mass, fuel heat capacity, fuel evaporation heat, cylinder pressure, heat loss, among others.

Figure 43 shows the behavior of the temperature with respect to the crank angle, in this case for the E0 mixture, although for all other mixtures the trend remains the same. There, it is observed that like the pressure curve, the temperature curve begins to increase in the compression stroke, reaching its highest peak at some point during the combustion process (See Figure 42). Then it begins to decrease during the expansion and exhaust strokes showing some temperature rises near 640 deg, i.e., during the exhaust of gases, which can be caused by reactions of unburned hydrocarbons or other elements.

Similar to pressure, each fuel mixture at a certain compression ratio has different temperature peaks at different angles, as shown in Figure 43. As expected, temperature peaks were decreasing for higher ethanol contents. For E84 the temperature decreased by 87 °C with respect to pure gasoline for CR11. Similarly, for each ethanol-gasoline mixture there was an average decrease of 15.5 °C between RC11 and RC14, without taking into account pure gasoline, as mentioned above, at high compression ratios present self-ignition.
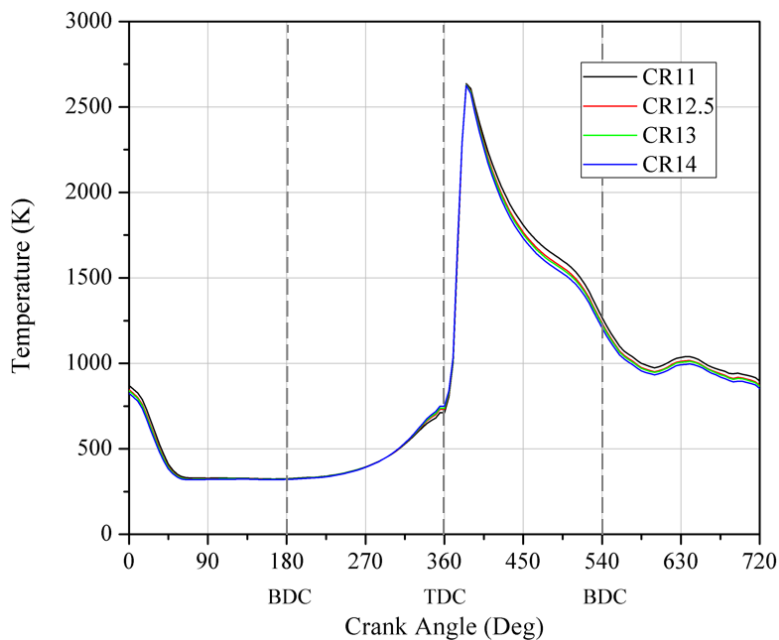
Figure 42. Temperature behavior according to crank angle in Cylinder 1 using E0.
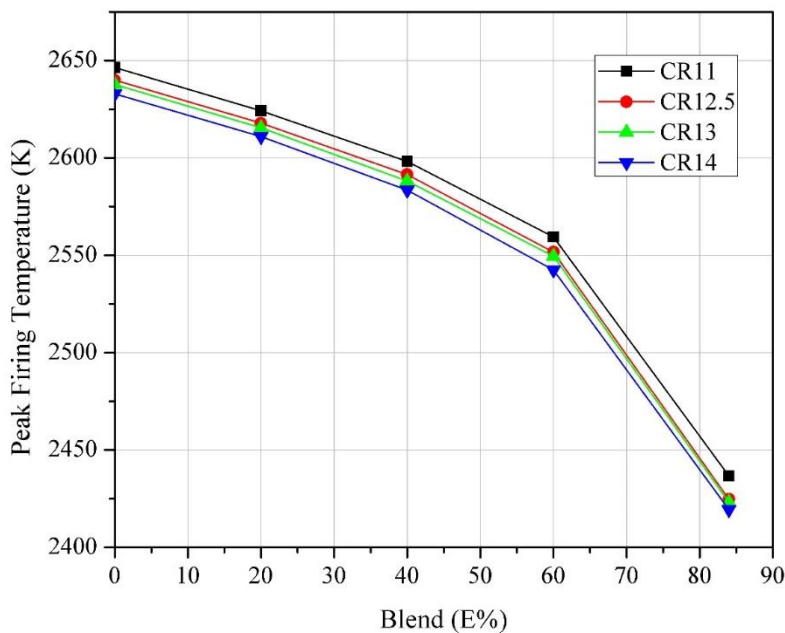
Figure 43. Peak Firing Temperature for each blend of ethanol-gasoline.

For the angle at which the peak of maximum temperature occurs (See Figure 44), it

increases up to mixture E60 and remains almost constant for E84. An average of 4.6 deg between

mixtures E0 and E84 is presented for all compression ratios. In addition, it should be noted that the change in peak temperature and crank angle where this happens are not very significant to vary the compression ratio.
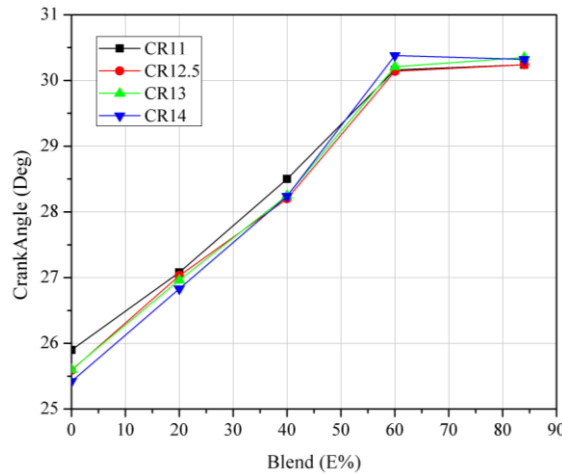
Figure 44. Crank angle where temperature peak occurs.

From the temperature curve as a function of the crankshaft angle, the mean Wall heat transfer temperature, the Wall heat transfer coefficient depending on crank angle and the temperature gas as shown in the Equation 66, AVL-BOOST calculates the mean effective temperature for wall heat transfer in the cylinder. This temperature (See Figure 45) presents a decreasing behavior as the ethanol content increases due to the higher amount of fuel but with lower calorific value, also, the decrease of the temperature is due to the higher vaporization heat of the ethanol against the gasoline, creating a cooling load inside the cylinder when the fuel evaporates. As for the compression ratio, the average temperature increases as higher pressure conditions are created inside the cylinder.

$$T_{g,eff} = \frac{1}{CD * \overline{h_w}} \cdot \int T_G(\alpha) \cdot h(\alpha) \cdot d\alpha \quad (66)$$
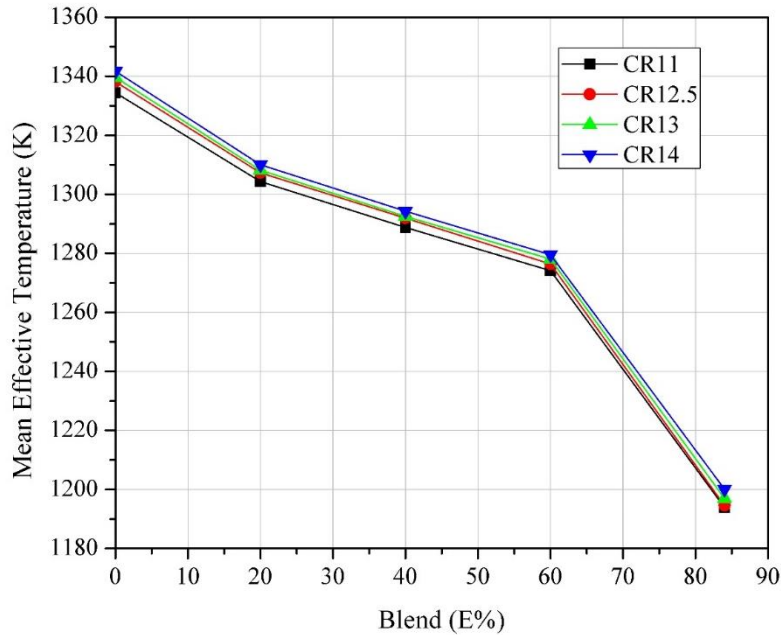
*Figure 45.*Mean Effective Temperature for each blend of ethanol-gasoline.

The heat transfer to the walls of the combustion chamber, i.e., the cylinder head, the piston, and the cylinder liner, is calculated from Equation 67.

$$Q_{wi} = A_i \cdot \alpha_w \cdot (T_c - T_{wi}) \quad (67)$$

Therefore, the amount of heat that is lost through the walls depends directly on the value of the heat transfer coefficient. Figure 46 shows the curves of each compression ratio for the mean effective heat transfer coefficient, which decreases as the ethanol/gasoline mixture increases and increases at high compression ratios. This coefficient is calculated by the Woschni model, which was the heat transfer model selected for the simulations. The heat transfer coefficient value represented in Figure 46 is a mean value, i.e., the average of all values in each crank angle evaluated by the program.

The reduction in the mean effective heat transfer coefficient between mixtures E0 and E84 is approximately 6% for all compression ratios. This coefficient depends on several

variables, which make this increase with the compression ratio, between compression ratios 11 and 14 there is an increase of about 10% for all mixtures.

As said before, the heat lost through the walls depends on the heat transfer coefficient and, on the temperature of the gas inside the cylinder. Both the heat transfer coefficient (Figure 46) and the temperature inside the cylinder (Figure 45) decrease with the increase in ethanol content, therefore, and as presented in Figure 47, the lost heat also decreases under this same criterion. The difference in energy lost between mixtures E0 and E84 is around 210 J. On the other hand, at the compression ratio of 14 there are greater energy losses, with an increase of approximately 6% for all the mixtures.
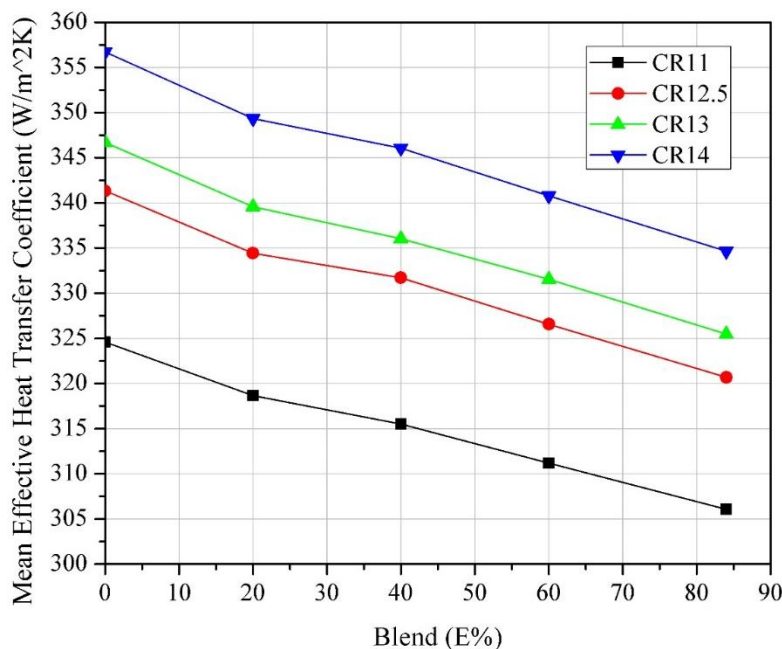
*Figure 46.*Mean Effective Heat Transfer Coefficient for each blend of ethanol-gasoline.
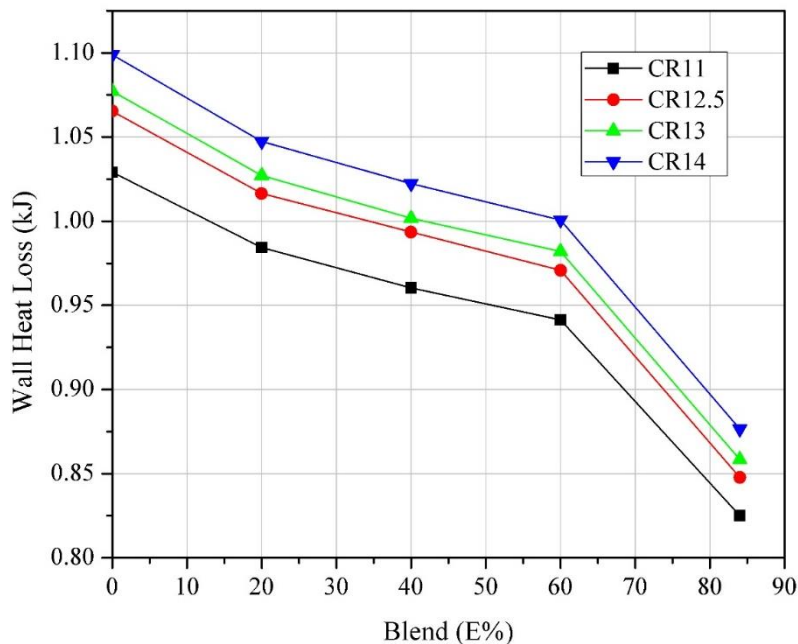
Figure 47. Wall Heat Transfer for each blend of ethanol-gasoline.

4.5 Fuel economy

On the other hand, a brief economic analysis will be carried out to determine the cost for one gallon of each of the mixtures in Colombia. For the above, the price of gasoline and fuel ethanol in Colombia was consulted and the price was determined based on the volumetric composition of each blend.

As of November 2019, the price of gasoline for the City of Bogota is $9,705/gal (Ministry of Mines and Energy, 2019) and that of fuel ethanol is $7,862/gal. The price to calculate will be per gallon of each of the mixtures (FedeBiocombustible, 2019).

Table 21 shows that the gallon of pure gasoline is $1,474 more expensive than the gallon of an E84 blend, which represents a significant long-term savings. But in Colombia this high ethanol blend is not used due to lack of regularization, in addition neither transportation fleet nor the physical infrastructure are conditioned to handle this percentage. Therefore, although it is not

part of this study was calculated the price of a gallon of fuel for the mixture E10, which is the

mixture currently regulated by resolution 40181 of 2018. The price difference is $184.

Table 21

Cost of 1 gallon of each of the simulated ethanol-gasoline blends

	Gaso line	Etha nol	Cost
E0	1	0	$ 9.705
E10	0,9	1	$ 9.521
E20	0,8	0,2	$ 9.336
E40	0,6	0,4	$ 8.968
E60	0,4	0,6	$ 8.599
E84	0,2	0,8	$ 8.231

The previously mentioned savings must be analyzed under specific conditions, that is, if

the fuel is going to burn in the same engine as for the gasoline, it is possible that there is not

really an economic saving, since the engine does not have the necessary conditions for a correct

ethanol combustion, there will be greater fuel consumption which would balance the prices.

On the other hand, as described for Figure 21, there are combinations of mixture and

compression ratio that obtain power values very similar to those of pure gasoline at a

compression ratio of 11, that is, E20 at a compression ratio of 12.5 and 13 and E40 with a

compression ratio of 14.

Therefore, in order to determine from the point of view of fuel cost if the use of ethanol is

viable, the cost of producing the power shown for each of the points taken will be calculated. For

this, the power data indicated for a cycle will be taken, since data is available for the specific fuel

consumption indicated. Additionally, as previously calculated, the time in seconds needed to

perform a cycle at 2500 rpm is 0.048 seconds, kWh is calculated.

From the kWh and together with the IFSC the amount of fuel mass needed is calculated (Table 22), this mass is divided according to the corresponding proportion of the mixture, and it is converted into volume from the density, from where the final price is obtained.

Table 22

Indicated power, work, isfc and total mass for the selected simulations.

	Indicated Power (kW)	kWh	isfc (g/kWh)	Mass (kg)
E0-CR11	58.69	7.8253E-04	286.0634	2.239.E-04
E20-CR12.5	58.21	7.7613E-04	284.2576	2.206E-04
E20-CR13	58.21	7.8200E-04	281.7847	2.204E-04
E40-CR14	58.21	7.7613E-04	282.9499	2.196E-04

Table 23

The cost of the fuel required to achieve the specified engine power for each mixture.

	Mass		Volume		Cost	
	Gasoline	Ethanol	Gasoline	Ethanol		
E0-CR11	2.239E-04	0.000E+00	8.213E-05	0.000E+00	$	0.797
E20-CR12.5	1.732E-04	4.743E-05	6.354E-05	1.586E-05	$	0.741
E20-CR13	1.730E-04	4.738E-05	6.347E-05	1.584E-05	$	0.740
E40-CR14	1.269E-04	9.272E-05	4.656E-05	3.100E-05	$	0,696

For about the same amount of power, the decrease in fuel cost is $0.101/cycle between mixture E0 to RC11 and mixture E40 to RC14. Therefore, it is concluded that in economic terms the use of fuel ethanol is viable, due to its lower price compared to ethanol.

Conclusions

Torque and Power decrease for higher concentrations of ethanol in gasoline and increase as cylinder compression ratio increases. There was a 17% decrease in torque and power for the E84 mixture versus gasoline. In turn, mixtures such as E20 at a compression ratio of 13 and E40 at a compression ratio of 14 obtained torque and power values similar to those of gasoline, demonstrating that it is possible to improve the performance of biofuels if they are burned under specific conditions, as different from those of gasoline.

The lower calorific value of ethanol implies higher specific consumption of gasoline the higher the percentage of mixture in gasoline. For the E84 mixture there was an increase of around 16% of the bsfc compared to gasoline, decreasing to 9.7% the specific consumption increase if the E84 mixture is burned at a compression ratio of 14. There are also alternative mixtures that compare the bsfc of gasoline: E20 to RC12.5, E40 to RC13, and E60 to RC14.

AVL BOOST does not capture the formation of formaldehydes and acetaldehydes because the internal calculations for the determination of the mass fractions of each species that compose the exhaust gases are carried out via chemical equilibrium. It would be necessary to use a mechanism of chemical kinetics for the numerical determination of this type of emissions.

The intake valve remains open for 70 degrees after the BTC in the compression stroke which causes a backflow that decreases the mass inside the cylinder, therefore, the engine intake characteristics do not represent the right conditions for the rotation speed regime used.

Composition of the gases products of the composition do not vary significantly with the compression ratio. The mass fraction for unburned gasoline and CO decreases with increasing ethanol content, the latter being almost zero for the E84 mixture. As for the mass fractions for the rest of the species (ethanol, NO, H_2O, CO_2 and N_2), the relationship with the ethanol content is directly proportional.

The maximum peak in the pressure curves occurs after the TDC, i.e., during the expansion stroke, which causes the pressure inside the cylinder to decrease with respect to that which can be reached. Therefore, the spark angle can be advanced to achieve better yields. Higher compression ratios produce higher pressure values, and conversely the ethanol content decreases these values.

There are different efficiencies that show the performance of an internal combustion engine at mechanical, chemical and thermodynamic levels. The mechanical efficiency measures the proportion of power lost by friction of the mechanical elements of the engine, with a constant friction power for all the simulations the mechanical efficiency decreased with respect to the ethanol content and increased with the compression ratio.

The thermal efficiency for the simulations was between 41% and 38%, typical values for gasoline engines. The decrease in temperature inside the cylinder for higher ethanol blends decreased the thermal efficiency, with a variation for E84 where it increased.

The price per gallon of gasoline with respect to the E84 blend would be $1,474 more expensive, due to the subsidized price of ethanol in the country. The mixture of regulated gasoline in E10 and under the methodology used for the approximate calculation of a market price, acquiring a gallon of this type of fuel means a saving of $184 for users.

Specific combinations of ethanol content and compression ratio achieve power values similar to those of gasoline: E20-CR12.5, E20-CR13, and E40-CR14. With these mixtures, yields equivalent to those of gasoline are achieved with lower fuel costs.

Ethanol is a biofuel that is currently booming due to the need and importance of protecting the environment and complying with increasingly stringent environmental laws. But despite its advantages as a biological product, there are still pollutant emissions that need to be reduced, especially aldehyde emissions. Therefore, the parameters and characteristics of the engines must be adjusted to take maximum advantage of the properties of ethanol and minimize the pollution produced.

From the literature review, it is concluded that automobiles in Colombia do not have the necessary capabilities to burn ethanol properly, which could present economic problems, physical damage to automobiles and an increase in the concentration of emissions of aldehydes and nitrogen oxides despite the decrease in CO_2 and CO.

Recommendations

For further work based on the present, it is recommended to initially conduct an experimental investigation on a spark ignition engine, of which the geometry data is known previously, and to determine by analysis of its pressure curve the values for the Vibe function for different ethanol-gasoline mixtures.

If possible, it is recommended to determine the Vibe function of two zones, since AVL BOOST will be able to determine the formation of chemical species during the combustion process with greater precision, achieving more realistic values in terms of formaldehyde and acetaldehyde formation

References

Agencia Nacional de Petróleo. (s.f). Etanol. Recuperado de: http://www.anp.gov.br/producao-de-
biocombustiveis/etanol

Agencia Nacional de Petróleo. (2019). Etanol. Recuperado de:
http://www.anp.gov.br/biocombustiveis/etanol

Álvarez, J., Callejón, I., Forns, S., Balsells, D., Casanova, J., Bonet., O.,… Villa, J. (2005).
Motores alternativos de combustión interna. Barcelona, España: Edicions UPC.

Amaris, J., Manrique, D., y Jaramillo, J. (2015). Biocombustibles líquidos en Colombia y su
impacto en motores de combustión interna. Una revisión, *Fuentes: El Reventón
Energético, 13* (2), 23-34. Recuperado de
https://revistas.uis.edu.co/index.php/revistafuentes/article/view/5236/5538

ANSYS. (2019). ANSYS CFX. Recovered: https://www.ansys.com/products/fluids/ansys-cfx

ANSYS. (2019). ANSYS Fluent. Recovered: https://www.ansys.com/products/fluids/ansys-
fluent

Arshad, M. (2018). *Optimization of chemical kinetic mechanism for efficient computation of combustion process in advanced internal combustion engine configuretions* (Doctoral dissertation). Florida Institute of Technology, U.S.

Asociación de Empresas de Energías Renovables. (2018). ¿Qué es la biomasa?. Recuperado de: https://www.appa.es/appa-biomasa/que-es-la-biomasa/

AVL. (2019). AVL BOOST. Recovered: https://www.avl.com/boost

AVL FIRE. (2019). AVL FIRE. Recovered: https://www.avl.com/fire

Barros, P., & Sodré, J. (2016). Simulation of Aldehyde Emissions from an Ethanol Fueled Spark Ignition Engine and Comparison with FTIR Measurements. *In Journal of Physics: Conference Series, 745* (3), 1-8. Recovered from https://iopscience.iop.org/article/10.1088/1742-6596/745/3/032023/pdf

Biofuel. (2010). Biofuel Chemistry: How they Burn?. Recovered from http://biofuel.org.uk/how-do-biofuels-burn.html

Biofuels. (s.f). What are biofuels?. Recovered from https://www.shell.com/energy-and-innovation/new-energies/biofuels.html#iframe=L3dlYmFwcHMvMjAxOV9CaW9mdWVssc19pbnRlcmFjdGl2ZV9tYXAv

Bittencourt, G., Olivera, R., Carvalho, A. (2012). Determinantes das exportações brasileiras de etanol. *Capa, 21* (4). 4-19. Recuperado de https://seer.sede.embrapa.br/index.php/RPA/article/view/262/pdf

Buitrago, R. (2014). Evaluación de los efectos ambientales de la gasolina, Diésel, biodiesel y etanol carburante en Colombia por medio del análisis de ciclo de vida. [Master's Thesis]. National university of Colombia.

Brunetti, F. (2012). Motores de combustao interna. Sao Paulo, Brasil: Blucher

Cardona, C. (2009).Perspectivas de la producción de biocombustibles en Colombia: contextos

latinoamericano y mundial. *Engineering magazine, 29.*109- 120.

Castelo, J., Cepeda, C., Bonilla, M., Acosta, J., Moreano, G., Almacaña, E., Villalba, R. (2017).

Estudio comparativo de potencia, torque y emisiones contaminantes en un motor de

combustión interna de encendido provocado (MEP) con combustible extra, e5 y e10 a una

altura de 2700 M.S.N.M. *Infociencia, 11 (1).* 132-138. DOI:

http://dx.doi.org/10.24133/infociencia.v11i1.1024

Caton, J. (2016). An introduction to thermodynamic cycle simulations for internal combustion

engines. United Kingdom: John Wiley & Sons Ltd.

Cengel, Y., & Boles, M. (2011). Termodinámica. New York, United States of America:

McGraw- Hill.

Cerveny, P., & Gravante, S. (s.f). WAVE. Recovered:

https://software.ricardo.com/products/wave

Ceviz, M., & Yüksel, F. (2005). Effects of ethanol- unleaded gasoline blends on cyclic

variability and emissions in an SI engine. *Applied Thermal Engineering, 25* (5-6), 917-

925.

Chang, R., & College, W. (2002). *QUÍMICA* (Quinta ed.). México, D.F: Mc Graw Hill.

Chawla, K., Lins, C., McCrone, A., Musolino, E., Riahi, L., Sawin, J., Sims, R.,… & Sverrisson,

F. (2014). Renewables 2014 Global Status Report. *Renewable Energy Policy Network for*

the 21st Century.

Congreso de la Republica de Colombia. (19 Septiembre 2001). Por la cual se dictan normas sobre el uso de alcoholes carburantes, se crean estímulos para su producción, comercialización y consumo, y se dictan otras disposiciones. [Ley 693 de 2001]. Bogotá.

Congreso de la Republica de Colombia. (9 de Agosto de 2019). Por medio del cual se establece una tarifa diferencial para los sistemas de transporte masivo y se dictan otras disposiciones. [Proyecto de Ley 46 de 2019]. Bogotá.

De Cerqueira, R., & Leal, M. (2007). O Biocombustível no Brasil. *Novos estudos CEBRAP,* (78), 15-21. Recovered from http://www.scielo.br/pdf/nec/n78/03.pdf

Demostenes, C., Ribao, J., Cavalcante, F., Olivera, M., & Silva, C. (2016). On-board Monitoring and Simulation of Flex Fuel Vehicles in Brazil, *Transportation Research Procedia, 14.* 3129- 3138. DOI: https://doi.org/10.1016/j.trpro.2016.05.253

Deparment of Energy. (s.f). Vehículos de combustible flexible. Recuperado de https://afdc.energy.gov/vehicles/flexible_fuel.html

Departamento Nacional de Planeación. (31 Marzo de 2008). Lineamiento de política para promover la producción sostenible de biocombustibles en Colombia. [Conpes 3510 de 2008]. Bogotá

Dongyoung, J., Kwanhee, C., Cha- Lee, M., Younsung, L., Jongtae, L.,…& Simsoo, P. (2017). The impact of various ethanol-gasoline blends on particulates and unregulated gaseous emissions characteristics from a spark ignition direct injection (SIDI) passenger vehicle. *Fuel, 2019 (1).* 702-712. DOI: https://doi.org/10.1016/j.fuel.2017.08.063

El Nuevo Siglo. (2019, Octubre 24). Plantean aumentar diesel y gasolina verde en el país. *El Nuevo Siglo*.

Eyidogan, M., Ozsezen, A., Canakci, M., & Turkan, A. (2010). Impact of alcohol–gasoline fuel blends on the performance and combustion characteristics of an SI engine. *Fuel, 89 (10).* 2713- 2720. DOI: https://doi.org/10.1016/j.fuel.2010.01.032

Fabricio, A. (Julio de 2015). *Universidad Tecnológica Equiccial.* Obtenido de http://repositorio.ute.edu.ec/bitstream/123456789/14047/1/63733_1.pdf

FedeBiocombustible. (2019). Precios de alcohol Carburante (Ethanol). Recovered from: https://www.fedebiocombustibles.com/estadistica-precios-titulo-Alcohol_Carburante. (Etanol).htm

Ferguson, C., & Kirkpatrick, A. (2016). Internal combustion engines: applied thermosciences (3rd Ed). John Wiley & Sons.

García, H., y Calderón, L. (2012). Evaluación de la política de Biocombustibles en Colombia. Recuperado de https://www.repository.fedesarrollo.org.co/bitstream/handle/11445/338/Repor_Octubre_2 012_Garcia_y_Calderon.pdf?sequence=3&isAllowed=y

Girardi, E. (2019). Agronegócio sucroenergético e desenvolvimiento no Brasil. *Confins. Revue franco- brésilienne de géographie,* (40). Recovered from https://journals.openedition.org/confins/19517#ftn2

Glassman, I., Yetter, R., & Glumac, N. (2015). Combustion (5th Ed). Pennsylvania: El Sevier.

Government of Canada. (2018). Ethanol. Recovered: https://www.nrcan.gc.ca/energy/efficiency/energy-efficiency-transportation-and-alternative-fuels/alternative-fuels/biofuels/ethanol/3493

GT-Power. (2019). GT-Power Engine Simulation Software. Recovered:

https://www.gtisoft.com/gt-suite-applications/propulsion-systems/gt-power-engine-

simulation-software/

Gravante, S. (2019). VECTIS. Recovered: https://software.ricardo.com/products/vectis

GREENDELTA. (2018). OPENLCA. Recovered: http://www.openlca.org/

Heermann, D. (1990). Computer- Simulation Methods. Berlin, Alemania: Springer Berlin

Heidelberg

Hernandez, A., Escobar, R., García, J., Gómez, J., Higareda, T., Olivares, V. (2019). Theoretical

analysis of the power of a spark ignition internal combustion engine with different fuel

blends. *IAPE'19.* DOI*:* http: //dx.doi .org / 10.17501

Heywood, J. (1988). Internal Combustion Engine Fundamentals. New York, United States of

America: McGraw- Hill.

Larsson, T., Stenlaas, O., & Erlandsson, A. (2019). Future Fuels for DISI Engines: A Review on

Oxygenated, Liquid Biofuels 2019-01-0036, *SAE Technical Paper.*

DOI: https://doi.org/10.4271/2019-01-0036

Leong, S., Muttamara, S., & Laortanakul, P. (2002). Applicability of gasolina containing etanol

as Thailand's alternative fuel to curb toxic VOC pollutants from automobile emiission.

Atmospheric Environment, 36 (21), 3495- 3503.

Mantilla, J., Aguirre, B., & Sarmiento, L. (2008). Evaluación experimental de un motor

encendido por chispa que utiliza biogás como combustible. *Ingeniería e Investigación*,

131-141.

Marinov, N. (1999). A detailed chemical kinetic model for high temperature ethanol oxidation. *International Journal of Chemical Kinetics, 31 (3).* DOI: https://doi.org/10.1002/(SICI)1097-4601(1999)31:3<183::AID-KIN3>3.0.CO;2-X

Merker, G., Schwarz, C., & Teichmann, R. (2012). Combustion Engines Development. London, United Kingdom: Springer.

Ministerio de Ambiente y Desarrollo sostenible. (25 Septiembre de 2017). Por la cual se expide el límite del indicador de cociente del inventario de emisiones de gases de efecto invernadero de Etanol Anhidro Combustible Desnaturalizado y se adoptan otras disposiciones. [Resolución 1962 de 2017]. Bogotá.

Ministerio de Ambiente y Desarrollo sostenible, y Ministerio de Minas y Energía. (20 Mayo de 2016). Por la cual se modifica la Resolución 898 de 1995 en lo relacionado con los parámetros y rquisitos de calidad del Etanol Anhidro Combustible y Etanol Anhidro Combustible Desnaturalizado utilizado como componentes oxigenante de gasolinas y se dictan otras disposiciones. [Resolución 0789 de 2016]. Bogotá.

Ministério de Meio Ambiente. (2015). O que são os poluentes atmosféricos?. Recovered from: http://www.ebc.com.br/infantil/voce-sabia/2015/08/poluicao-do-ar-o-que-sao-os-poluentes-atmosfericos

Ministerio de Minas y Energía. (28 Febrero 2019). Por la cual se establece la mezcla mínima de biocombustible para uso en motores diésel de las fuentes móviles terrestres que se utilicen para la actividad minera. [Resolución 40188 de 2019]. Bogotá.

Ministerio de Minas y Energía. (2019). Precios de combustibles. Recuperado de https://www.minenergia.gov.co/precios-de-combustible

Ministerio de Minas y Energía. (2019). Precios de combustible año 2019. Recovered from:

https://www.minenergia.gov.co/precios-ano-2019

Mitsutani, C. (2010). *A logística do etanol de cana de açúcar no Brasil: condicionantes e*

perspectivas (Tese de doutorado). Universidade de São Paulo, Brasil.

Mouthón, L. (2008, Octubre 27). Importaciones desplazan el 26% de producción de etanol. *El*

Heraldo.

NASA. (2019). Carbon Dioxide. Recovered from: https://climate.nasa.gov/vital-signs/carbon-

dioxide/

NASA. (2019). The causes of climate change. Recovered from https://climate.nasa.gov/causas/

NASA. (2019). What is the greenhouse effect?. Recovered from

https://climate.nasa.gov/faq/19/what-is-the-greenhouse-effect/

National Geographic. (2019). Biomass energy. Recovered from

https://www.nationalgeographic.org/encyclopedia/biomass-energy/

Nigro, N., Storti, M., & Ambroggi, L. (1999). Modelización numérica de un motor de

combustión interna monocilíndrico encendido por chispa. *Revista Internacional de*

Métodos Numéricos para Cálculo y Diseño de Ingeniería., 34.

Noqueira, T., Dominutti, P., De Carvalho, L., Fornaro, A., & Andrade, M. (2014). Formaldehyde

and acetaldehyde measurements in urbn atmosphere impacted by the use of etanol

biofuel: Metropolitan Area of Sao Paulo (MASP) 2012-2013. *Fuel,* (134), 505- 513. DOI:

https://doi.org/10.1016/j.fuel.2014.05.091

Onorati A., Ferrari G., D'Errico, G., "1D Unsteady Flows with Chemical Reactions in the

Exhaust Duct-System of S.I. Engines: Predictions and Experiments". SAE Paper No.

2001-01-0939.

OpenFOAM. (2019). About OpenFOAM. Recovered: https://www.openfoam.com/

Petrobras. (2019). Composição de preços ao consumidor. Recovered from

http://www.petrobras.com.br/pt/produtos-e-servicos/composicao-de-precos-de-venda-ao-

consumidor/gasolina/

Pulkrabek, W. (1997). *Engineering Fundamentals of the Internal Combustion Engine.* New

Jersey: Prentice Hall. Recuperado el Abril de 2019

Rodriguez, J. (2018). *INTRODUCCIÓN A LA TERMODINÁMICA.* México.

Santos, A. (2008). A influência do uso do Etanol combustível nas emissões dos gases do efeito

estufa nos motores do ciclo otto. [Undergraduate thesis]. Escola de Engenharia Mauá do

Centro Universitário do Instituo Mauá de Tecnologia. São Caetano do Sul. Brasil.

Sanz, C. (2017). *Optimización del cierre de la válvula de admisión de u motro de combustión*

interna alternativa.

Schwingel, A., Viera, L., De Oliveira, G., Ziani, F., Coronel, D. (2018). Análise empírica da

competitividade do etanol brasileiro 199-2016. *Administração e Negócios da Amazônia,*

10 (3). 53- 72. Recuperado de

https://pdfs.semanticscholar.org/0aa9/9bb5643f0b8c964b40a1a4c6da3e9185153a.pdf

Semana. (2018, Agosto 11). Colombia, en la ruta de los biocombustibles. *Semana.*

Serrato, C., y Lesmes, V. (2016). *Metodología para el cálculo de energía extraída a partir de la*

biomasa en el departamento de Cundinamarca (Tesis de grado). Universidad Distrital

Francisco Jose de Caldas, Colombia. Recuperado de

http://repository.udistrital.edu.co/bitstream/11349/3687/1/Documento%20final%20Metod

olog%C3%ADa%20Potencial%20Energ%C3%A9tico%20Biomasa.pdf

Soustelle, Michel. (2011). An Introduction to chemical kinetics. ISTE Ltd. WILEY.

Stone, R. (2012). Introduction to Internal Combustion Engines. China: Palgrave Macmillan

Suarez, R., Clirotte, M., Arlitt, B., Nakatani, S., Hill, L., Winkler, K, … Astorga, C. (2012).

Intercomparison of ethanol, formaldehyde and acetaldehyde measurements from a flex-

fuel vehicle exhaust during the WLTC. *Fuel, 203 (1).* 330-340. DOI:

https://doi.org/10.1016/j.fuel.2017.04.131

Suarez, R., Cairotte, M., Arlitt, B., Nakatani, S., Hill, L., Winkler, K.… Astorga, C. (2017).

Intercomparison of ethanol, formaldehyde and acetaldehyde measurements from a flex-

fuel vehicle exhaust during the WLTC. *Fuel, 203*, 330-340. Recovered from

https://www.sciencedirect.com/science/article/pii/S0016236117305598

Turns, S. (2011). An Introduction to Combustion. Concepts and Applications. New York:

McGraw-Hill.

Turus, S. (2012). An Introduction to Combustion concepts and applications. (3rd Ed). New York:

McGraw Hill.

UFPS. (13 de Junio de 2016). *Universidad Francisco de Paula Santander*. Obtenido de

https://ww2.ufps.edu.co/universidad/informacion-institucional/1042

UFPS. (2018). *Ingeniería Mecánica*. Obtenido de https://ww2.ufps.edu.co/oferta-

academica/ingenieria-mecanica

UFSC. (2019). *Universidad Federal de Santa Catarina*. Obtenido de http://estrutura.ufsc.br/

United Nations. (2017). UN Comtrade Database. Recovered from https://comtrade.un.org/

United States Environmental Protection Agency. (2017). Technical Overview of Volatile

Organic Compounds. Recovered from https://www.epa.gov/indoor-air-quality-

iaq/technical-overview-volatile-organic-compounds

Virtualengine. (s.f). Virtualengine: the end user computing and cloud solution specialists.

    Recovered: https://virtualengine.co.uk/

Yang, J., Roth, P., Dubin, T., Shafer, M., Hemming, J., Antkiewicz, D.,…& Karavalakis, G.

    (2019). Emissions from a flex fuel GDI vehicle operating on ethanol fuels show marked

    contrasts in chemical, physical and toxicological characteristics as a function of ethanol

    content. *Science of the Total Environment,* (683), 749- 761. DOI:

    https://doi.org/10.1016/j.scitotenv.2019.05.279

Yeliana, C., Cooney, J., Worm, D., Michalek, J., & Naber. (2008). Wiebe function parameter

    determination for mass fraction burn calculation in an ethanol- Gasoline Fuelled si

    engine. *Journal of KONES Powertran and transport, 15 (3).* 567-574.

Yüksel, F., & Yüksel, B. (2004). The uses of etanol- gasolina blend as a fuel in an SI engine.

    Renewable energy, 29 (7), 1181-1191

Zink, J. (2011). *The John Zink Combustion Handbook.* Oklahoma: CRC.

Satratta, J. (2000). Biocombustibles: los aceites vegetales como constituyentes principales del

    biodiesel. Departamento de Capacitación y desarrollo de Mercado. Recuperado de:

    https://pdfs.semanticscholar.org/58bb/85dbc16dbe919fb6d4d2a8e91d1c44a391af.pdf

ANP. (2019). Agencia Nacional de Petróleo, Gás natural e Biocombustiveis. Recovered:

    http://www.anp.gov.br/

Cassiano, D., Ribau, J., Cavalcante, F., Oliveira, M., Silva, C. (2016). On board monitoring and

    simulation of flex fuel vehicles in Brazil. Science Direct, 14. 3129- 3138. Doi:

    10.1016/j.trpro.2016.05.253

Fridell, E., Eugensson, M., Modanova, J., Tang, L., Sjoberg, K., Forsberg, B. (2010). A

    comparasion of emissions from ethanol and petrol fueled cars. IVL. Recovered:

    https://www.ivl.se/download/18.343dc99d14e8bb0f58b75e4/1445517474842/B1962.pdf

Doğan, B., Erol, D., Yaman, H., & Kodanli, E. (2017). The effect of ethanol-gasoline blends on

    performance and exhaust emissions of a spark ignition engine through exergy

    analysis. Applied Thermal Engineering, 120, 433-443.

Corrêa, S. M., Arbilla, G., Martins, E. M., Quitério, S. L., de Souza Guimarães, C., & Gatti, L. V. (2010). Five years of formaldehyde and acetaldehyde monitoring in the Rio de Janeiro downtown area–Brazil. Atmospheric Environment, 44(19), 2302-2308.

REA. (2019). The Association for Renewable Energy & Clean Technology. Recovered: https://www.r-e-a.net/

Oih, A., Tromboni, P., Correia, L., Camargo, A., Marchetti, C., Borsoi, C. (2010). Evolution of flex- fuel technology: a case study on Volkswagen Brazil. XXXIV Encontro da ANPD. Recovered: http://www.anpad.org.br/admin/pdf/gct1500.pdf

Álvarez, J., Callejón, I., Forns, S., Balsells, D., Casanova, J., Bonet, O., Carrera, X…Villa, J. (2005). Motores alternativos de combustión interna. UPC: Barcelona.